2800 East Old Shakopee Road
Mailing Address/Box 1249
Minneapolis, Minnesota 55440

CD

CONTROL DATA CORPORATION

Dynamic Characteristics
of
Observed Sudden Warmings

Final Report

Contract NASW 3761

May 1983 - May 1986

by

D.G. Dartt and D.E. Venne

September 1986

Summary

The following study investigates the planetary wave
dynamics of stratospheric sudden warmings in the northern
hemisphere for a large number of observed events that
occurred during winters from 1970-75 and 1978-81. The
analysis describes wave propagation and zonal flow
interaction from the troposphere upwards to near 50 km, and
in some years to near 80 km. Analysis is primarily
concentrated in the stratosphere and mesosphere using
meteorological parameters derived from Selective Chopper
Radiometer (SCR) measurements on Nimbus 4 and 5 and
Stratospheric and Mesospheric Sounder (SAMS) measurements
on Nimbus 7. National Meteorological Center data are used
below 30 km. Three primary topics are covered in this
study: (1) the interaction of zonally propagating and
quasi-stationary planetary waves during warming events; (2)
planetary wave influence on zonal flow near the
stratopause; and (3) planetary wave propagation to near 80
km as seen from SAMS data. This final report consists of
draft manuscripts on each topic.

In (1), filters are applied to one particularly good
winter of daily planetary wave data to separate westward
and eastward propagating components from the
quasi-stationery (QS) component. For waves 1 and 2, the QS
component is prominent during the warming process. The
propagating components attain their largest amplitude in
the polar stratosphere (30 mb, 65°N) near the end of the
warming process. At this time, interference between QS and
propagating components produces vacillations in
Eliassen-Palm (EP) wave flux, EP flux divergence and zonal
flow. In the meridional plane, the propagation of the
amplifying QS wave 1 and 2 components are compared to the
indexes of refraction (Q_n) derived from zonal flow.
Upward propagating waves are refracted towards large values
of Q_n. However, waves retain some of their propagation
characteristics of lower altitudes and do not directly
propagate up the gradient of Q_n. Periods of strong
upward wave propagation into the stratosphere have
associated minimal latitude gradients of Q_n in the lower
stratosphere.

In (2), the relationship between zonal flow change
near the stratopause (1 mb), and upward propagating wave
activity in the lower stratosphere (50 mb), and polar zonal
temperature tendency (2 mb) is explored using Transformed
Eulerian Mean diagnostics applied to large stratospheric
volumes. Some 14 wave events from 1970-75 and 1978-81 are

compared, and a composite relationship among the above variables is calculated at various stages of the stratospheric warming process. The 5-day zonal flow change is given as a function of observed wave forcing and of the stratospheric temperature tendency which indirectly gives the strength of the residual circulation. The very rapid mid-winter breakdown in zonal flow of the mesospheric jet may have practical applications for space shuttle and hypersonic flight. Prediction of 1-mb zonal flow is investigated using measurements of vertically propagating wave activity in the lower stratosphere and zonal temperature tendency in the upper stratosphere.

In (3), the mesospheric limit of vertical wave propagation is examined using two winters of SAMS data. Wave 1 appears to propagate upward and decelerate zonal flow in mid-latitudes to altitudes near 70 km, wave 2 to altitudes of 60 km. During large wave events, evidence of a two-cell residual circulation exists similar to the model results of Dunkerton, et al. (1981). Above 65 km, a region of EP flux divergence frequently occurs during winter, leading to wave-forced acceleration of zonal flow averaging about 5 ms^{-1}day^{-1}. The primary source of this divergence is wave 2, whose vertical propagation is generally restricted in the easterly shear region above the mesospheric wind maximum in high latitudes. The EP flux divergence above 65 km is poorly correlated with zonal-flow change, indicating that other mechanisms of flow change such as gravity wave dissipation and diabatic cooling are likely to be more important.

TABLE OF CONTENTS

The Interaction of Quasi-Stationary and Zonally Propagating
Planetary Waves During Winter, 1973-74

Denis G. Dartt

Abstract

Eliassen-Palm diagnostics of the primary planetary waves and their interaction with the zonal flow are described from the middle troposphere to the upper stratosphere during winter, 1973-74. Using filters the planetary waves are further decomposed into quasi-stationary and zonally propagating components and the dynamics of each component is analyzed. The sequence of wave activity consists of amplification and propagation to the upper stratosphere of wave 1 in late December, wave 2 during January and wave 1 again in late February. All wave events have a strong quasi-stationary component of Eliassen-Palm (EP) wave flux. The propagating components constructively and destructively interfere with the quasi-stationary component to produce pulses of upward EP flux in the manner described by Salby(1984). For wave 1, the westward propagating component is largest and attains an amplitude of about 40%·the quasi-stationary component approximately ten days following the quasi-stationary maximum. By themselves, the propagating components do not contribute significantly to the observed EP flux.

Cross-sections of quasi-stationary EP flux reveal the locations of wave activity and the paths of propagation to the upper stratsophere. An index of refraction analysis based on zonal wind indicates that the upward propagating waves are horizontally refracted towards maximum values of Q_m. However, the waves retain some of their propagation characteristics of lower levels and do not directly propagate up the gradient of Q_m. Periods of strong upward wave propagation into the stratosphere have associated minimal latitude gradients of Q_m at 50 mb.

1. Introduction

The purpose of this paper is to discuss the application of
Eliassen-Palm planetary wave diagnostics to one winter of particularly
good planetary wave data, 1973-74. In this winter, Nimbus 5 Selective
Chopper Radiometer derived temperature and geopotential height fields in
the upper stratosphere are combined with NMC data below 30 km to analyze
planetary wave propagation and wave-zonal mean flow interaction from
0-50 km. The completeness of daily data allow a separation of the
quasi-stationary and primary eastward and westward zonal propagating
components and an analysis of their contribution to the winter dynamics.

The ensuing discussion describes the propagation of planetary
waves 1 and 2 and the forcing of the zonal flow by these waves in terms
of 5-day average Eliassen-Palm (EP) flux parameters throughout the
winter. This is followed by a discussion on the separation of
quasi-stationary and zonally propagating components along with an
assessment of their importance to the winter dynamics. Finally,
cross-sections of quasi-stationary wave EP fluxes for the major events
are discussed with regard to sources of wave activity and paths of
propagation to the upper stratosphere. An index of refraction analysis
is used to indicate how the zonal wind field may influence the
propagation of the major waves.

Supporting data and analysis of dynamics during the 1973-74
winter include the studies by Quiroz (1975), McGregor and Chapman (1979)
and Labitzke and Goretzki (1982). Quiroz gives a synoptic
interpretation of stratospheric warmings using data from NOAA
satellites. McGregor and Chapman (1979) discuss the behavior of
planetary waves 1 and 2 in temperature in the upper stratosphere;
Labitzke and Goretzki (1982) give a detailed chronology of sensible heat
and momentum fluxes at 30 mb.

2. Data

All parameters were computed from daily planetary wave coefficients of height and temperature. This calculation was performed for seven latitude circles (25, 35, 45, 55, 65, 75, 79°N) and 11 altitudes (850, 500, 200, 100, 50, 30, 10, 5, 2, 1, and 0.4 mb) for the winter season, November 1983 to March 1984. For the six lowest levels, wave amplitude and phase are based on NMC gridded values interpolated to 20° longitude intervals. Zonally averaged east-west winds below 100 mb were derived from NMC wind grids; otherwise all wave analysis for wind is based on the geopotential height field using the geostrophic approximation as described by Eliasen (1958). Wave coefficients at the five upper levels are based on temperature fields derived statistically from NMC 10-mb temperature and various nonlinear combinations of SCR channel radiances from Nimbus 4 and 5. The regression coefficients utilized in the temperature analysis were derived from co-located rocketsonde temperature, NMC 10-mb temperature and smoothed satellite radiances. Hovland and Wilcox (1979a, 1979b) give a detailed discussion of the regression and gridding procedures. The upper level geopotential height fields were derived hydrostatically using the NMC 10-mb height field and the statistically derived upper-level temperature fields.

3. Computations of EP Diagnostics

The respective horizontal (H) and vertical (Z) EP flux components for each wave were defined (after Palmer, 1981) by:

$$F_H = - \rho_s \exp(-z/H_0) r_0 \cos \phi \, (\overline{u'v'}) \tag{1}$$

$$F_Z = \rho_s \exp(-z/H_0) r_0 f \cos \phi \, (\overline{v'\theta'})/\bar{\theta}_z \tag{2}$$

where $\overline{u'v'}$ and $\overline{v'\theta'}$ are the respective longitudinally integrated meridional transport of zonal momentum (u') and potential temperature (θ') by the meridional wind (v') for a given wave; $z = -H_0 \ln(p/1000)$

is a vertical coordinate defined in terms of pressure (p) and constant
scale height, H_o = 6400 m; $\bar{\theta}_z$ is the vertical lapse of zonal
potential temperature, ϕ is latitude and r_o = 6370 km, the earth's
radius; ρ_s = 1000 g m^{-3}, a reference 1000 mb density, and
$f = 2\Omega \sin \phi$, the coriolis parameter.

The divergence of the EP flux components is given by:

$$\nabla \cdot \vec{F} = (1/r_o \cos \phi)(\cos \phi \, F_H)_\phi + (F_Z)_z \tag{3}$$

where the subscripts ϕ and z indicate partial derivatives with respect
to latitude and altitude. Equation (3) defines the planetary wave
forcing term in the momentum equation based on the transformed Eulerian
mean formulation (Palmer, 1981). The momentum equation is given by:

$$\bar{u}_z = f\bar{v}^* + (\rho_s r_o \cos \phi)^{-1} \exp(z/H_0) \nabla \cdot \vec{F} \tag{4}$$

where $\bar{u}_z$ is the time derivative of zonal wind and $\bar{v}^*$ is the meridional
component of the residual circulation which intrinsically opposes the
planetary wave forcing term (O'Neill and Youngblutt, 1982).

In the EP flux analysis below, the discussion is based on time
histories of vertical and horizontal components and on cross sections of
EP flux vectors on given days. The scaling used with EP flux vector
cross sections is used throughout so the results can be compared. Both
flux components are multiplied by $2\pi r_o \cos \phi$ to produce longitudinally
averaged fluxes, and the meridional flux in (1) is multiplied by
(.0132). The latter scaling ensures that when the meridional and
vertical fluxes are equal, the flux vector will be drawn at a 45° angle
from the horizontal on cross sections. The units of EP flux are
10^{15} g m s^{-2}. In the computation of EP flux divergence (3),
vertical derivatives typically represent changes over an approximate
10-km interval.

4.   Description of Primary Wave EP Fluxes

A chronology of wave 1 and 2 propagation at 200, 30 and 2 mb is shown in Figures 1-4 in terms of 5-day averages of EP flux components. Figure 1 shows two wave 1 events (December 23 - January 3 and February 16-26) when amplification of flux occurred in middle latitudes, 200 to 2 mb. The vertical EP flux is damped with altitude and also occurs slightly later at higher levels, consistent with the tropospheric source of wave activity. The wave 1 EP flux at higher altitudes also appears to be shifted to higher latitudes. Both of the wave events have flux maxima between 45° and 55°N at 200 mb. These maxima appear near 55° to 65°N at 30 and 2 mb. Figure 2c indicates that substantial wave activity in low and middle latitudes of the upper troposphere is diverted southward by strong equatorward flux. During the first wave event, poleward flux northward of 50° is evident at 200 mb prior to the vertical flux maximum. Figure 2 indicates there is no apparent polar focusing for the second event. At 30 and 2 mb, enhanced equatorward flux is associated with the large values of vertical flux.

Wave 2 vertical EP flux at 200 mb is comparable in magnitude to wave 1, but Figure 3c shows that intervals of wave 2 amplification are conversely related to intervals of wave 1 amplification, Figure 1c. At 30 and 2 mb, wave 2 upward flux is about one-half the magnitude of the wave 1 component. At 200 mb, wave 2 poleward flux is closely associated with upward flux leading to strong polar focusing, Figure 4c. At stratospheric levels, however, upward and equatorward components occur coincidently, as was evident for wave 1. Superposed on the seasonal EP flux variations at 200 mb are vacillations of 10 to 20 days period.

A direct measure of planetary wave forcing of the zonal flow is given by the EP flux divergence term in (4). A comparison of the zonal wind with EP flux divergence due to waves 1-6 throughout the winter at 55°N is shown in Figure 5. Figures 1 and 3 show this to be the primary latitude of vertical wave forcing. In the upper stratosphere, the primary zonal flow deceleration occurs from Dec. 27-Jan. 11 and from Feb. 10-Mar. 7. These times of zonal wind change compare favorably with

the times of maximum wave forcing in Figure 5b. However, the wave forcing typically is about a factor of five larger than the observed wind change. Thus, the wave forcing is opposed by a poleward residual circulation, $\bar{v}^*$, as in (4). In the transformed Eulerian mean framework, the downward branch of this circulation in high latitudes produces the adiabatic warming characteristic of the stratospheric warming process (O'Neill and Youngblut, 1982).

Figure 5 suggests that the overall effect of the upward propagating waves is to decelerate the zonal flow throughout the winter. The maintenance of the zonal flow is by the winter radiation imbalance between the pole and equator.

Figure 6(a) and (b) show the individual contributions of waves 1 and 2 to the EP flux divergence at 55°N. The primary wave events have their own characteristic forcing of the zonal flow. For the wave 1 event in the latter part of December, wave forced deceleration occurs from 15-50 km, and reaches a maximum of over 15 m s^{-1}day^{-1} between 35-40 km on Dec. 27. For the wave 1 event in late February, the wave-forced deceleration lasts from February 15 to March 17, reaches a maximum of near 15 m s^{-1} day^{-1} at 45-50 km and produces the major spring zonal wind reversal. For the midwinter wave 2 event, Figure 6b, wave-forced deceleration occurs from the surface to near 50 km, attaining a value of 10 m s^{-1}day^{-1} at this altitude.

For wave 2, Figure 6b, EP flux convergence appears to originate in the troposphere, while for wave 1, the convergence appears first in the lower stratosphere. From 5-15 km, weak EP flux divergence occurs for wave 1, perhaps indicating a weak source of wave activity in this region. Below 20 km the EP flux divergence for wave 1 is somewhat correlated with EP flux convergence for wave 2. This pattern may be evidence of nonlinear wave-wave interactions (Palmer and Hsu, 1983).

5. Separation of Quasi-Stationary and Propagating Waves

Selected daily time series of wave 1 and 2 cosine and sine coefficients were filtered to separate quasi-stationary and transient components in order to determine their contributions to the winter dynamics. A low-pass filter was first applied to these time series to isolate the quasi-stationary components. A band-pass filter was used to isolate the westward and eastward propagating components whose period was in the range 12-35 days. Inspection of the variability of planetary wave parameters indicated significant variability on these time scales. The frequency response of both the low-pass and band-pass filters is indicated in Figure 7. The band-pass filter has symmetric and antisymmetric components to separate westward and eastward propagating waves. The effect of the antisymmetric filter is to shift the phase of the output by one quarter cycle relative to the symmetric filter. For an eastward propagating component, the cosine coefficient leads the sine coefficient in time by one quarter period; for a westward propagating component, the sine leads the cosine by the same interval. This characteristic is used to separate eastward and westward propagating components whose period is in the range 12-35 days.

Both filters are applied to time series of wave coefficients of geopotential height, temperature and component winds. These filtered data were used to determine the EP fluxes of each propagating component as in (1) and (2). Figure 8 shows the amplitudes of the quasi-stationary (QS), westward propagating and eastward propagating components of waves 1 and 2 at 55°N in the lower stratosphere. The wave 1 QS and westward propagating components are observed to vary in a similar fashion, with the latter lagging the former by about 10 days. The westward propagating amplitude is roughly 35-45 percent of the QS amplitude. The eastward propagating wave 1 amplitude is smaller and relatively constant. For wave 2, the eastward propagating component attains a value about 35 percent of the QS component following its maximum. Figure 9 indicates the magnitude and vector direction of the QS EP flux for both waves at 30 mb. The early winter and spring wave 1

events involve primarily the QS component as does the midwinter wave 2
event. The QS EP vector direction for the early winter event is upwards
and towards the equator (135°); for the midwinter wave 2 and spring
wave 1 events, the vector direction is almost directly upward (90°).
The EP fluxes of the westward and eastward propagating components are
less than 10 percent of the QS component and are not shown. Thus, by
themselves, these waves do not seem to transport significant sensible
heat or momentum in the stratosphere. A recent model study by Robinson
(1985) indicates that alternating wave 1 and wave 2 behavior may result
from non-linear wave-wave interactions between quasi-stationary waves 1
and 2 and westward propagating wave 1. For the 1973-74 winter these
three wave components are prominent, and the successive amplification of
QS wave 1, westward propagating wave 1, and QS wave 2 is observed.

There are also significant EP flux variations resulting from the
interference of the QS and propagating waves in the manner described by
Madden (1983) and Salby (1984). To analyze this effect, the meridional
transport of potential temperature in (2) was decomposed into

$$\overline{v'\theta'} = \overline{v_q'\theta_q'} + \overline{v_t'\theta_t'} + \overline{v_q'\theta_t'} + \overline{v_t'\theta_q'} \tag{5}$$

where the subscripts q and t indicate quasi-stationary and transient
components. Here the transient components are defined to be all the
residual propagating waves after subtraction of the QS component (low
pass filtered) from the time series. Accordingly, EP fluxes were
calculated for the quasi-stationary $(\overline{v_q'\theta_q'})$ and transient $(\overline{v_t'\theta_t'})$
components and for their interaction $(\overline{v_q'\theta_t'} + \overline{v_t'\theta_q'})$.

Figure 10 indicates the daily magnitude of the various terms
in (5) for wave 1 and 2 at 30 mb. The total daily variability of
vertical EP flux arises primarily as a result of the QS component and by
the interference of the transients with the QS component. There is
particularly large interference of QS and transient wave 1 in the last
half of February and early March. Interference of transient and QS wave

2 is also pronounced in midwinter. The transients, themselves, appear to contribute relatively little to the EP flux, especially for wave 1.

The overall effect of the QS transient interaction is for the wave activity to propagate upward in pulses as described by Salby (1934). As the transients intensify following QS wave amplification, Figure 8, the interference is exaggerated. The pulses evident in Figure 4c are extreme examples of this phenomenon.

Generally, the transient waves in geopotential height propagate westward while transient waves in temperature are erratic but characteristically propagate eastward. Both waves exhibit periods near 20 days. Pratt and Wallace (1976) observed similar wave properties in the mid-latitude troposphere during the winter months. There are several possible sources for these propagating waves. They may be normal modes that are excited by the QS component of forcing (Salby, 1984), linear transients resulting from a sudden change in tropospheric forcing, or perhaps non-linear transients occurring as a result of wave-wave interactions (Smith et al., 1984). The general occurrence of these propagating waves and their subsequent excitation following the QS component amplification suggests that these waves may be families of Rossby normal modes (Venne, 1985). However, these modes cannot be resolved here from data of limited latitude extent.

Vertical EP flux pulses can lead to similar pulses of wave forcing of the zonal flow by the EP flux convergence. In Figure 5, periods of alternating EP-flux forcing and zonal flow change with an approximate 20-day period occur intermittently in the stratosphere. The study by Robinson (1985) indicates that vacillations in wave 1 and the zonal mean wind may be caused by interference between wave 1 stationary and traveling components. The variations in zonal wind (Figure 5) and wave 1 components (Figure 8) observed here support Robinson's findings.

6. Cross Sections of QS Wave Properties During Major Events

As the QS waves are ultimately responsible for most of the wave activity that propagates into the stratosphere, their propagation is described in more detail below. Cross-sections of amplitude (A) and phase (B) of geopotential height, EP flux vector magnitude (C) and direction (D), and the squared value of the index of refraction (E) are given at three characteristic stages of the dynamic process. These stages are an initial state, an intermediate state with strong upward propagation in the upper troposphere, a mature state with strong upward propagation in the upper stratosphere. The computations of the index of refraction, Q_m, are described in the Appendix.

The December wave 1 event, Figure 11, shows the amplitude of geopotential height increasing from 400 to 800 m from 40-50 km, 55-65°N, in the 20-day period Dec 12-Jan 1. Initially the EP vectors, Figure 13d, show poleward and equatorward branches of wave propagation in the troposphere on either side of a narrow zone of vertical propagation at 55°N. Wave propagation in the equatorward branch is very strong, while the poleward branch is extremely weak, Figure 11c. Much of the wave activity in the equatorward branch does not reach the stratosphere, but propagates southward into low latitudes. The poleward branch splits near 15 km, with downward propagation to the troposphere below this level and equatorward propagation at higher altitudes. On December 27, the poleward branch appears to focus upward propagating waves into the polar stratosphere. This is coincident with a low value of Q_1 near 20 km, 45°N which appears to locally relax the normal equatorward gradient of this parameter observed at lower and higher levels. As the wave activity propagates upwards from below, contours of EP-flux magnitude develop a characteristic convex bubble shape in the stratosphere, Figure 11c. In the upper stratosphere these contours tilt

equatorward, as do the flux vectors. The upward propagating wave appears to be refracted toward the equator in response to the negative Q_1 region near the pole and larger Q_1 values in low latitudes. In lower latitudes the waves appear to be dissipated between 20 to 40 km as indicated by the minimum in EP flux. This is also a region of large Q_1, Figure 11e, which favors dissipation (Smith, 1983). At maturity, the EP flux vectors appear to be cut off from their baroclinic source in the lower troposphere as all wave activity propagates equatorward.

In contrast, the poleward branch of wave propagation is only weakly present for the spring event, Figure 12d, and the source region of vertical EP flux is further to the north in the latitude band, 40-60°N, Figure 12c. The EP vectors indicate that wave activity propagates almost vertically above the source. The wave amplifies from 700 to 1100 meters from 40 to 50 km in a period of about 10 days, Feb. 11-Feb 21. This is twice the rate of amplification of the previous wave 1 event. Figure 12e shows that near 20 km and 55°N the equatorward gradient of Q_1 is locally relaxed coincident with upward propagation from the troposphere on February 21. On March 2, Q_1 is relatively large in the upper stratosphere, and the direction of EP flux is almost vertical. Here Q_1 has increased as a result of the deceleration of zonal wind by the EP-flux convergence of wave 1 shown in Figure 6a. This occurs just prior to the zonal wind reversal in the upper stratosphere, Figure 5a. Thus, for this event the QS wave activity appears to be sharply focused into the region of large Q_1 prior to the occurrence of a critical line.

The altitude-latitude distribution of phase for both events in Figures 11b and 12b indicates that the waves propagate vertically into the stratosphere from the troposphere (baroclinic growth) and propagate equatorward in the upper stratosphere (barotropic decay). In the first event the primary baroclinic zone is near 55°N; for the second event, the baroclinic zone is broader and displaced towards the pole.

Figure 13 shows propagation of QS wave 2 during its intitial mid-winter amplification in early January. As wave 1 is damped, wave 2 amplifies from 50 to 400 m in the upper stratosphere. The origin of wave activity is 850-500 mb from 45-65°N, Figure 15c. With amplification, on January 6, poleward and upward flux occurs throughout the troposphere. Coincidentally, small values of Q_2, Figure 13e, occur near 20 km in low latitudes. These values should help focus the upward propagating waves poleward into the stratosphere. The EP flux propagates upward in the lower stratosphere around a meridional cell whose center is near 40°N, 100 mb as indicated by the nodes in geopotential phase, Figure 13b. Downwards in the troposphere some of the wave activity appears to be trapped in higher latitudes. This may be a consequence of negative values of Q_2 in the lower stratosphere extending to 55°N, Figure 13e. The EP fluxes for wave 2 in the troposphere appear about 5 times stronger than the fluxes for wave 1 events, Figures 11c, 12c.

7. Comparison of EP Flux and Index of Refraction at 50 mb

The previous cross sections indicate that near 20 km the latitude gradient of Q_m may change sign and thus by refraction change the horizontal direction of the upward propagating QS waves. Figure 14 for wave 1 and Figure 15 for wave 2 further explore the relation between Q_m and wave EP fluxes throughout the winter at 50 mb. On these diagrams Q_m is based on 5-day average zonal winds but is not filtered; thus, the variability of Q_m is influenced by the intermittent wave forcing caused by the interaction of QS and propagating waves. The QS wave EP flux is not affected by propagating waves so is inherently smoother.

In Figure 14, the primary intervals of maximum EP flux occur at times (December 27 and February 10) when the general latitude gradient of Q_1 is very weak in middle latitudes. On these occasions there appears to be little horizontal refraction of the upward propagating wave as the EP vectors are directed almost vertically (90°). In low latitudes, equatorward refraction in November, December and March is indicated by relatively high values of Q_1 (60) and wave fluxes with a

strong equatorward component (135°). In January poleward (45°) fluxes are indicated in low latitudes and Q_1 is large (>40) in middle latitudes. Thus, there appears to be some general reciprocity between the refraction of observed waves and the latitude gradient of Q_1.

Figure 15 shows that wave 2 does not amplify and vertically propagate until the early winter horizontal gradient of Q_2 is very weak. In late February wave 2 develops an equatorward component of propagation (135°) concurrently with a general increase in the equatorward gradient of Q_2.

Positive relations between Q_m gradient and the observed propagation of wave activity can lead to techniques of forecasting the QS component of sudden warmings in the stratosphere based on the initial states of the zonal flow field and of the EP fluxes emerging from the troposphere. The EP cross sections in Figures 11-13 and the time analysis in Figures 14 and 15 indicate that the QS waves appear to respond in a gradual way to the large scale gradients of Q_m in the stratosphere. However, the waves still retain characteristics of their past history and are not radically affected by local gradients of Q_m.

8. Conclusions

This study describes the analyses of Eliassen-Palm planetary wave dynamics and associated zonal flow interaction for winter 1973-74, an interval when upper stratospheric data were of good quality and complete. The year was characterized by quasi-stationary wave 1 propagation in late December and late February and wave 2 propagation throughout much of January and early February. Quasi-stationary waves propagating upwards from the troposphere are the primary source of wave activity in the stratosphere. However, zonal propagating waves whose periods are near 20 days constructively and destructively interfere with the QS component to produce upward propagating wave pulses in the manner described by Madden (1983) and Salby (1984). The propagating components

amplify following the maximum in the QS component and produce vacillations in wave EP flux. However, the propagating components by themselves do not appear to transport significant momentum or sensible heat upwards into the stratosphere.

The upward propagating QS wave decelerates the zonal flow throughout the stratosphere with maximum values of wave forced deceleration by EP-flux convergence attaining values of 10-15 m $s^{-1}day^{-1}$ from 40-50 km. This is about five times the observed wind change. Thus, the wave-forcing is opposed by a poleward directed residual circulation, whose descending branch produces adiabatic stratospheric warming in high latitudes.

Cross-sections of EP flux and associated wave parameters at various stages in the evolution of QS wave events are useful for identifying regions of forcing and paths of wave propagation into the stratosphere. Both QS wave 1 events have different sources of forcing and different paths of propagation in the meridional plane. For the December event, the source of wave activity appears to be the upper troposphere, 45-55°N. The wave activity propagates poleward in the lower stratosphere and equatorward in the middle and upper stratosphere. For the February event, the source of the wave activity is much more extensive latitudinally, and the wave activity propagates almost vertically to the upper stratosphere. Wave 2 in January indicates a cellular wave propagation circulation with poleward EP flux in the troposphere and equatorward fluxes in the stratosphere.

An index of refraction analysis indicates that the upward propagating QS waves are generally refracted in the stratosphere in accordance with the horizontal gradient of Q_m. However, because the waves retain some of their propagation characteristics of lower levels, they never appear to directly propagate perpendicular to the Q_m gradient. In the lower stratosphere near 20 km, the Q_m gradient is very weak at those times when wave activity propagates vertically to the upper stratosphere.

Calculation of the index of refraction for quasi-stationary waves

According to quasi-geostrophic theory (Matsuno, 1970), the index of refraction squared (Q_m) derived from the zonal flow may be used for describing the propagation of planetary waves in the meridional plane. Using ray tracing techniques, with appropriate assumptions (O'Neill and Youngblutt, 1982; Karoly and Hoskins, 1982), it is possible to describe the path of a propagating wave in terms of spatial variations of Q_m which is given, after Matsuno (1970), by:

$$Q_m = (1/\bar{\omega} \cos \phi)\bar{q}_\phi - (\Omega\, r_0/NH_0)^2 \sin^2\phi - (m^2/\cos^2\phi), \qquad A(1)$$

$$\bar{q}_\phi = \cos \phi \left\{ 2\,(\Omega + \bar{\omega}) - \bar{\omega}_{\phi\phi} + 3\bar{\omega}_\phi \tan \phi - (2\Omega r_0 \sin \phi)^2 (1/P)([P/N^2]\bar{\omega}_z)_z \right\},$$

$$\bar{\omega} = \bar{u}/(r_0 \cos \phi)$$

$$z = -H_0 \ln(P/P_0),$$

$$N^2 = (g/\bar{\theta})\bar{\theta}_z$$

where m is zonal wavenumber, $\bar{q}$ is zonal vorticity, $\bar{\omega}$ is zonal angular momentum, N is the Brunt-Väisälä frequency and other symbols were previously defined in Section 3. (The subscripts ϕ and z denote partial derivatives.) For a wave of fixed frequency away from the region of forcing, wave packets will propagate up the gradient of Q_m with a group velocity inversely proportional to Q_m. Matsuno (1970) used values of Q_m calculated from the climatological wind field to study the propagation of stationary waves from the troposphere upwards into the stratosphere. Smith (1983) has also used Q_m to help describe the interannual and seasonal variation of planetary waves. O'Neill and Youngblutt (1982) and Butchart, et al. (1982) have used Q_m to analyze the relation between wind fields and EP fluxes during stratospheric sudden warmings.

In the analysis here, Q_m is based on 5-day average zonal winds. Values of Q_m as specified above were also divided by $\sin^2 \phi$, a factor described by Palmer (1982) for correcting ray curvature in Mercator coordinates.

Q_m is a highly derived parameter that is sensitive to observed small-scale latitude variations in zonal wind. When latitude derivatives are determined from NMC data in the lower stratosphere, the resulting space and time variability of Q_m is excessive compared to other planetary wave parameters. To reduce this variability, latitude derivatives were computed from a third degree polynomial function that expresses the latitude variation of $\bar{u}$ from 35 to 75°N. The coefficients of the polynomial were determined by least squares analysis applied at each pressure level from 500 to 1 mb. Otherwise, unsmoothed values of $\bar{u}$ were used in A(1) in the calculation of $\bar{q}_\phi$ wherever $\bar{u}$ or its vertical derivative were required.

References

Butchart, N., S.A. Clough, T.N. Palmer and P.J. Trevelyan, 1982: Simulations of an observed stratospheric warming with quasigeostrophic refractive index as a model diagnostic. Quart. J. Roy. Met. Soc., 108, 475-502.

Eliasen, E., 1958: A study of the long atmospheric waves on the basis of zonal harmonic analysis. Tellus, 10, 206-215.

Hovland, D. and R. Wilcox, 1979a: Statistical retrieval of temperatures from SCR-B at 10 to 0.4 mb. Interim Report No. 1, Contract F49620-78-C0036 for Air Force Office of Scientific Research, by Control Data Corporation, Minneapolis, MN, 24 pp.

Hovland, D. and R. Wilcox, 1979b: Statistical retrieval of temperatures from SCR-A at 10 to 0.4 mb. Final Report, Contract NAS-5-23538 for NASA-Goddard Space Flight Center, by Control Data Corporation, Minneapolis, MN, 33 pp.

Karoly, D.J. and B.J. Hoskins, 1982: Three dimensional propagation of planetary waves. J. Met. Soc. Japan, 60, 109-122.

Labitzke, K. and B. Goretzki, 1982: A catalogue of dynamic parameters describing the variability of the middle stratosphere during northern winters, MAP Handbook 5, C.F. Sechrist, Jr., Editor, Available from SCOSTEP Secretariat, U. of Illinois, Urbana. 188 pp.

Madden, R.A., 1983: The effect of the interference of traveling and stationary waves on time variations of the large-scale circulation. J. Atmos. Sci., 40, 1110-1125.

Matsuno, T., 1970: Vertical propagation of stationary planetary waves in the winter Northern Hemisphere. J. Atmos. Sci., 27, 871-883.

McGregor, J. and W.A. Chapman, 1979: Stratospheric temperatures and geostrophic winds during 1973-74. Quart. J. Roy. Met. Soc., 105, 241-261.

O'Neill, A. and C.E. Youngblut, 1982: Stratospheric warmings diagnosed using the transformed Eulerian-mean equations and the effect of the mean state on wave propagation. J. Atmos. Sci., 39, 1370-1386.

Palmer, T.N., 1981: Diagnostic study of a wavenumber-2 stratospheric sudden warming in a transformed Eulerian-mean formalism. J. Atmos. Sci., 38, 844-855.

Palmer, T.N., 1982: Properties of the Eliassen-Palm flux for planetary scale motions. J. Atmos. Sci., 39, 992-997.

Palmer, T.N. and C.-P.F. Hsu, 1983: Stratospheric coolings and the role of nonlinear wave interactions in preconditioning the circumpolar flow. J. Atmos. Sci., 40, 2484-2496.

Pratt, R.W. and J.M. Wallace, 1976: Zonal propagation characteristics of large scale fluctuations in the mid-latitude troposphere. J. Atmos. Sci., 33, 1184-1194.

Quiroz, R.S., 1975: The stratospheric evolution of sudden warmings in 1969-1974 determined from measured infrared radiation fields. J. Atmos. Sci., 32, 211-224.

Robinson, W., 1985: A model of the wave 1-wave 2 vacillation in the winter stratosphere. J. Atmos. Sci., 42, 2289-2304.

Salby, M.L., 1984: Transient disturbances in the stratosphere: Implications for theory and observing systems. J. Atmos. Terr. Phys., 46, 1009-1047.

Smith, A.K., 1983: Stationary waves in the winter stratosphere: seasonal and interannual variability. J. Atmos. Sci., 40, 245-261.

Smith, A.K., J.C. Gille and L.V. Lyjak, 1984: Wave-wave interactions in the stratosphere: observation during quiet and active wintertime periods. J. Atmos. Sci., 41, 363-373.

Venne, D.E., 1985: Observations of long-period normal mode Rossby waves in the troposphere and stratosphere. (Submitted to J. Atmos. Sci.).
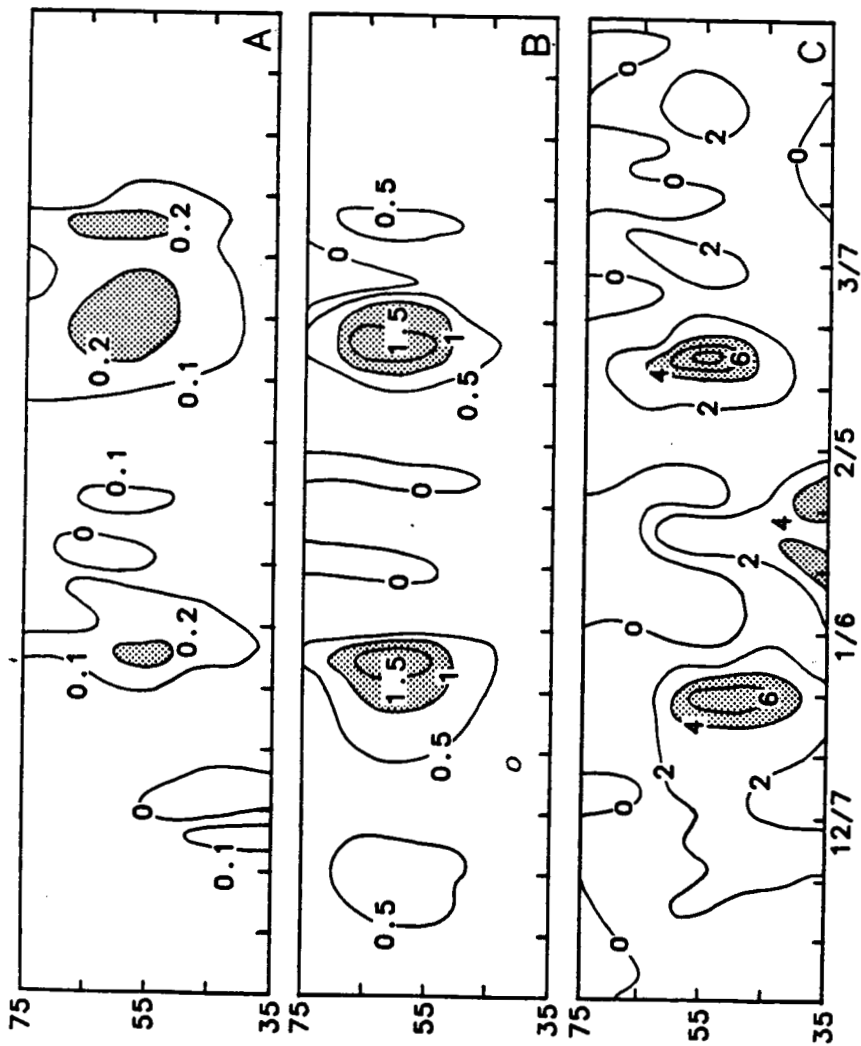
Figure 1. Vertical component of EP flux (10^{15}g m s^{-2}) for wave 1 at (A) 2 mb, (B) 30 mb and (C) 200 mb. Upward fluxes greater than 4 at 200 mb, 1 at 30 mb and 0.2 at 2 mb are shaded to highlight the major flux events.
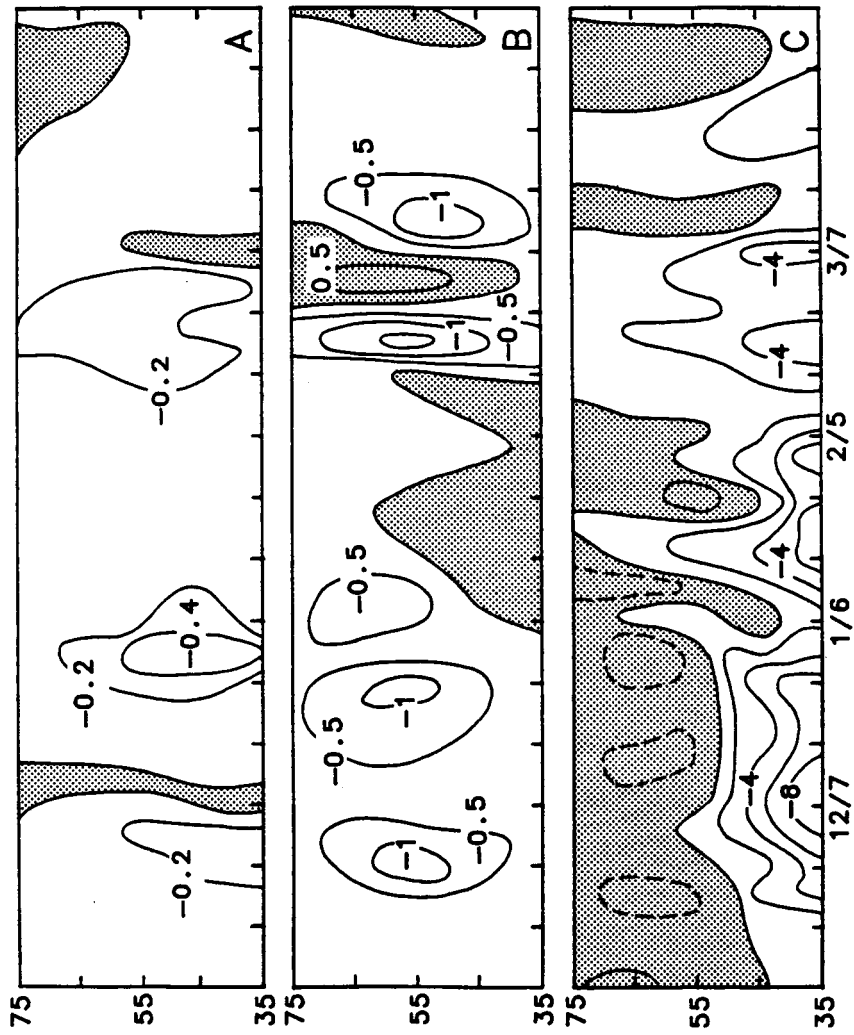
Figure 2. Horizontal component of EP flux (10^{15} g m s^{-2}) for wave 1 at (A) 2 mb, (B) 30 mb and (C) 200 mb during winter, 1973-74. Poleward components are shaded.
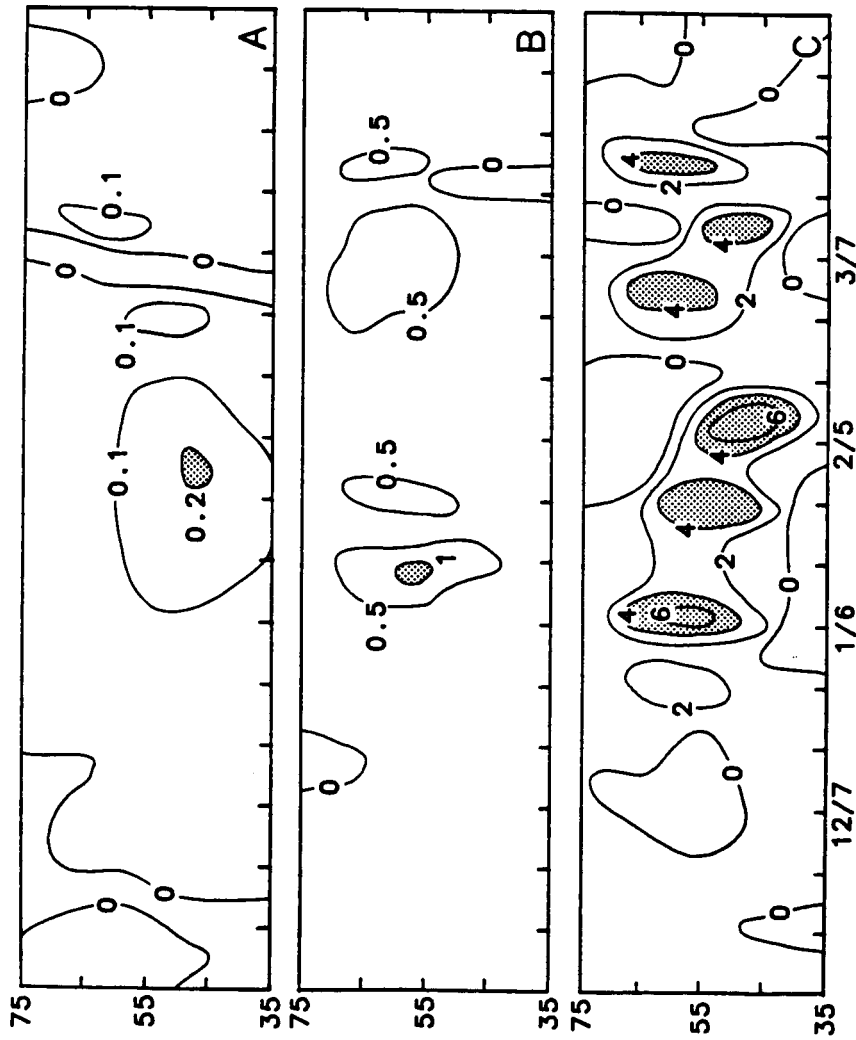
Figure 3. Vertical component of wave 2 EP flux at (A) 2 mb, (B) 30 mb, and (C) 200 mb. Units as in Figure 1.
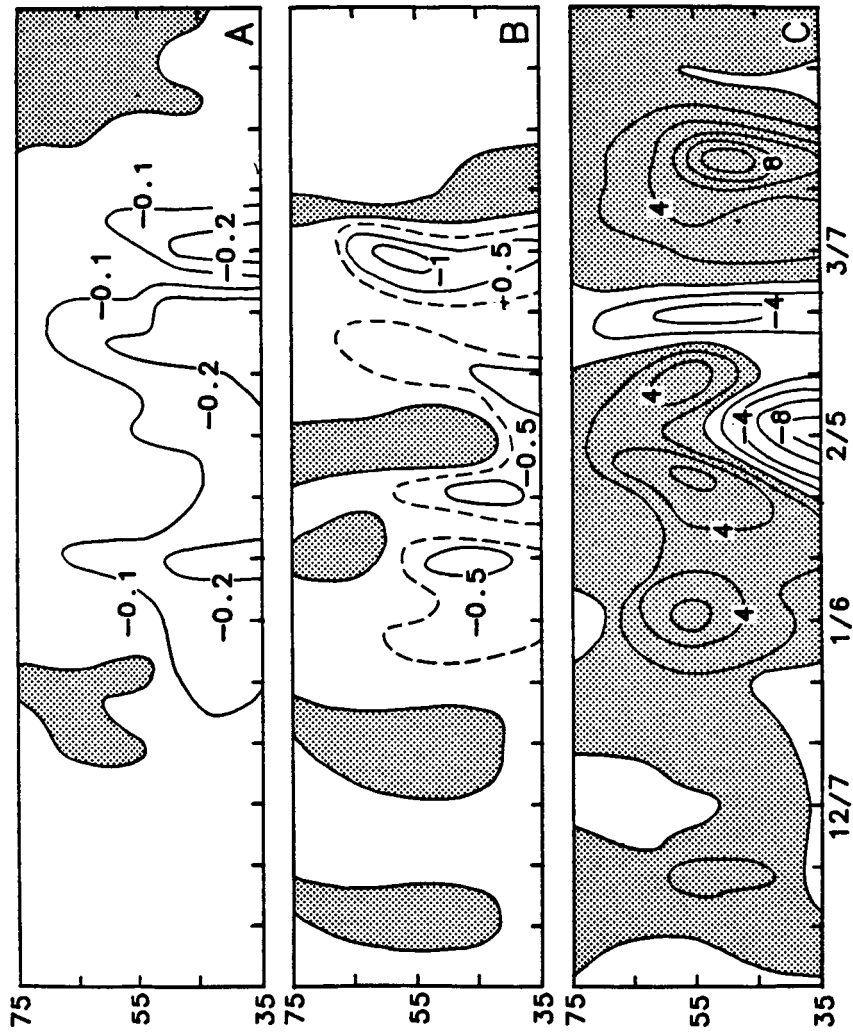
Figure 4. Horizontal component of wave 2 EP flux at (A) 2 mb, (B) 30 mb, and (C) 200 mb. Units as in Figure 2.
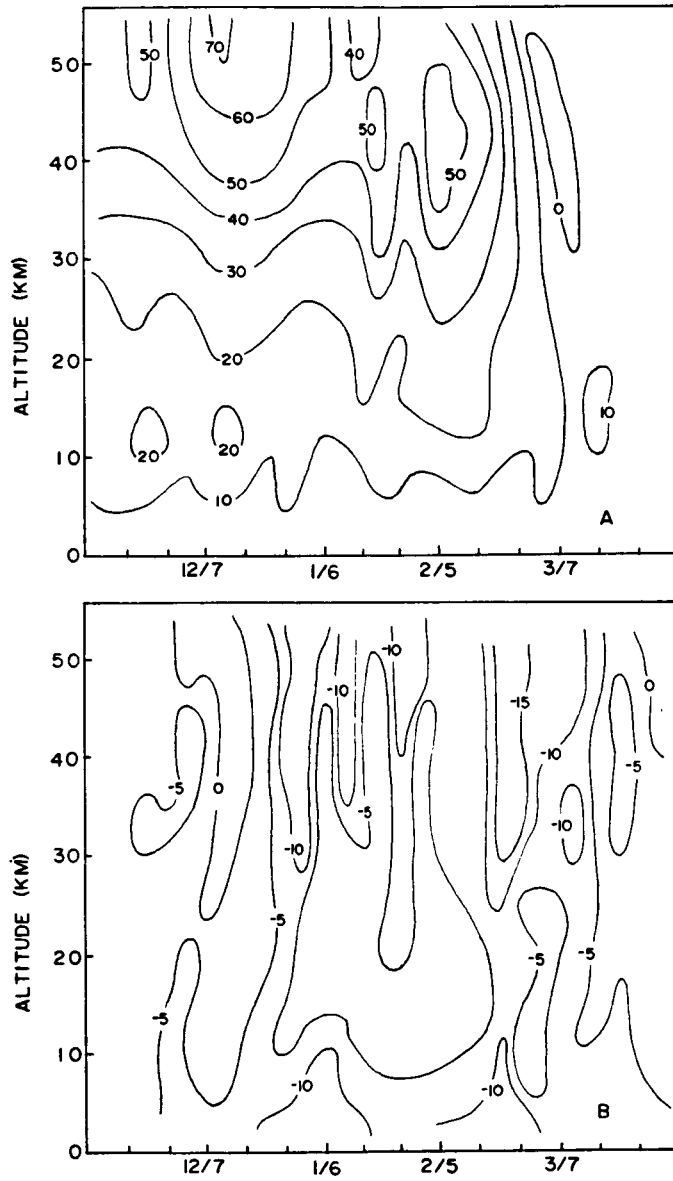
Figure 5. Time-altitude variation of (A) zonal
wind (m s^{-1}) and (B) EP-flux divergence
(m s^{-1}day^{-1}) for planetary waves 1-6
at 55°N.
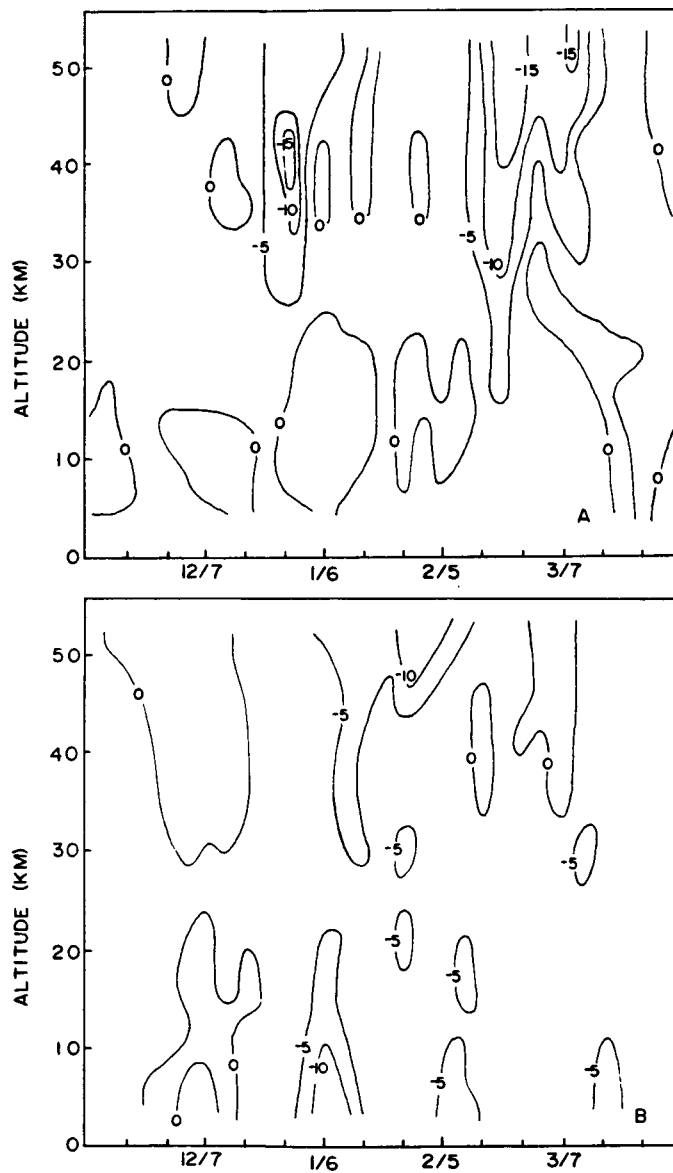
Figure 6. Time-altitude variation of EP flux
divergence (m s^{-1}day^{-1}) for (A)
wave 1 and (B) wave 2 at 55°N.
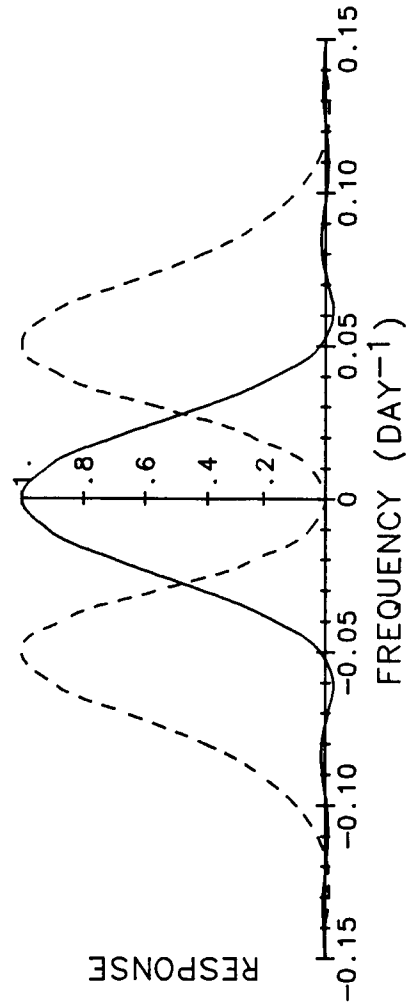
Figure 7. Frequency response of low-pass (solid line) and band-pass (dashed line) filters used to separate quasi-stationary and propagating waves. For the band-pass filter, the peak response is for a period of 20 days.
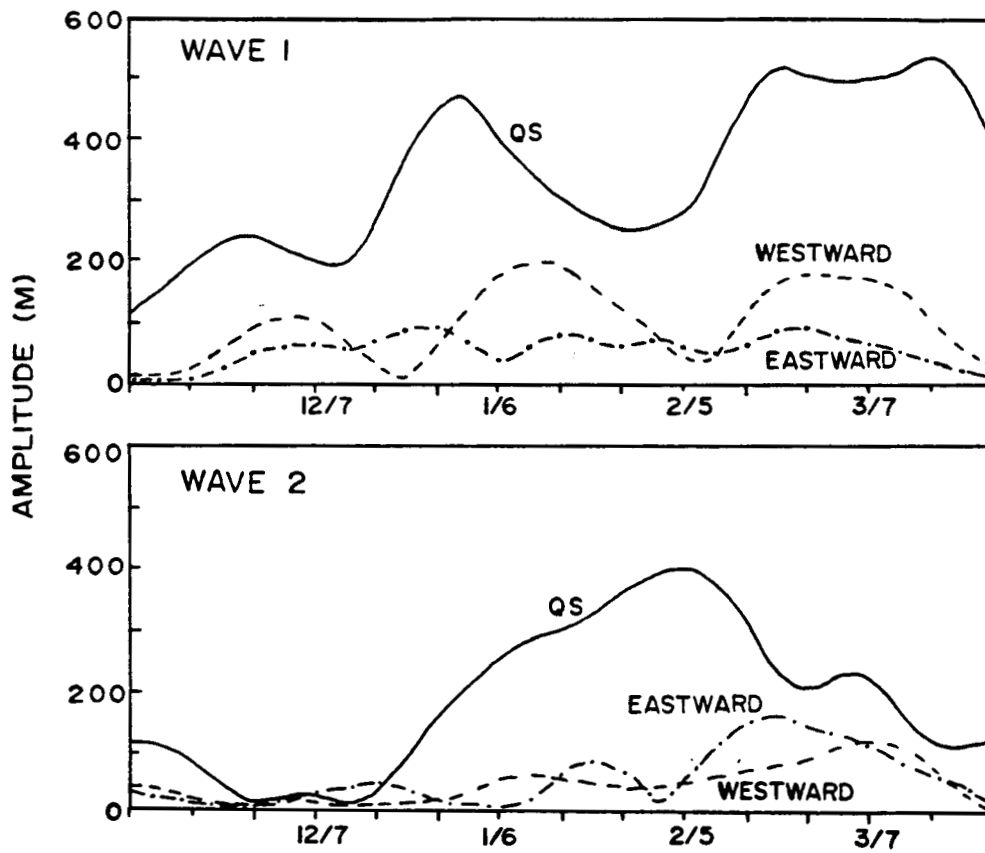
Figure 8. Amplitude (m) of quasi-stationary, westward propagating and eastward propagating waves at 30 mb, 55°N.
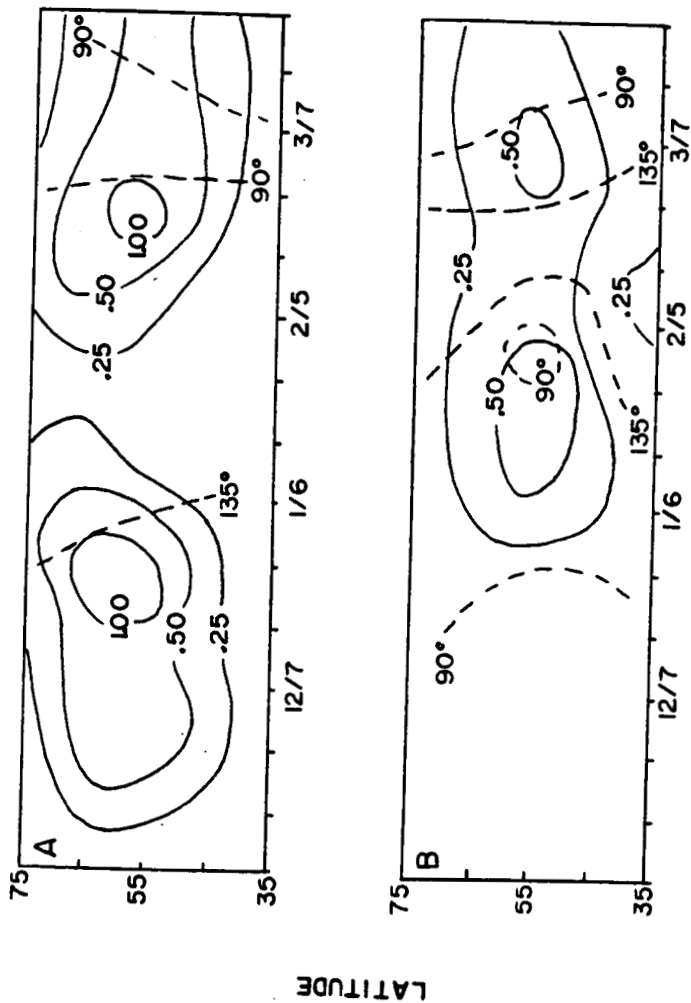
Figure 9. The magnitude of the quasi-stationary component of vector EP flux (10^{15} g m s^{-2}) at 30 mb for (A) wave 1 and (B) wave 2. The direction of the EP flux is indicated by dashed lines where 90^0 is upward and 180^0 is equatorward.
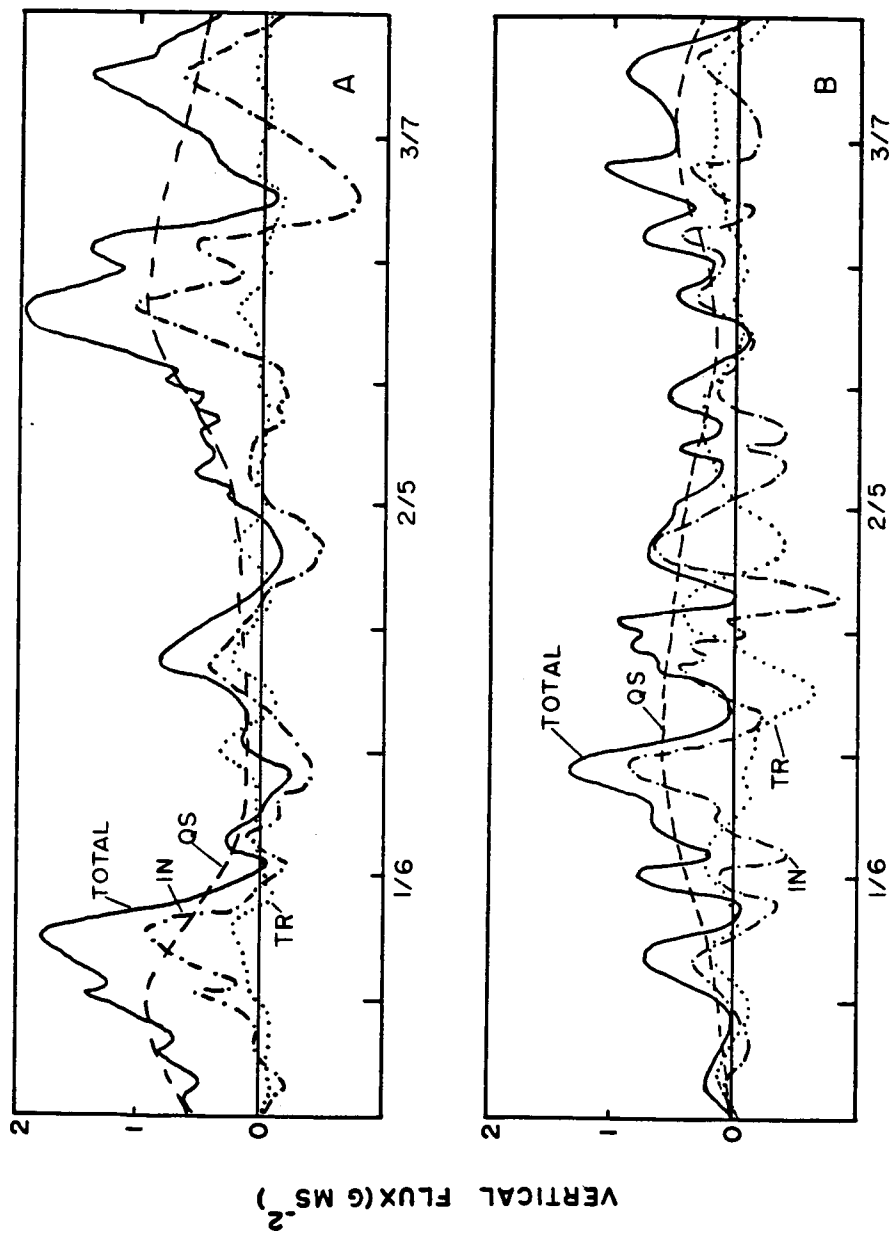
Figure 10. Daily components of 30 mb vertical EP flux for (A) wave 1 and (B) wave 2 at 55°N. The components are the total flux, the quasi-stationary flux $\overline{v'_q \theta'_q}$, the transient flux $\overline{v'_t \theta'_t}$, and the interactive flux $\overline{v'_q \theta'_t} + \overline{v'_t \theta'_q}$, and are denoted by TOTAL, QS, TR, and IN, respectively. Units are $(10^{15}$ g ms$^{-2})$.
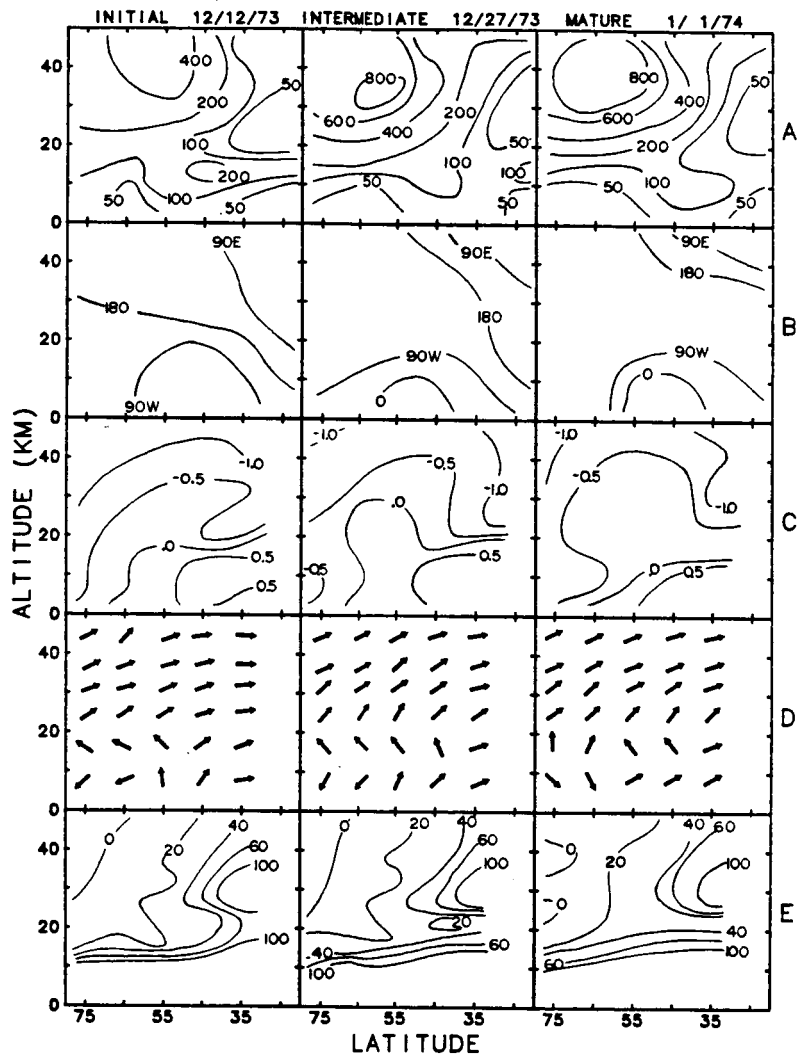
Figure 11. Evolutionary development of quasi-stationary wave 1 parameters for late December - early January event. The parameters are (A) amplitude (m) of geopotential height, (B) phase (westerly longitude of geopotential height maximum), (C) the $\log_{10}$ of the magnitude of the EP flux vector and (D) the direction of the EP fluxes and (E) the squared value of the index of refraction.
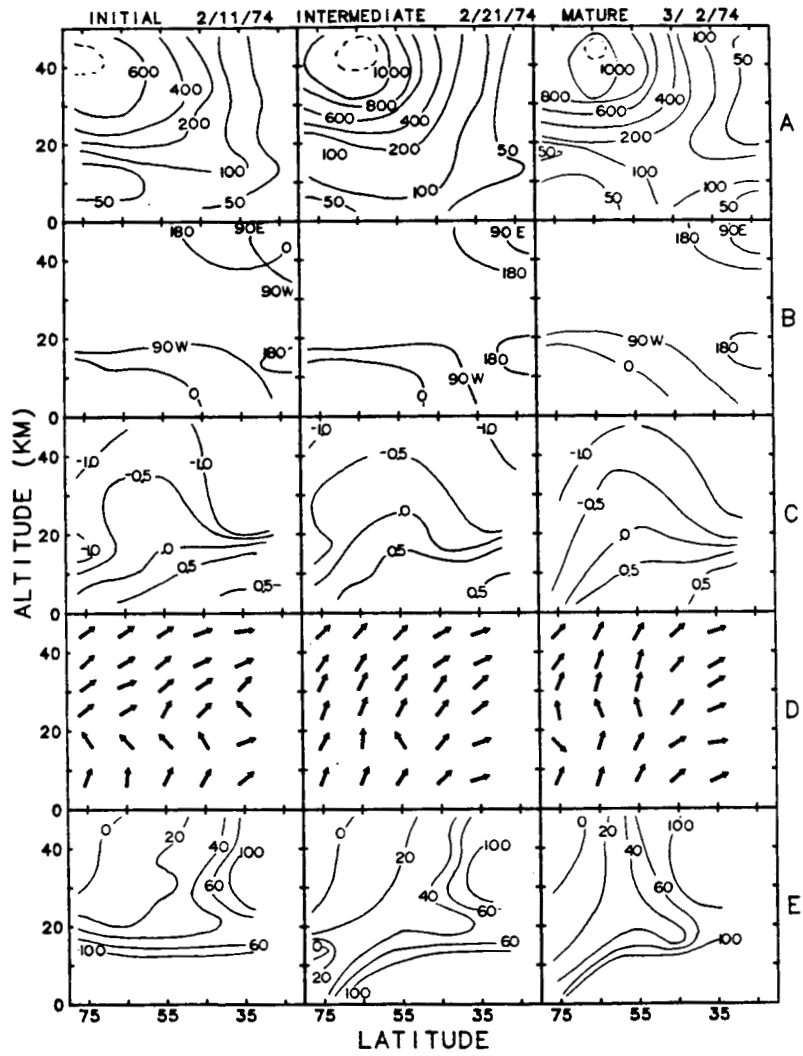
Figure 12. Evolutionary development of quasi-
stationary wave 1 parameters for late
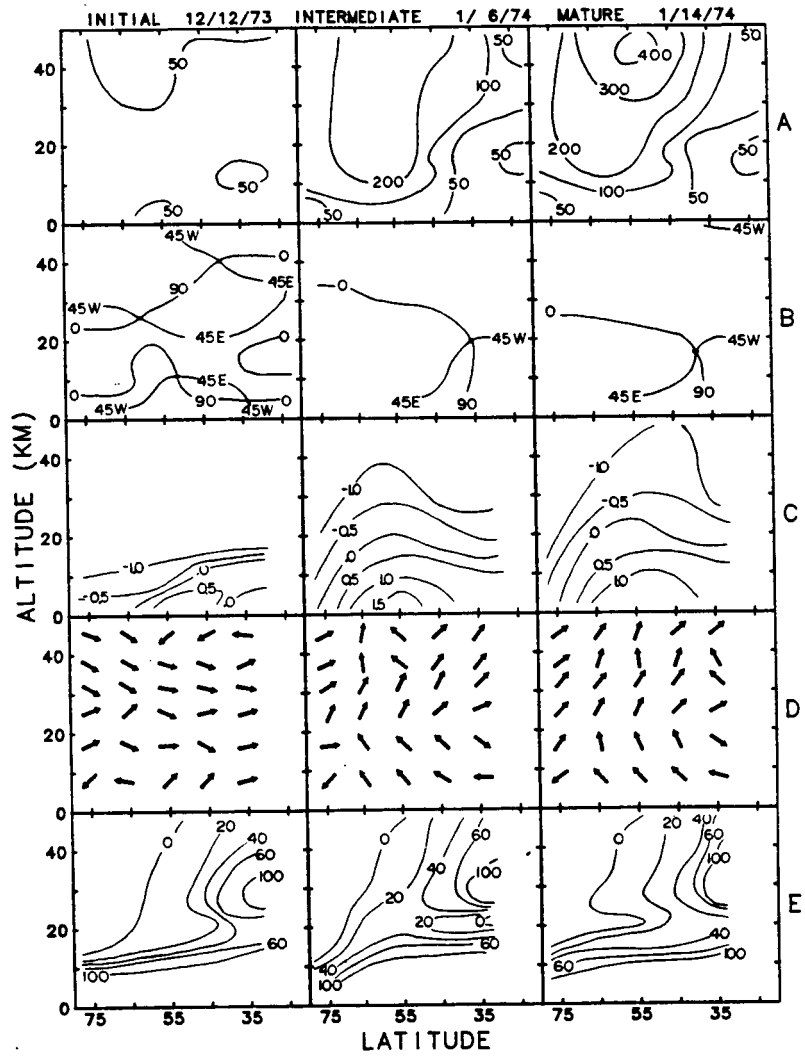February - early March event.

Figure 13. Evolutionary development of quasi-stationary wave 2 parameters for January event.
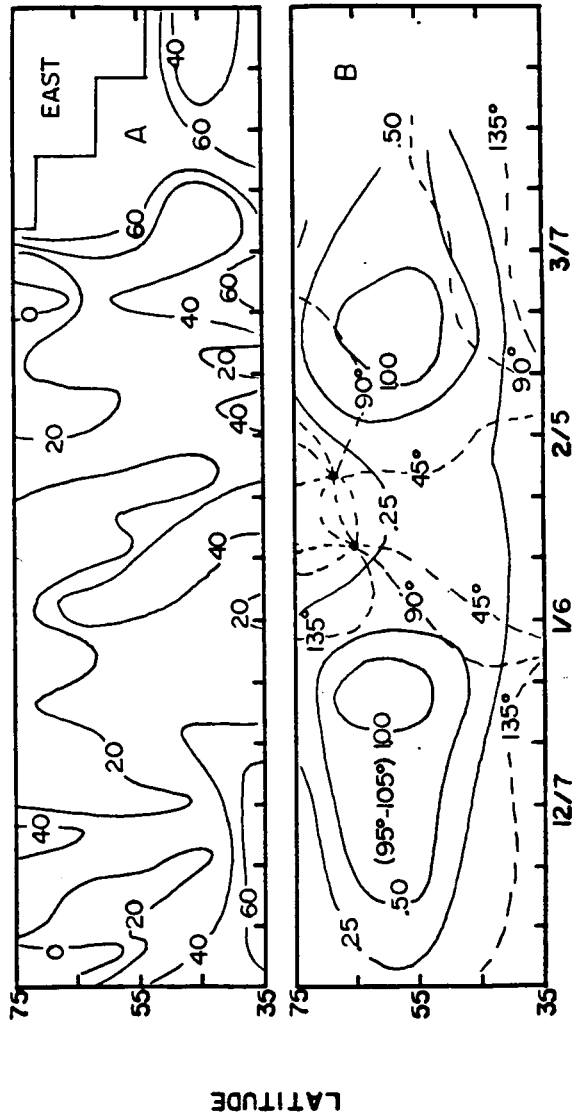
Figure 14. Time–latitude variation of (A) Q_1 and (B) wave 1 EP flux at 50 mb. In the lower diagram, the description of the EP flux is as described in Figure 9.
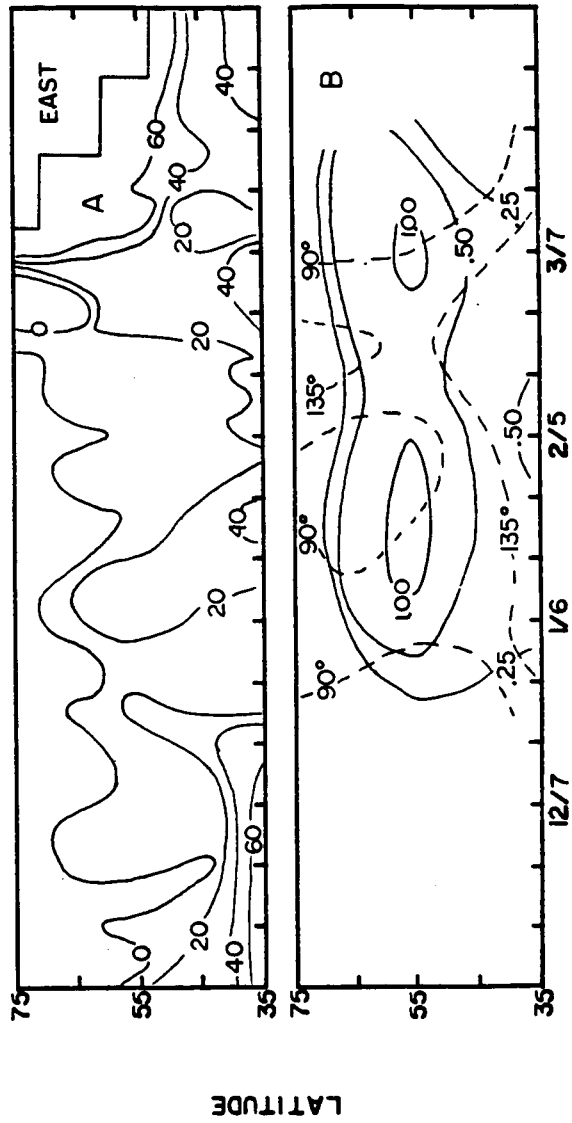
Figure 15. Time-latitude variation of (A) Q_2 and (B) wave 2 EP flux at 50 mb.

WINTER PLANETARY WAVE INFLUENCE ON ZONAL FLOW
NEAR THE STRATOPAUSE FROM SCR AND SAMS DATA

Denis G. Dartt

ABSTRACT

Eight years of upper stratospheric data from SCR and
SAMS instruments are used to examine the winter behavior of
zonal flow at 1 mb in relation to upward propagating
planetary wave activity from the lower stratosphere and
zonal temperature change in the vertical branch of the
residual circulation. Some fourteen wave events are
examined within the analysis period. Using a box framework
encompassing large volumes of the stratosphere, the wave
events are compared and a composite relationship between
primary variables is defined indicating the evolution of
the wave-zonal flow interaction process in the upper
stratosphere.

Zonal flow deceleration near 50 km occurs in response
to nonconservative wave forcing from below (20 km) and
zonal temperature increases in high latitudes near 40 km
which indirectly describe the residual circulation. Upward
propagating wave activity from below may be conservative in
nature and not always lead to zonal flow deceleration.
Also, upward propagating wave activity reaches a maximum in
the lower stratosphere following the primary zonal flow
deceleration at 1 mb. At this time, major planetary wave
dissipation occurs below 1 mb. The temperature tendency in
the upper polar stratosphere indicates the magnitude and
sense (ascending or descending branch) of the residual
circulation excited by the dissipating planetary waves. An
empirical method is examined for predicting zonal flow
change near the stratopause by monitoring upward
propagating wave activity from the lower stratosphere and
upper stratospheric temperature change in high latitudes.

1. Introduction

The following study investigates relationships during winter between zonal flow near the stratopause, upper stratospheric temperature and upward propagating planetary wave activity lower down in the stratosphere. The basic data are eight years of temperature and geopotential height derived from the SCR (Selected Chopper Radiometer) instruments on Nimbus 4 and 5 (1970-1975) and the SAMS (Stratospheric and Mesospheric Sounder) instrument on Nimbus 7 (1978-81) with NMC (National Meteorological Center) grids used 30 km and lower.

The primary variables examined are Eliassen-Palm (EP) wave fluxes which characterize wave propagation in the altitude-latitude plane, the convergence of the EP flux which describes the planetary wave forcing of the zonal mean wind, zonal wind and temperature, and the vertical and meridional components of the residual circulation. All such parameters are based on the transformed Eulerian-Mean formalism as described by Palmer (1981) and O'Neill and Youngblut (1982). From the long period of record, fourteen wave events occurred which resulted in stratospheric warming. The linear planetary wave dynamics of these events are summarized and compared, with regard to the behavior of zonal flow at 1 mb, in proximity to the stratopause. In terms of data, the current study supplements the investigation of Labitzke and Goretzki (1982) who described daily planetary wave behavior near 25 km (30 mb) for this same period.

The deceleration of stratospheric zonal flow by upward propagating planetary waves has been described by Palmer (1981), O'Neill and Youngblut (1982) and most recently by Dunkerton and Delisi (1985). In the upper stratosphere and lower mesosphere, the calculated wave forcing is larger than the observed flow change and is opposed by the Coriolis torque of the poleward directed residual circulation. The downward branch of the residual circulation in high latitudes causes adiabatic zonal stratospheric warming during wave events. Dunkerton, et al. (1981) consider the enhanced residual circulation during stratospheric warmings to be a natural linear response of the diabatic zonal flow to upward propagating and dissipating planetary waves as the atmosphere attempts to maintain thermal wind balance. In the current study, variations in zonal flow near the stratopause are analyzed as a function of lower stratospheric wave forcing and an indirect measure of the residual circulation given by zonal temperature change in high latitudes. An understanding of the behavior of these primary variables over a large data set will be useful for the eventual prediction of middle atmospheric zonal flow.

The following discussion first illustrates the general behavior of planetary wave variables for 1970-71, a winter with complete upper stratospheric data and two well-defined wave events. This includes wave propagation from the troposphere upwards into the stratosphere during stratospheric warmings (Section 3), the forced deceleration of the zonal flow by the

propagating waves (Section 4) and the role of the residual
circulation in restoring the zonal flow (Section 5). In Section
(6), a chronology of the primary dynamic parameters
characterizing the warming process is shown for eight winters.
Event comparisons (Section 7) and composite relationships
(Section 8) are then described. Finally, the usefulness of the
parameters are considered in a heuristic model for predicting the
behavior of 1-mb zonal flow.

2.   Data and Details of Computation

Middle atmospheric temperatures (at 10, 5, 2, 1, .4 mb)
from November, 1970 to April, 1975 were derived at Control Data
from SCR A and B radiances from NIMBUS 4 and 5. The technique
involved establishing regression relationships between SCR
channel radiances and rocketsonde temperatures from colocated
data. These regression coefficients were then used to convert
orbital radiances to temperature. The regression coefficients
were a function of latitude and were updated at 6-month intervals
throughout the period to account for possible sensor
degradation. Space-time interpolation of orbital temperatures to
1200Z was then performed at intervals of 20 degrees longitude and
10 degrees latitude. The details of this data reduction process
are described in Hovland and Wilcox 1979a, 1979b and Roe, et al.,
1982.

SAMS temperatures (at 3 and 1 mb) from NIMBUS 7 were used for the upper stratosphere for winters 1978-81. These limb sounder data are averages of two orbits per day with an effective observation time near 2100 local time (Barnett and Corney, 1984). After comparisons with NMC temperature in the altitude range 30-10 mb, SAMS temperatures were combined directly with the 1200Z temperature from NMC at 10 mb, to extend upward temperature profiles in the latitude range 25-67.5°N.

For both data sets, geopotential height was computed hydrostatically in the upper stratosphere using NMC 10-mb geopotential height as a base level. This was followed by computation at all levels of planetary waves (wave numbers 1-6) of geopotential height, temperature and geostrophic zonal and meridional wind. These data were further used to calculate daily momentum flux and sensible heat flux by each planetary wave using the formulation of Eliasen (1958). From these parameters, the Eliassen-Palm flux, $\vec{F}$, and the EP flux divergence, $\nabla \cdot \vec{F}$, were calculated (Palmer, 1981):

$$F_\phi = -\rho_s \exp(-z/H) \gamma_0 \cos \phi \, \overline{u'v'} \tag{1}$$

$$F_z = -\rho_s \exp(-z/H) \gamma_0 f \cos \phi \, \overline{v'\theta'}/\theta_z \tag{2}$$

$$\nabla \cdot \vec{F} = (1/\gamma_0 \cos \phi) \frac{\partial}{\partial \phi} (\cos \phi \, F_\phi) + \frac{\partial}{\partial z} (F_z) \tag{3}$$

-39-

where $\rho_s = 1000$ gm^{-3}, $z = -H\ln(P/1000$ mb$)$, $H = 6400$ m, γ_o is the earth radius, ϕ is latitude, p is pressure (mb), and $f = 2\Omega\sin\phi$ is the Coriolis parameter. The planetary wave geostrophic zonal wind, u', and meridional wind, v', were used along with zonal potential temperature, $\bar\theta$, and temperature lapse, $\bar\theta_z$, to calculate the zonal momentum flux, $\overline{u'v'}$, and normalized sensible heat flux, $\overline{v'\theta'}/\bar\theta_z$.

The geostrophic momentum flux was further adjusted for zonal flow variations using the technique of Robinson (1986) which improves the interpretation of the EP flux divergence.

The Cartesian representation of EP flux vectors is utilized as described by Palmer (1981). The EP flux components (F_ϕ, F_z) are multiplied by $2\pi\gamma_o\cos\phi$; further, the horizontal component is multiplied by a constant (.0132) which scales vectors for plotting in a plane where 10-km altitude is equivalent in distance to 10° of latitude (Fig. 1).

The basic diagnostic equations of transformed Eulerian-mean dynamics linking planetary waves and time changes in zonal flow in the altitude-latitude plane are:

$$\frac{\partial\bar{u}}{\partial t} = f\bar{v}^* + (1/\rho_s\gamma_o\cos\phi)\exp(z/H)\vec\nabla\cdot F \qquad (4)$$

$$\frac{\partial\bar\theta}{\partial t} = -\bar\theta_z\bar{w}^* + J \qquad (5)$$

where $\bar{v}^*$ and $\bar{w}^*$ are respectively the meridional and vertical components of the residual circulation which occurs as a result of nonconservative wave action; $\bar{J}$ is the diabatic cooling rate. Values of $\bar{J}$ for the upper stratosphere used in the evaluation of (5) were from Crane et al. (1980). Equation (5) is a simplified form of the complete thermodynamic equation in the transformed Eulerian mean formalism and has been used by Palmer (1981) and O'Neill and Youngblut (1982).

In the above computations, horizontal derivatives were estimated over 20° latitude intervals with the exception of 65°N where zonal winds from SAMS data were determined by differencing geopotential height between 67.5°N and 55°N. Vertical derivatives were estimated by differencing alternating pressure levels, a distance of approximately 10 km. Five-day averaging was used to smooth all parameters.

3.   **Wave Propagation into the Upper Stratosphere**

In a companion paper (Dartt and Venne, 1986), numerous EP flux diagrams are shown, illustrating the detailed propagation of wave activity from the troposphere into the stratosphere and mesosphere during intervals of enhanced winter wave activity associated with sudden warmings. A general characteristic of these events is that baroclinic wave growth into the stratosphere occurs in the latitude band 55-65°N. The waves are then progressively refracted equatorward with increasing altitude into the stratosphere and lower mesosphere.

Figures 1 and 2 illustrate the respective propagation of planetary waves 1 and 2 into the stratosphere in the early stage of the major mid-winter warming in 1970-71. Beginning on December 22, wave 1 EP unit flux vectors begin to develop a strong vertical component in middle latitudes between 10-20 km before turning equatorward at higher levels. From December 22 to January 6, wave 1 EP fluxes progressively show continued upward and also poleward wave propagation. During this interval, the magnitude of EP flux, indicating propagating wave activity, increases nearly an order of magnitude above 30 km. Wave 2 upward propagation on December 22 in Figure 2 is initially similar to wave 1. However, with increasing time, wave 2 upward propagation is diminished both at high latitudes and stratospheric altitudes. On January 1 and 6, downward EP flux occurs for wave 2 poleward of 55°N above 30 km, and the magnitude of EP flux for wave 2 is about a factor of 10 less than for wave 1.

4.   Wave-Induced Zonal Flow Changes

The divergence of EP flux, $\nabla \cdot \vec{F}$, is a direct measure of the planetary wave induced forcing of the zonal flow in (4). From (4), non-conservative waves will decelerate the flow through convergence of EP flux, a dissipative wave process.

Alternatively, the zonal flow will accelerate through divergence of EP flux, a wave generation process. Conservative or freely propagating waves will have no effect on the zonal flow.

Figure 3 shows the effects of nonconservative wave action on the zonal flow of the upper stratosphere. The upward propagating wave activity from below induces deceleration of the winds near 50 km beginning about Dec. 17. The wave forcing intensifies in early January and extends downward to near 30 km. A second period of wave forced deceleration near March 7, also leads to a deceleration of zonal flow. Figure 4 indicates the contribution to $\nabla \cdot \vec{F}$ by planetary waves 1 and 2, the two prominent stratospheric components. Initially, near December 17, both components act to decelerate the zonal flow above 40 km. However, in early January, wave 1 forced deceleration becomes very strong, but is opposed by wave 2 which is accelerating the zonal flow. Wave 2 divergence at this time coincides with the appearance of downward EP flux for this component in Fig. 2. In the middle of January near 30 km, the opposite occurs. Wave 2 is decelerating the zonal flow while wave 1 is indicating weak acceleration. This pattern of alternating wave 1 and 2 wave forcing of opposite sign is indicative of non-linear wave-wave interactions (Palmer and Hsu, 1983).

While the simultaneous occurrence of zonal flow deceleration and EP flux convergence indicates a cause and effect relation, the magnitude of both changes are quite different. For example, near 50 km in early January, wave forced deceleration is of the order of 30 $ms^{-1}day^{-1}$; the actual wind deceleration is of the order of 6 $ms^{-1}day^{-1}$. Figure 5 compares wind tendency ($\Delta u/\Delta t$) with wave forcing at selective stratospheric pressure levels. At 30 and 50 mb, $\nabla \cdot \vec{F}$ and $\Delta u/\Delta t$ are near the same magnitude, but not particularly well correlated. Increasing with altitude, the time variation of $\Delta u/\Delta t$ and $\nabla \cdot \vec{F}$ become better correlated, however, $\nabla \cdot \vec{F}$ forcing is noticeably larger than the observed flow deceleration. Thus, the effects of planetary waves on the zonal flow of the upper stratosphere must be damped by the residual circulation term in (4).

5.   Residual Circulation

The role of the meridional component of the residual circulation, $\overline{v}^*$, is to compensate for excess wave forcing through a Coriolis torque in (4). Figure 6a indicates this component in the upper stratosphere at 55°N, determined as a residual between observed wind change and $\nabla \cdot \vec{F}$ over a 5-day interval. A poleward component is enhanced during late December near 1 mb in response to the upward propagating waves. The variability of $\overline{w}^*$ at 65°N over the winter is indicated in Fig. 6b. In early

January, maximum downward motion is indicated near 40 km corresponding to the strong poleward component near 50 km. Near January 16, a descent of the poleward component to 35 km occurs. At this time, ascending motion is indicated at higher altitudes, descending motion at lower altitudes. In the ascending branch adiabatic cooling occurs; in the descending branch adiabatic warming occurs.

Observationally, $\bar{w}^*$ is only a function of the zonal temperature tendency near the pole and climatological cooling rates; $\bar{v}^*$ on the other hand, is determined almost independently by examining highly derived properties of planetary waves ($\nabla \cdot \vec{F}$) and zonal flow. The close relationship of these two variables in the meridional plane is quite remarkable, demonstrating the link between nonconservative wave action and changes in the zonal state.

6.   Chronology of Stratospheric Dynamics

A condensed description of planetary wave-zonal flow interaction from available upper stratospheric data in the 1970-81 period is given in Figs. 7-14. Variations in zonal flow at 1 mb are examined as a function of: (1) the amplitude of vertical EP flux at 50 mb, (2) a large volume measurement of EP flux convergence, (3) zonal temperature change at 2 mb (SCR) or 3 mb (SAMS) at 65°N and (4) the squared values of the index of refraction (Q_i) for planetary waves 1 and 2 at 30 mb which are

useful as indicators of planetary wave dissipation in the lower stratosphere (Smith, 1983). A simple box model is used to describe the primary aspects of wave-zonal flow interaction. Each box encompasses a 20° latitude belt and has a lower boundary at 50 mb (20 km) and an upper boundary near 1 mb (48 km). Planetary wave forcing is monitored at the lower boundary in terms of the 5-day average of the vertical EP flux integrated over the latitude band. The 50-mb level was chosen as a lower boundary as it is an altitude where the primary component of wave propagation is vertical and thus defines the primary waves penetrating the upper stratosphere. Also the vertical distance between 50 and 1 mb would typically require a few days of wave propagation based on the vertical group velocity (Karoly and Hoskins, 1982). Thus, the box model is also useful for a cursory examination of prediction of middle atmosphere zonal flow in terms of lower stratospheric wave forcing. At the top of the box the vertical component of EP flux is very small compared to the flux at the lower boundary and for the current analysis is assumed to be zero. Along the north and south boundaries the density weighted horizontal component of EP flux is numerically integrated with height from 20 to 48 km and the horizontal difference is determined. This value is normalized by the ratio of vertical to horizontal box dimensions and is then added to the vertical component at the lower boundary to obtain a measure of

$\nabla \cdot \vec{F}$ over a deep layer and wide latitude band. The term, net

flux, is used to describe this measure of nonconservative wave

flux within the volume. With the use of models for adjacent

latitude bands, the latitude transfer of wave activity (i.e.

polar focusing) can be investigated. In Figs. 7-14, the 50-mb EP

flux is indicated for wave 1 and also integrated for all waves,

1-6. In the stratosphere, the difference between the flux for

wave 1 and that for the integrated flux is primarily the result

of wave 2. Also, in these diagrams, the primary warming and

cooling periods are indicated. These are numbered

chronologically for later reference in Table 1. A warming period

is characterized by an increase in upper stratospheric

temperature (65°N), a decrease in zonal wind and an increase in

wave forcing and net flux. A cooling period shows opposite

characteristics.

1970-71

As discussed earlier and shown for the box model at 55°N

in Fig. 7, this year is characterized by a major midwinter event

during December and early January, and a minor event in March.

The zonal flow deceleration at 1 mb is well correlated with the

increases in wave activity and increases in zonal temperatures

for both events. During December, much of the upward propagating

wave activity appears to be conservative, as the vertical wave flux is larger than the net flux. At the beginning of the January cooling period, upward propagating EP flux is still large, but diminishes rapidly. Planetary wave zonal flow interaction is now more confined to the lower stratosphere as indicated by zonal flow deceleration at 30 mb and the large values of Q_i indicating dissipation near this altitude. Figure 8 shows wave flux parameters and 1-mb zonal flow for overlapping 20° latitude bands. Even though the 50-mb vertical EP flux is larger from 45-65°N than neighboring latitude bands, the net flux is similar for all three latitude bands. The zonal flow at each latitude undergoes nearly the same deceleration.

1971-1972

Figure 9 indicates that the wave 1 flux is weak compared to the integrated flux, and net flux in the 45-65°N band is generally less than the previous year. Events during late December and in February produce decelerations of 1-mb zonal flow. As in the previous winters, warmings are characterized by an increase in wave activity, coolings are characterized by a rapid decrease in upward propagating wave activity.

1973-74

Figure 10 indicates two relatively minor wave events in terms of zonal flow deceleration, one in late December, the second in late February. Wave 1 is prominent for both events. The temperature at 2 mb increases gradually for both events.

1974-75

Figure 11 indicates that near the end of December, a large wave event occurred as indicated by zonal wind and temperature change from December 17 to January 1. However, the details of the event are obscured by a data gap. In January and early February, there is very little net wave flux within the 45-65°N latitude band and the upper stratospheric flow accelerates sharply, accompanied by rapid polar cooling. Near the end of February, a moderate wave event results in a marked deceleration of 1-mb flow and zonal temperature increase.

1979-80

Figure 12 indicates the EP flux has a strong wave 1 component and vascillates with about a 20-day period throughout much of the winter. This is primarily the result of the interference of quasi-stationary and zonally propagating wave 1

component (Dartt and Venne, 1986). The zonal flow shows similar vascillating behavior with intermittent deceleration from late December onward. The vascillations are not so pronounced in polar temperature which indicates two warming intervals. Thus, the residual circulation may not respond as rapidly to variations in planetary wave forcing as the zonal flow.

1980-81

A long period of large amplitude vertical wave flux occurs in January resulting in a large decrease in zonal wind and increase in temperature over a 30-day period, Fig. 13. As in 1970-71, in early winter, the wave flux appears to act conservatively and is not utilized within the zonal band. In March, an increase in lower stratospheric wave activity produces only a minor change in zonal wind and temperature in the upper stratosphere. At 30 mb large values of Q_i and zonal flow deceleration indicate that much of the upward propagating wave activity is dissipated in the lower stratosphere.

1972-73 and 1978-79

These two winters have only partial data and are shown jointly in Fig. 14. In 1972-73, only the second stage of the major midwinter wave 1 warming is indicated. However, the earlier stage with missing data indicates substantial upper stratospheric zonal flow deceleration and temperature increase as compared to the latter event.

In 1978-79, large wave 1 fluxes produce moderate zonal flow deceleration from late December through early February. Large wave 2 fluxes in middle February do not appear to effect zonal flow at 1 mb or to produce an enhanced residual circulation as indicated by an increase in temperature. Again, large values of Q_1 and zonal wind deceleration at 30 mb suggest that much of the upward propagating wave activity is dissipated in the lower stratosphere.

7.   Comparative Properties

Table 1 compares the time integrated properties of 1-mb zonal flow, upper stratospheric temperature and wave forcing for all events in Figs. 7-14. The events are stratified according to duration. Events of long duration produce extensive zonal flow deceleration from 45-65°N and are based on sustained periods of vertical planetary wave flux. Events of intermediate and short duration generally have less effect on zonal flow and have less wave flux. For all wave events, vertical wave flux at 50 mb is greater from 45-65°N than in the 35-55°N and 55-75°N bands. However, the net flux which measures the nonconservative wave forcing within the band is only slightly stronger from 45-65°N than neighboring bands. From 35-55°N, the net flux is almost equivalent to the lower boundary flux, indicating that most upward propagating wave activity is used to decelerate zonal flow. For other latitudes bands there is a net loss of wave activity through the latitude boundaries.

Zonal warming during wave events is greater to the north than to the south. This indirectly indicates the increase in strength of the residual circulation with latitude which opposes the wave forced deceleration of zonal flow. The Coriolis torque ($f\bar{v}^*$) of the residual circulation (4) will be stronger in higher than lower latitudes both because of f and $\bar{v}^*$. Thus, wave forcing in low latitudes need not be as large as in high latitudes to equivalently decelerate the zonal flow. Table 1 indicates that zonal flow deceleration at 45°N is typically as large as at 55°N or 65°N, even though the net flux is somewhat less. The relative strength of the upper stratospheric residual circulation may be weaker in late than in middle winter. Late winter events (13, 4 and 10) indicate small zonal temperature increases compared to earlier events of similar duration.

For all eight years, Figs. 7-14, 1-mb flow was decelerated in early January in response to upward propagating waves. In some years, the mesospheric jet is again restored in late winter (1971, 1972, 1975). In these years, there is an extended period in late January and February when wave 1 vertical EP flux diminishes to near zero at 50 mb. Initially, adiabatic cooling by the ascending branch of the residual circulation helps to restore the jet to its earlier amplitude. When wave activity vanishes, the primary cooling will be by radiative processes.

8.   Composite Relationships

Figure 15 indicates the time-latitude structure of 5-day 1-mb zonal flow change, upper stratosphere temperature change, and net wave flux at 50 mb for composite 5-day average parameters over all 8 years. Six characteristic steps of upper stratospheric temperature and zonal flow change were defined and then identified from serial data. Composites were calculated at each step and also, 5 days prior to and 5 days after. These time sequences are analyzed in Fig. 15 as a function of the average time separation of the characteristic steps. Individual events may be either compressed or extended in time with regard to the average event. However, they typically will exhibit each individual step.

The characteristic steps are defined in terms of the 5-day tendency in 1-mb zonal flow at 55°N and 5-day tendency of upper stratospheric temperature (2-mb SCR or 3-mb SAMS) at 65°N. These tendencies are forward time differences relative to values of net wave flux. Step (1) corresponds to the time of early winter maximum westerly flow acceleration at 1 mb occurring in late November or early December, i.e. Fig. 3. Fig. 15 shows that the mesospheric jet is intensifying with moderate cooling occurring near the pole. Upward propagating wave activity is weak at 50 mb as is the net flux from 1-50 mb. The upper

-53-

stratospheric cooling rate at 65°N is considerably less than the calculated radiative rate of nearly 15°K (5 days)$^{-1}$, Crane, et al. (1980). This suggests that some adiabatic warming of polar regions is already occurring, perhaps due to dissipating planetary waves or gravity waves. Step (2) corresponds to the time of initial zonal temperature rise at 65°N. Moderate zonal flow deceleration begins and is largest at 45°N. Net wave flux increases especially in middle latitudes. Warmings may exhibit a pulse-like nature as a result of the interference of a strong quasi-stationary wave component and weaker amplitude zonally propagating waves (Dartt, 1986). Step (3) indicates the time of maximum upper stratospheric temperature increase associated with the first such pulse. Temperature increases of 4°K (5 days)$^{-1}$ in polar regions are associated with flow deceleration of 5 ms^{-1}(5 days)$^{-1}$ in middle latitudes. The net wave flux has increased slightly in high latitudes (65°N) from Step (2). Step (4) corresponds to the time of maximum upper stratospheric heating which may follow Step (3) or in some warmings follows directly from Step (2). Substantial flow deceleration occurs from 45-65°N with the maximum occurring at 55°N. Prior to Step (4) net wave flux increases over the entire latitude range. On a composite basis, the maximum stratospheric temperature increase appears to precede the maximum zonal flow decrease by about 1 day. Step (5) corresponds to the time of maximum upper stratospheric temperature decrease at 65°N following the warmings. Winds undergo very sudden

acceleration in middle latitudes. At this step, upward wave propagation from below is maximum as is the net flux. However, practically all of this wave activity is dissipated lower down in the stratosphere and does not reach 1 mb. The major stratospheric cooling occurs in the ascending branch of the residual circulation above the altitude of major wave-zonal flow deceleration. This cooling is much stronger than that occurring earlier in winter (Step 1).

The second part of Fig. 15 shows a composite single pulse warming occurring after a mid-winter cooling. Step (6) is the period of cooling that usually follows late winter warming events. There were no significant monthly differences in the relationships between flow deceleration, temperature increase and net flux during intervals of stratospheric heating. Thus, Steps (2) and (4) are the same for both the first and second composite events.

Figure 16 shows 5-day zonal flow tendency at 1 mb expressed as a function of high latitude (65°N) upper stratospheric temperature increase and net wave flux for the various latitude bands. Also indicated is the sign of the vertical component of the residual circulation at 65°N (2-mb SCR or 3-mb SAMS). These diagrams are composites based on all available 5-day winter data over the entire 8-year period. In regions of dense data the rms variability of individual values of

zonal wind tendency about the contour (mean) value is in the range from 3 to 6 ms^{-1}(5 days)$^{-1}$. This rms variability is smallest at 55°N and largest at 65°N.

In the right portion of these diagrams, zonal wind deceleration is proportional to increasing stratospheric temperature and to increasing net wave flux. At 65°N, net wave flux is the primary variable, while at 45°N, stratospheric temperature increase is most important as indicated by the change in slope of the contours. Changes in zonal flow are jointly subject to the constraints of equation (4) which specifies dynamics in terms of wave activity at a given latitude and to the thermal wind relationship which specifies zonal wind (shear) in terms of large scale latitudinal gradients of temperature. At 65°N, the net flux is inherently most important as the temperature tendency is defined at this latitude. At 45°N, wind changes appear most dependent on changes in meridional temperature gradient brought about by temperature increases in high latitudes. At 55°N, the flow deceleration is intermediate between that observed at 45°N and 65°N. For net flux values in the range 1-2 x 10^{15} g ms^{-2}, there is a tendency for the wind deceleration to diminish with temperature increases of 4-8°K (5 days)$^{-1}$. This is consistent with the idea of the residual circulation opposing the wave forcing. For larger temperature increases, this effect is suppressed by the large

scale thermal wind balance. Dunkerton, et al. (1981) indicate that the response of the zonal flow to wave forcing is substantially weaker, narrower (in latitude) and taller (in altitude) than the observed wave forcing. Thus, the residual circulation should be intense on the northern flank of wave forcing, contributing to the pattern seen in Fig. 16b.

In the left hand portion of Fig. 16, zonal flow acceleration is proportional to upper stratospheric cooling at all latitudes. Most of the extreme values of zonal flow acceleration occur when the vertical component of the residual circulation at 65°N (2 or 3 mb) is upward indicating adiabatic cooling. As discussed previously, this is a time of lower stratospheric wave dissipation.

9. Possible Forecasts of 1-mb Zonal Flow

For future applications of hypersonic flight planning and perhaps space shuttle operations, it would be useful to be able to predict in advance the behavior of the mesospheric jet. When fully developed, this zonal belt of west winds attains strengths in the middle atmosphere in excess of 100 ms^{-1} and would influence transcontinental flight duration and fuel requirements. Further, the rapid deceleration of zonal flow and dissipation of planetary waves during sudden warmings may lead to regional turbulence affecting spacecraft re-entry.

The previous comparisons of 1-mb zonal flow, upper stratosphere temperature and lower stratospheric vertical wave flux suggest that monitoring the latter two variables should provide information on subsequent winter mesospheric flow change. Figure 17 is a diagram, much like Fig. 16b, indicating the composite 5-day predictive 1-mb zonal flow change based on current information on vertical wave flux at the lower stratospheric boundary (50 mb) and the temperature tendency over the past 5 days. All available 5-day averages over the eight-year period are included in the composite. Estimated rms variability of zonal wind change ranges from near ± 5 ms^{-1} (5 days)$^{-1}$ during times of rapid cooling and low amplitude wave flux to more than ± 10 ms^{-1} (5 days)$^{-1}$ during times at high amplitude wave flux and rapid heating. In this latter case, the past 5-day temperature tendency is unable to predict the rapid wind acceleration that follows the sudden warming. While the rms difference is large, there is some overall skill indicated in the 5-day prediction of zonal flow.

Based on the above evidence, it would appear that further refinements of empirical models such as those above, would prove useful for predicting zonal flow change in the middle atmosphere. Such optimization should include investigation of averaging and tendency intervals, choice of the lower boundary, the significance of wave fluxes from neighboring latitude bands and methods of parameterizing dissipation in the lower

stratosphere. In particular, if the upper stratosphere temperature tendency were evaluated on a shorter term basis than 5 days, the rms variability of Fig. 17 would be reduced. Further, single point wave flux diagnostics, as recently described by Plumb (1985), could also be explored for predicting large scale longitudinal variations of the stratospheric and mesospheric flow.

10.   Conclusions

Eight years of planetary wave data in the upper stratosphere have been analyzed to determine the effect of upward propagating waves on the zonal flow at 1 mb. Midwinter deceleration of the middle atmosphere jet commonly occurs in response to upward propagating planetary waves 1 and 2. The jet which is strongest in late December undergoes a rapid deceleration in January. Westerly zonal flow at 1 mb may diminish by amounts approaching 80 ms^{-1} and easterlies may occur in high latitudes. An indirect measure of the large scale residual circulation opposing the wave forcing is the zonal temperature tendency at 2 or 3 mb in high latitudes. This zonal temperature tendency is also a useful predictor of zonal flow change at higher altitudes.

The primary vertical planetary wave flux from the lower
stratosphere occurs from 45-65°N, but the nonconservative wave
flux extends outward to neighboring latitudes and decelerates
zonal flow. The Robinson (1986) correction of geostrophic
momentum fluxes in the middle atmosphere has the effect of
spreading the dissipation of planetary waves over a wide latitude
band. If not applied, much of the middle atmosphere planetary
wave dissipation shifts equatorward. In most years, the
deceleration of 1-mb zonal flow begins first in lower latitudes,
35-45°N and may overall be as large as in more northern
latitudes. The mesospheric jet nearly regains its early season
strength during February in three of the eight winters studied.
This occurs when planetary wave activity is minimal in the lower
stratosphere for extended periods.

While upward propagating wave activity from the lower
stratosphere appears to be directly responsible for 1-mb zonal
flow deceleration, it, by itself, is not necessarily a good
predictor. Significant conservative wave activity may precede
the zonal flow deceleration at higher levels as wave activity
propagates equatorward. Also, at the final stage of the warming,
when wave activity is strongest, planetary waves are dissipated
lower down in the stratosphere. At this time, zonal flow
acceleration occurs at 1 mb in response to adiabatic cooling in
the upward branch of the residual circulation and also because of
radiative cooling.

A heuristic box model indicates that much of the zonal wind variability at 1 mb can be explained in terms of variations of lower boundary wave flux, the net nonconservative wave flux within a relatively large volume, upper stratospheric temperature tendency in polar regions and a measure of lower stratospheric planetary wave dissipation. Experiments with some of these parameters suggest a capability of predicting middle atmosphere zonal flow on a short-term basis.

References

Barnett, J. J. and M. Corney, 1984: Temperature comparisons between NIMBUS 7 SAMS, rocket/radiosondes and the NOAA 6 SSU. _J. Geophys. Res._, 89, 5294-5302.

Crane, A. J., J. D. Haigh, J. A. Pyle and C. F. Rogers, 1980: Mean meridional circulations of the stratosphere and mesosphere, _Pageoph_, 118, 307-328.

Dartt, D. and D. Venne, 1986: Planetary wave propagation and zonal flow interaction, 0-80 km, observed from NMC-SAMS data. (Submitted for publication)

Dartt, D., 1986: The interaction of quasi-stationary and zonally propagating planetary waves during winter, 1973-1974. (Submitted for publication)

Dunkerton, T. J., C.-P. F. Hsu and M. E. McIntyre, 1981: Some Eulerian and Lagrangian diagnostics for a model stratospheric warming, _J. Atmos. Sci._, 38, 819-843.

Dunkerton, T. J. and D. P. Delisi, 1985: The subtropical mesospheric jet observed by the Nimbus 7 Limb monitor of the stratosphere, _J. Geophys. Res._, 90, 10681-10692.

Eliasen, E., 1958: A study of the long atmospheric waves on the basis of zonal harmonic analysis. _Tellus_, 10, 206-215.

Hovland, D. And R. Wilcox, 1979a: Statistical retrieval of temperatures from SCR-B at 10 to 0.4 mb. Interim Report No. 1, Contract F49620-78-C0036 for Air Force Office of Scientific Research, by Control Data Corporation, Minneapolis, MN, 24 pp.

Hovland, D. and R. Wilcox, 1979b: Statistical retrieval of temperatures from SCR-A at 10 to 0.4 mb. Final Report, Contract NAS-5-23538 for NASA-Goddard Space Flight Center, by Control Data Corporation, Minneapolis, MN, 33 pp.

Karoly, D. J. and B. J. Hoskins, 1982: Three-dimensional propagation of planetary waves. _J. Met. Soc. Japan_, 60, 109-122.

Labitzke, K. C. and B. Goretzki, 1982: A catalogue of dynamic parameters describing the variability of the middle stratosphere during the northern winters. Middle Atmosphere Program, Handbook for MAP, Vol 5, (edited by C. F. Sechrist, Jr.). 1-28.

O'Neill, A. and C. E. Youngblut, 1982: Stratospheric warmings
    diagnosed using the transformed Eulerian-Mean equations
    and the effect of the mean state on wave propagation. J.
    Atmos. Sci., 39, 1370-1386.

Palmer, T. N., 1981: Diagnostic study of a wave number-2
    stratospheric sudden warming in a transformed
    Eulerian-Mean formalism. J. Atmos. Sci., 38, 844-855.

Palmer, T.N. and C.-P. F. Hsu, 1983: Stratospheric coolings and
    the role of nonlinear wave interactions in preconditioning
    the circumpolar flow. J. Atmos. Sci., 40, 2484-2496.

Plumb, R. A., 1985: On the three-dimensional propagation of
    stationary waves. J. Atmos. Sci., 42, 217-229.

Robinson, W. A., 1986: The application of the quasi-geostrophic
    ELiassen-Palm flux to the analysis of stratospheric data.
    J. Atmos. Sci., 43, 1017-1023.

Roe, J., D. Hovland and R. Wilcox, 1982: Statistical retrieval
    of temperatures at 10 to 0.4 mb from SCR-B, 1975-76.
    Final Report, Contract NAS5-26252 for NASA-Goddard Space
    Flight Center, by Control Data Corporation, Minneapolis.,
    MN, 15pp.

Smith, A. K., 1983: Stationary waves in the winter stratosphere:
    Seasonal and interannual variability. J. Atmos. Sci., 40,
    245-261.

Event	Duration (days)	Upper Stratosphere Zonal Temperature Increase (°K)			Zonal Flow Decrease at 1 mb (ms⁻¹)			Vertical EP Flux at 50 mb (10¹⁵ g ms⁻²)			Net Flux in Box Model (10¹⁵ g ms⁻²)		
		45°N	55°N	65°N	45°N	55°N	65°N	35-55°N	45-65°N	55-75°N	35-55°N	45-65°N	55-75°N
1) 12/7/70-1/16/71	40	11	25	36	72	73	75	12.5	18.3	14.4	9.9	12.0	10.3
2) 2/15/71-3/27/71	40	17	30	39	79	72	60	6.6	9.9	8.4	6.4	7.9	6.3
13) 1/21/80-3/1/80	40	5	11	19	53	83	91	12.1	18.0	14.5	11.3	12.8	-
14) 12/22/80-2/5/81	45	9	18	28	72	81	80	9.0	17.6	14.6	9.8	10.3	-
(INTERMEDIATE DURATION)													
3) 12/7/71-1/6/72	30	9	13	26	47	60	20	6.3	9.9	7.6	5.6	6.0	4.4
4) 1/31/72-2/25/72	25	2	8	9	43	52	42	7.1	11.4	8.4	-	-	-
7) 12/12/73-1/16/74	35	16	20	21	55	25	8	5.6	9.1	7.9	5.7	7.6	6.0
8) 1/26/74-2/25/74	30	6	14	22	43	44	51	6.9	10.6	8.4	6.5	10.0	7.1
11) 1/16/79-2/10/79	25	5	7	16	45	50	47	6.0	12.5	11.8	-	-	-
(SHORT DURATION)													
5) 12/27/72-1/11/73	15	10	22	24	65	44	18	-	-	-	-	-	-
6) 1/21/73-1/31/73	10	5	3	2	10	33	44	4.3	6.8	6.2	4.4	5.5	4.8
9) 12/12/74-1/1/75	20	10	24	34	84	81	58	-	-	-	-	-	-
10) 2/20/75-3/7/75	15	6	14	26	59	69	54	3.9	5.9	5.1	-	-	-
12) 12/27/79-1/16/80	20	13	21	25	49	26	22	4.8	10.3	4.4	3.1	4.1	-

Table 1: Time integrated zonal parameters for individual warning events.
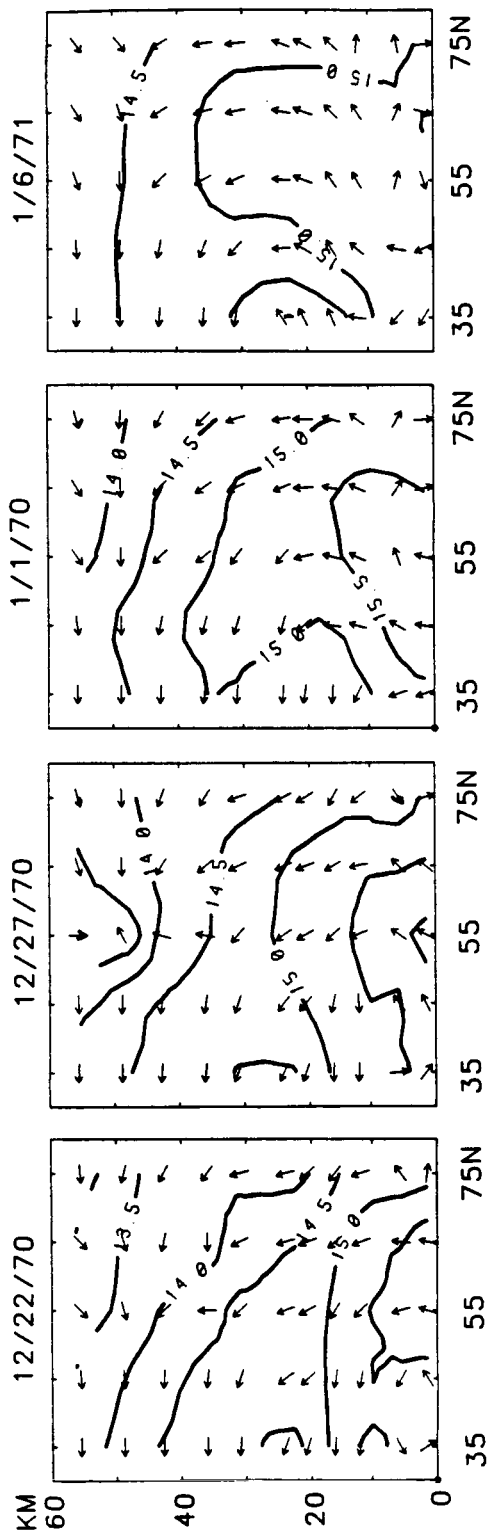
Figure 1. EP wave 1 flux during 1970-71 mid-winter warming. Contour values are $\log_{10}$ of the EP flux magnitude. Units are g ms^{-2}.

PRECEDING PAGE BLANK NOT FILMED
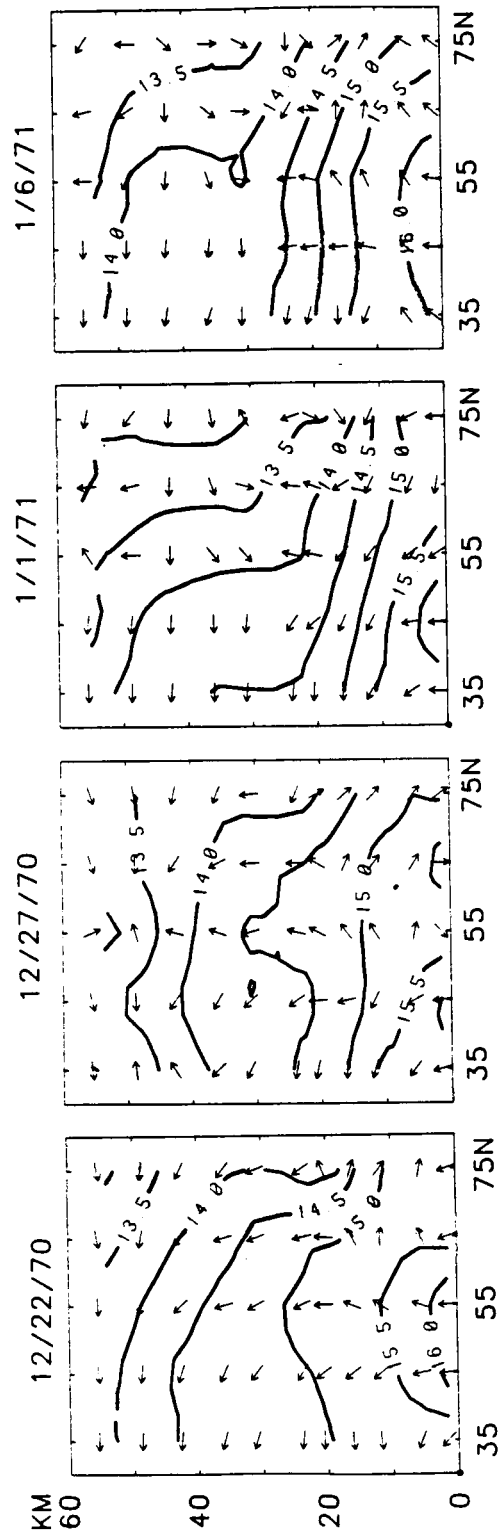
Figure 2. EP wave 2 flux during 1970-71 mid-winter warming.
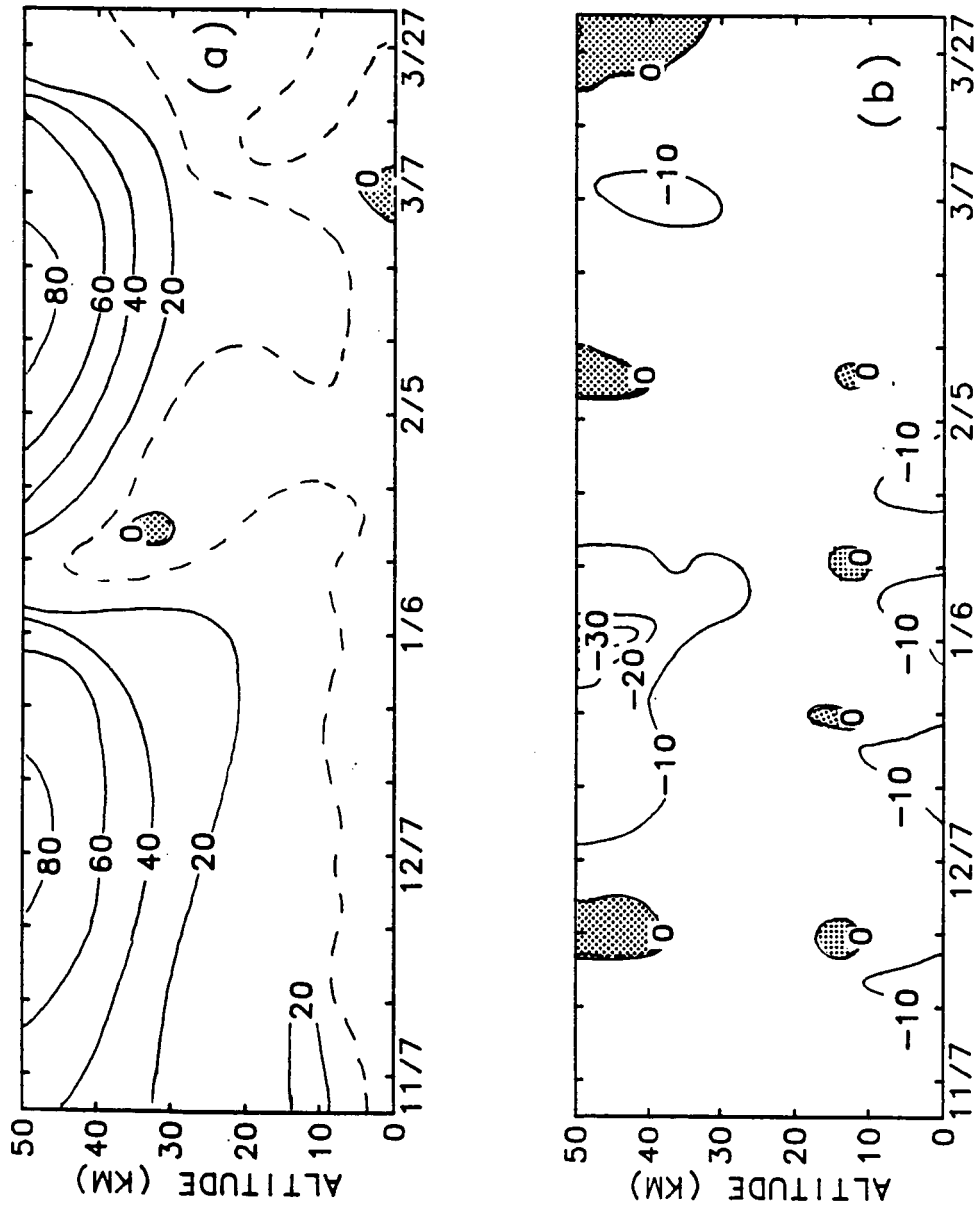
Figure 3. Time altitude sections of (a) zonal wind (ms^{-1}) and (b) EP flux divergence for waves 1-6 (ms^{-1}day^{-1}) at 55°N during winter, 1970-71. In (a) easterlies are shaded; in (b) positive values of EP flux divergence are shaded.
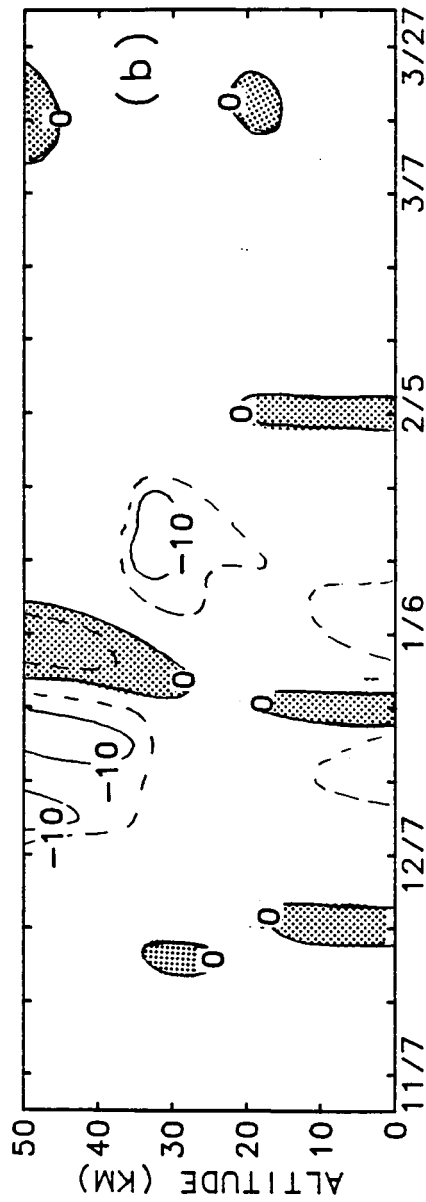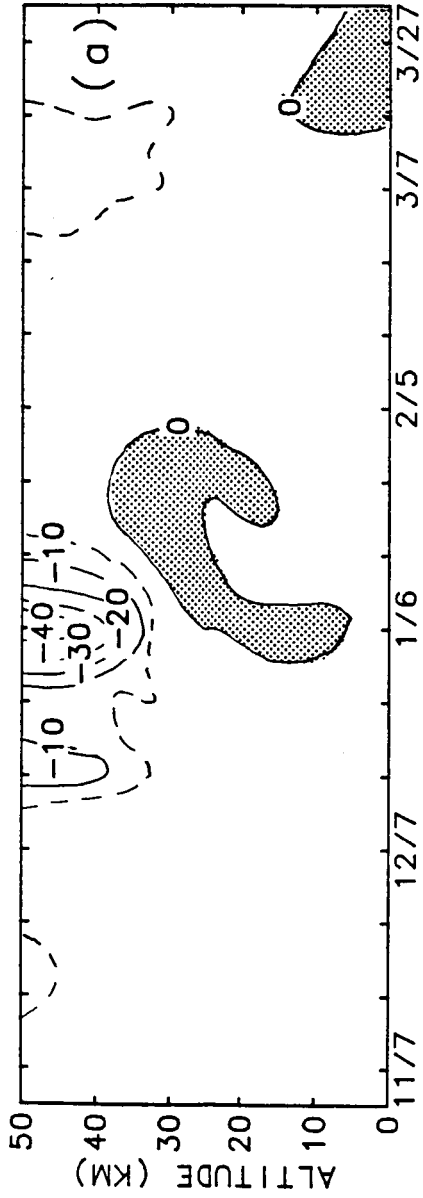
Figure 4. Time altitude sections of EP flux divergence ($ms^{-1}day^{-1}$) for (a) wave 1 and (b) wave 2.
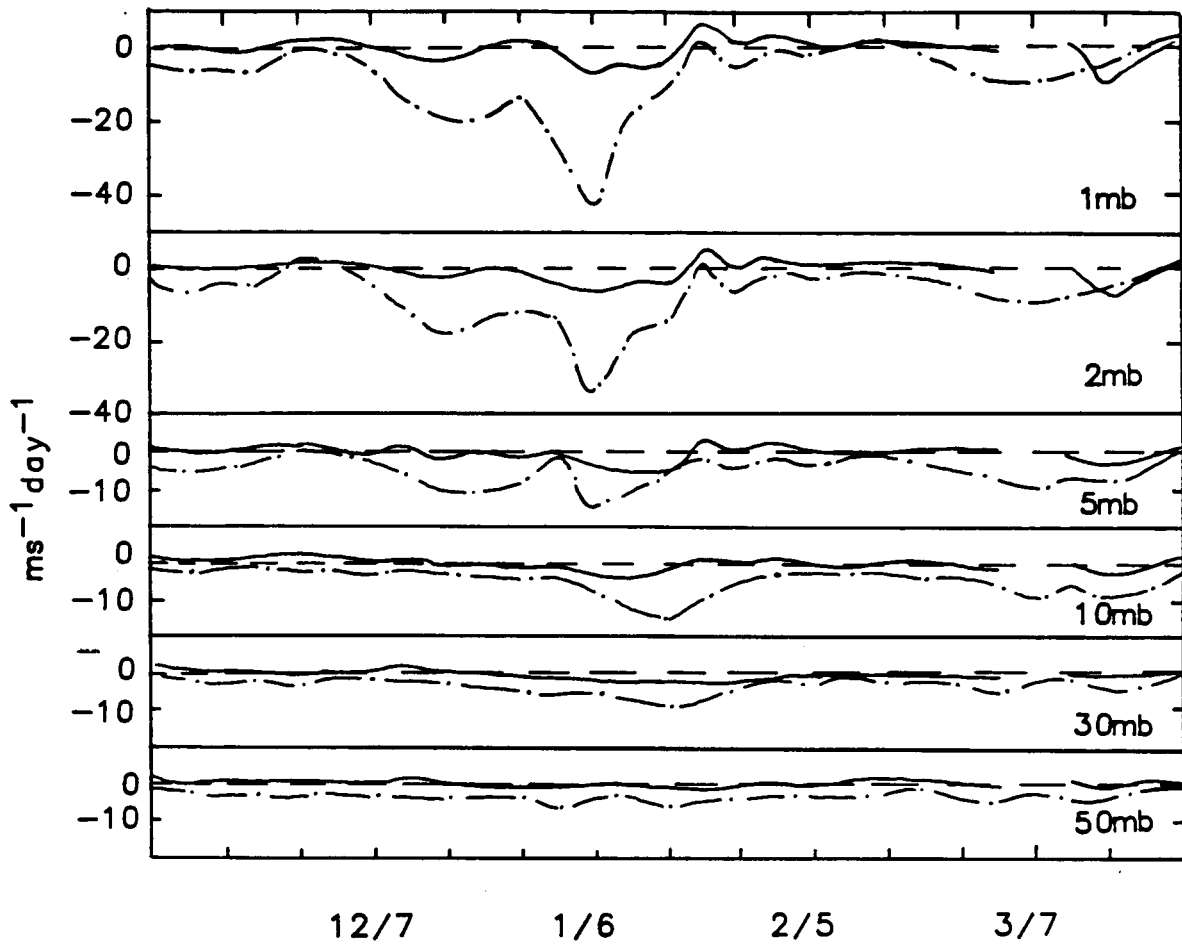
Figure 5. Time variations of $\Delta\bar{u}/\Delta t$ (solid line) and EP flux
forcing of the zonal flow (dot-dash line) at selected
stratospheric pressure levels, 55°N, 1970-71.
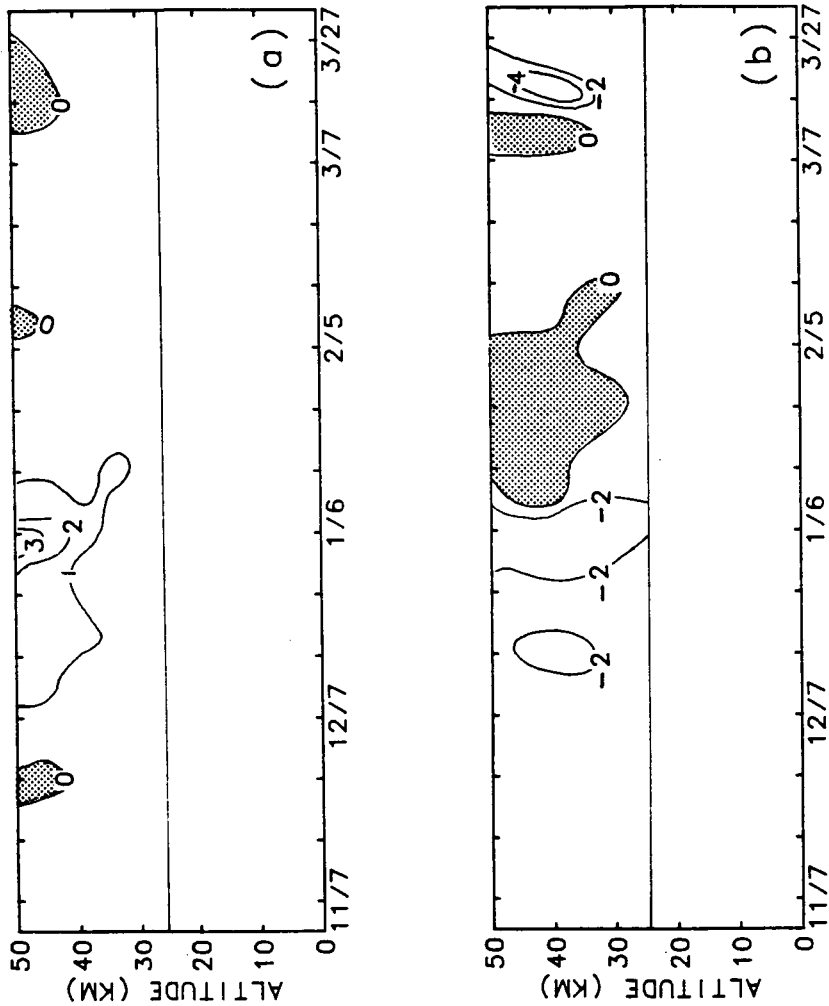
Figure 6. Stratospheric time-altitude sections of (a) $\bar{v}^*$, the meridional component of the residual circulation (ms^{-1}) at 55^{0}N, (b) $\bar{w}^*$, the vertical component of the residual circulation (ms^{-1}x10^{-3}) at 65^{0}N during winter 1970-71. In (a) flow from the north is shaded; in (b) ascending motion is shaded.
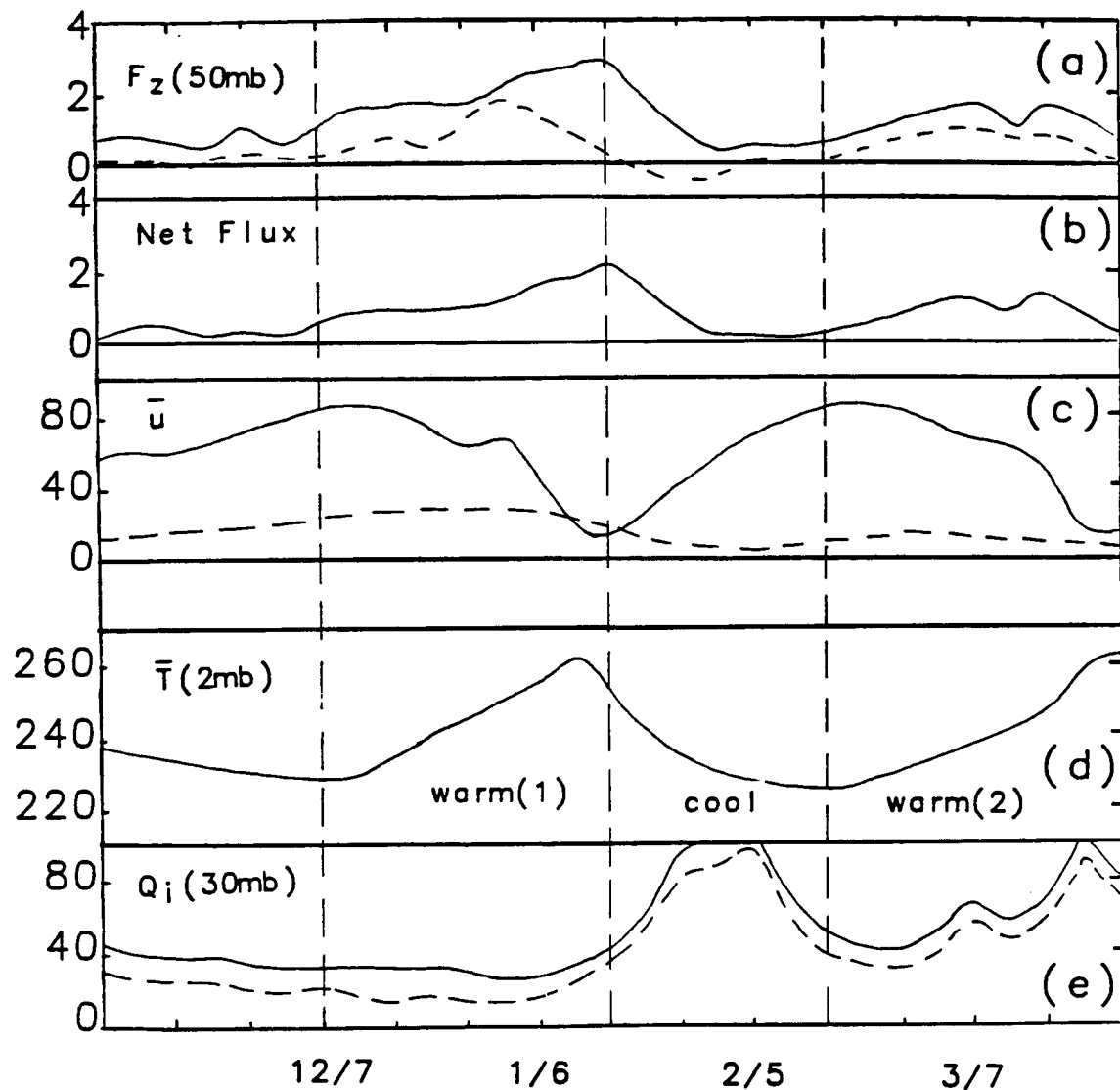
Figure 7. Time variation of wave zonal flow interaction in the stratosphere for latitude band 45-65°N in 1970-71: (a) vertical component of EP flux at 50 mb for waves 1-6 (solid line) and wave 1 (dashed line), $(10^{15} g \; ms^{-2})$, (b) net wave flux from 50 to 1 mb, $(10^{15} g \; ms^{-2})$, (c) zonal flow (ms^{-1}) at 55°N at 1 mb (solid line) and 30 mb (dashed line), (d) zonal temperature (°K) at 2 mb, 65°N, and (e) squared value of the index of refraction at 30 mb for wave 1 (solid line) and wave 2 (dashed line).
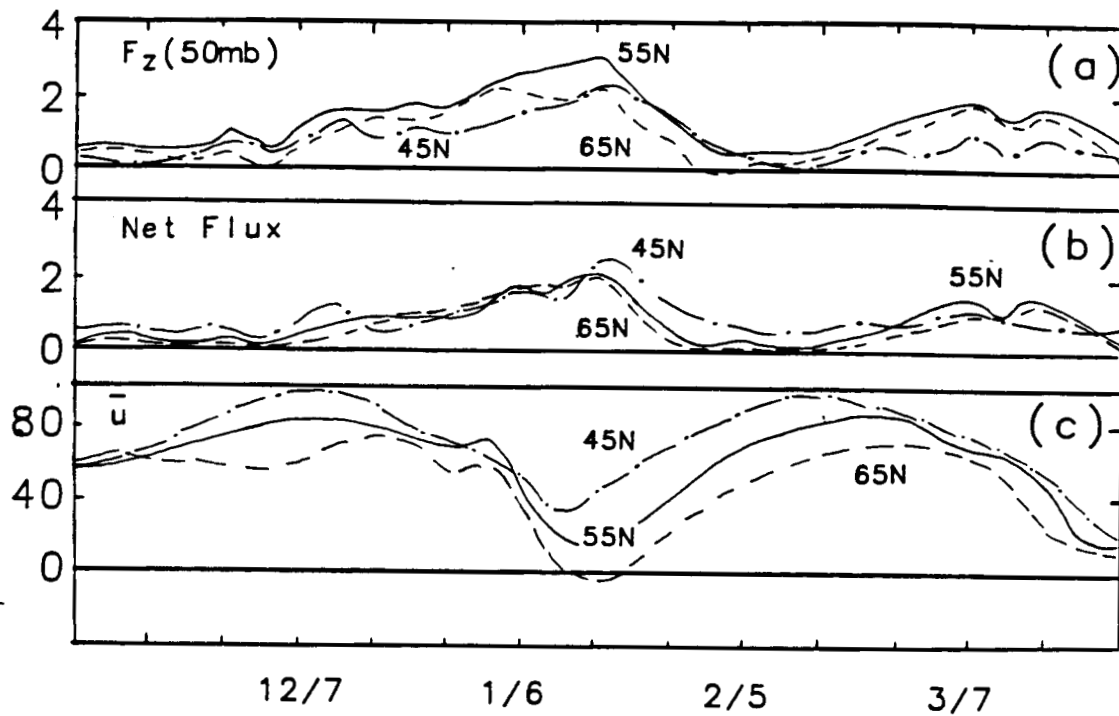
Figure 8. Time variation of wave-zonal flow interaction in the stratosphere for neighboring latitude bands, 35-55°N, 45-65°N and 55-75°N in 1970-71: (a) vertical component of EP flux at 50 mb (10^{15}g ms^{-2}), (b) net wave flux from 50 to 1 mb (10^{15}g ms^{-2}) and (c) zonal flow (ms^{-1}).
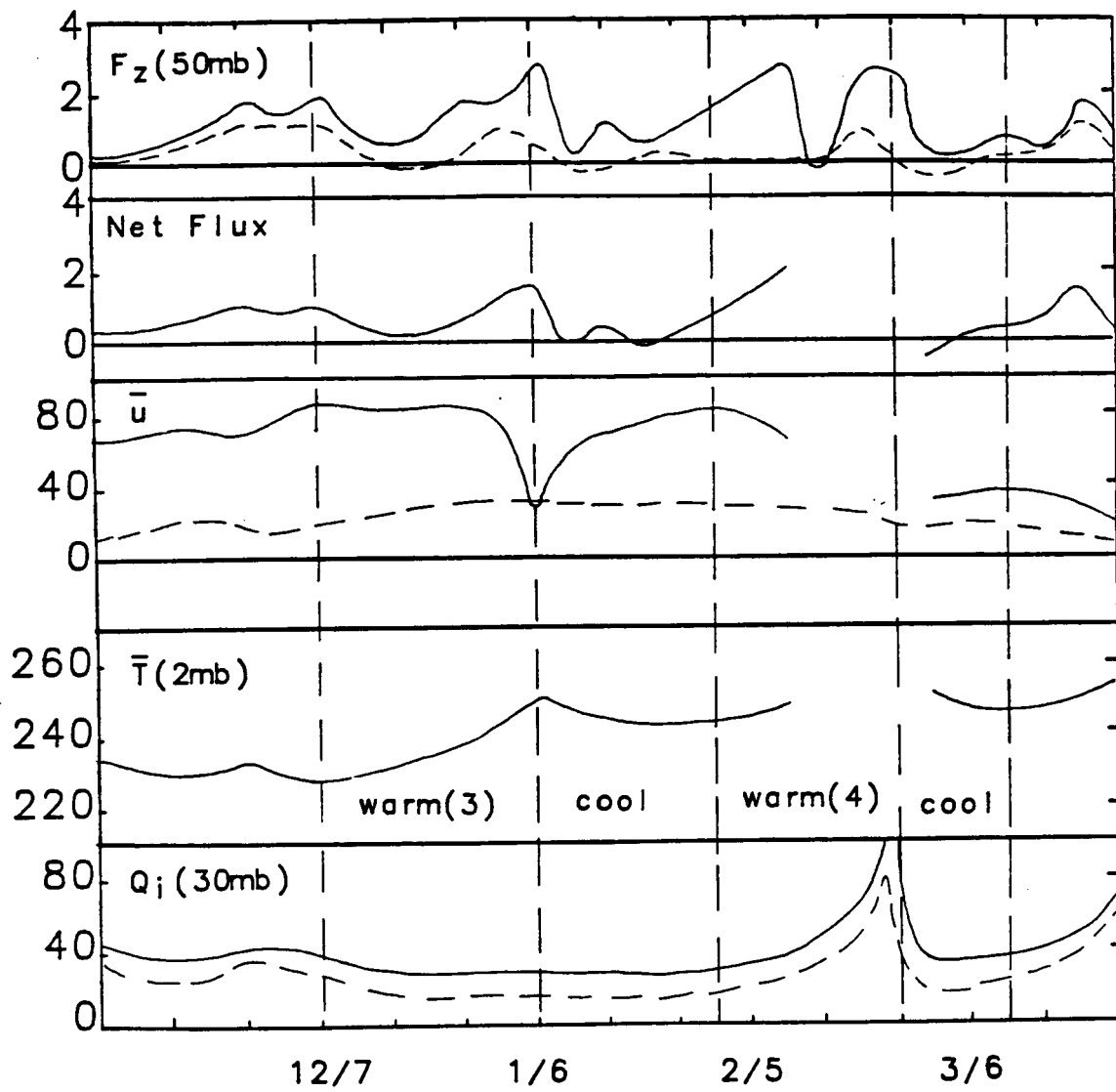
Figure 9. Same as Figure 7 for 1971-72.
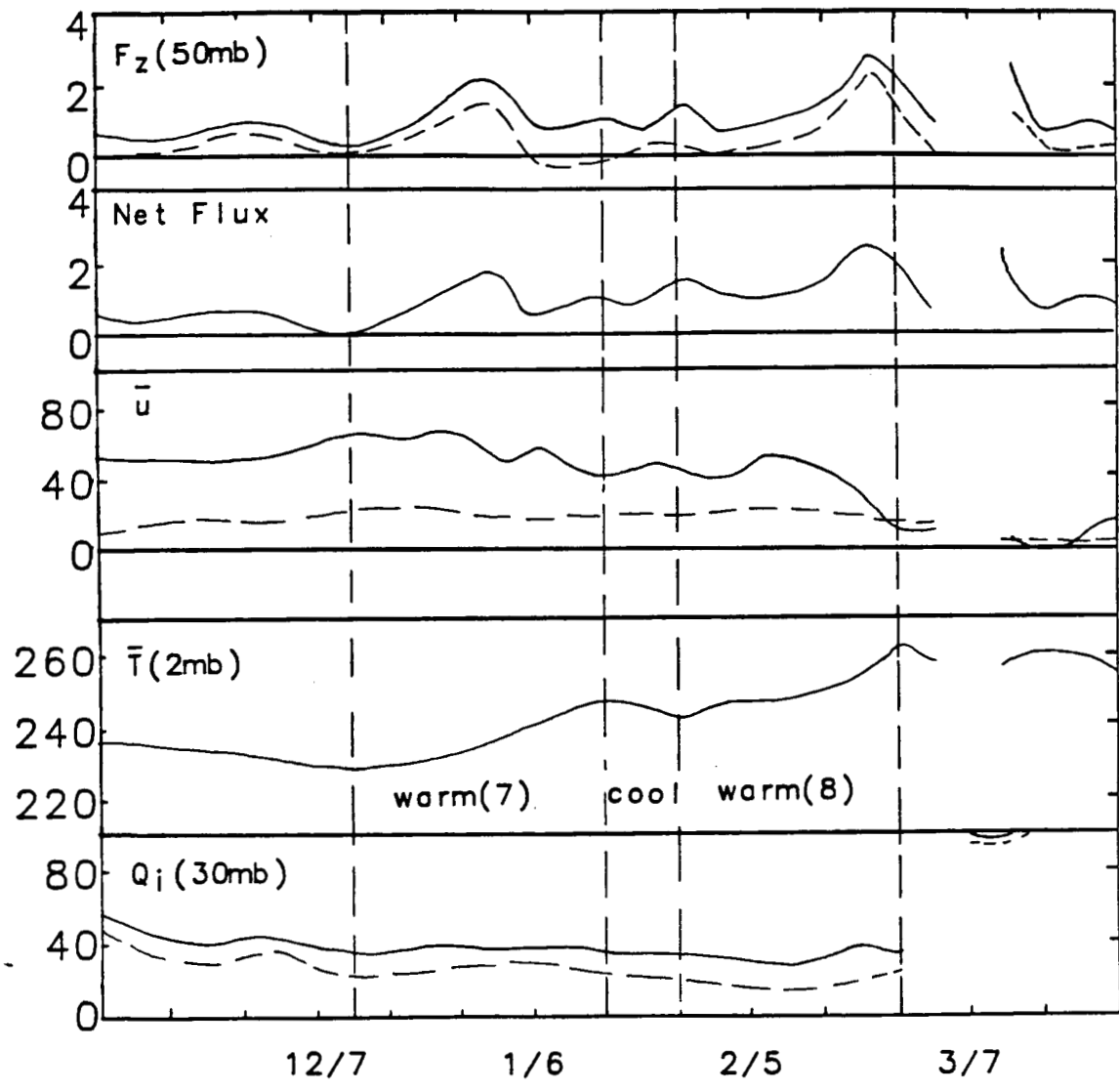
Figure 10. Same as Figure 7 for 1973-74.
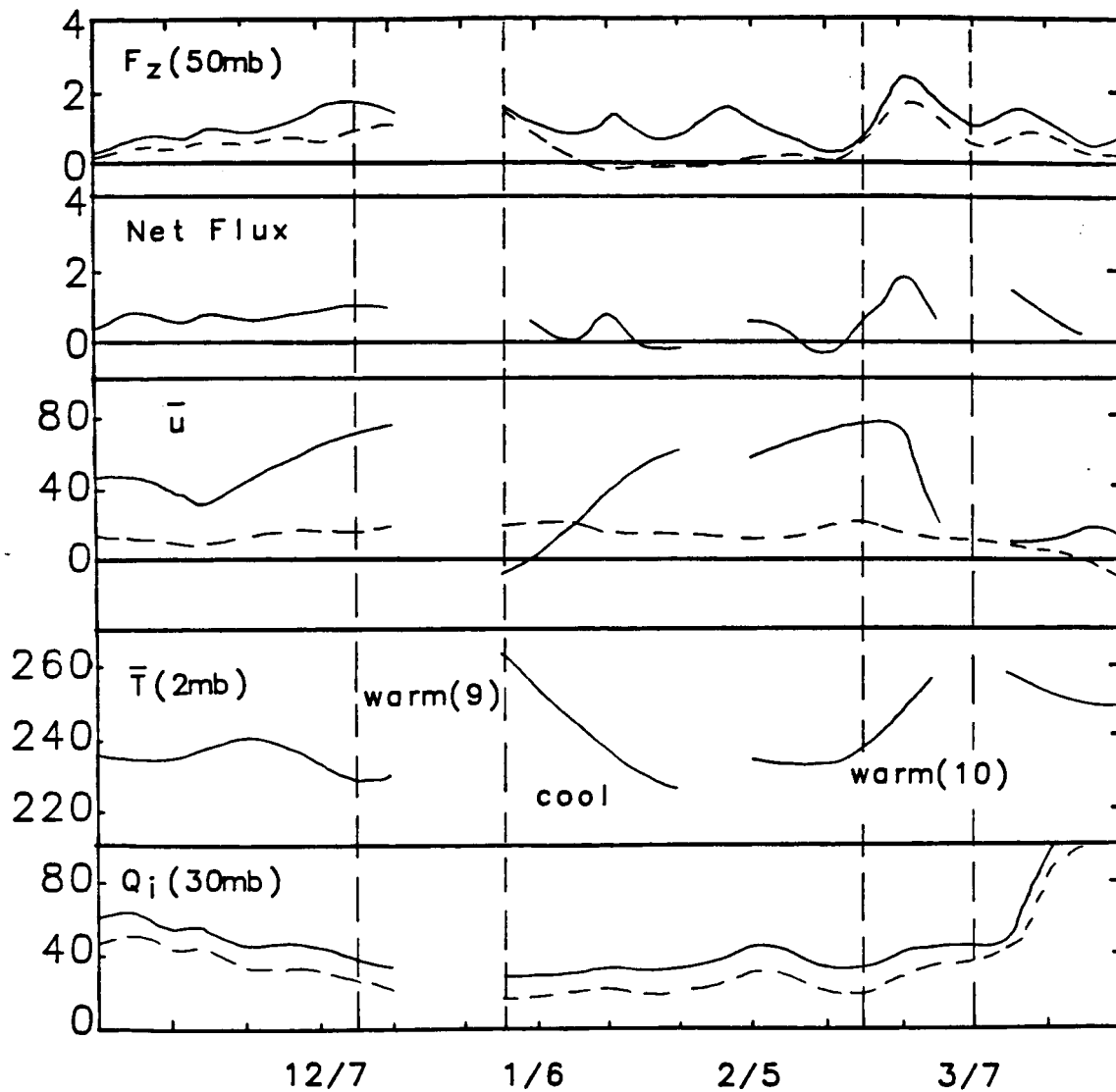
Figure 11. Sames as Figure 7 for 1974-75.
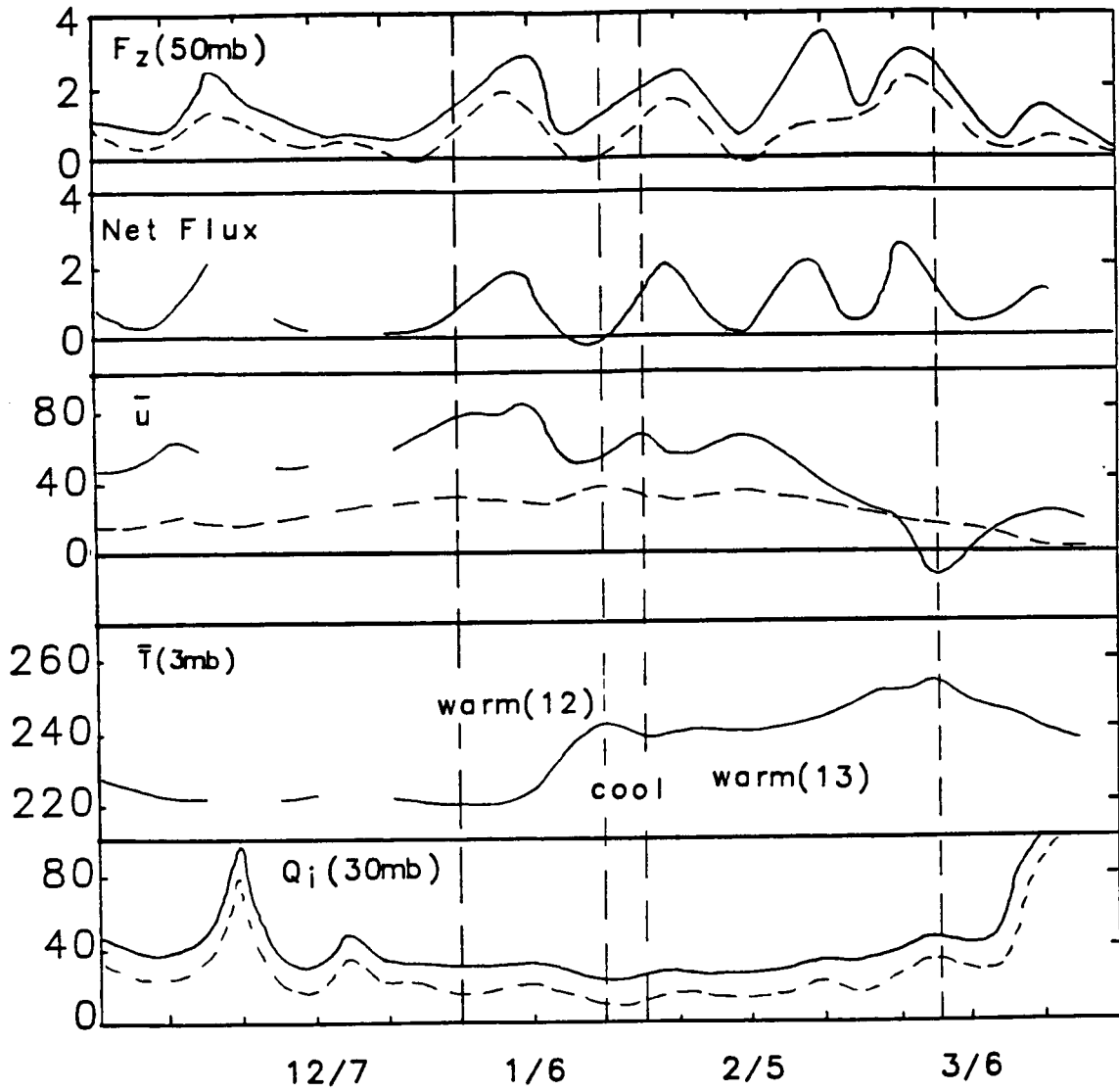
Figure 12. Same as Figure 7 for 1979-80, except 3 mb temperature
is used in place of 2 mb temperature.
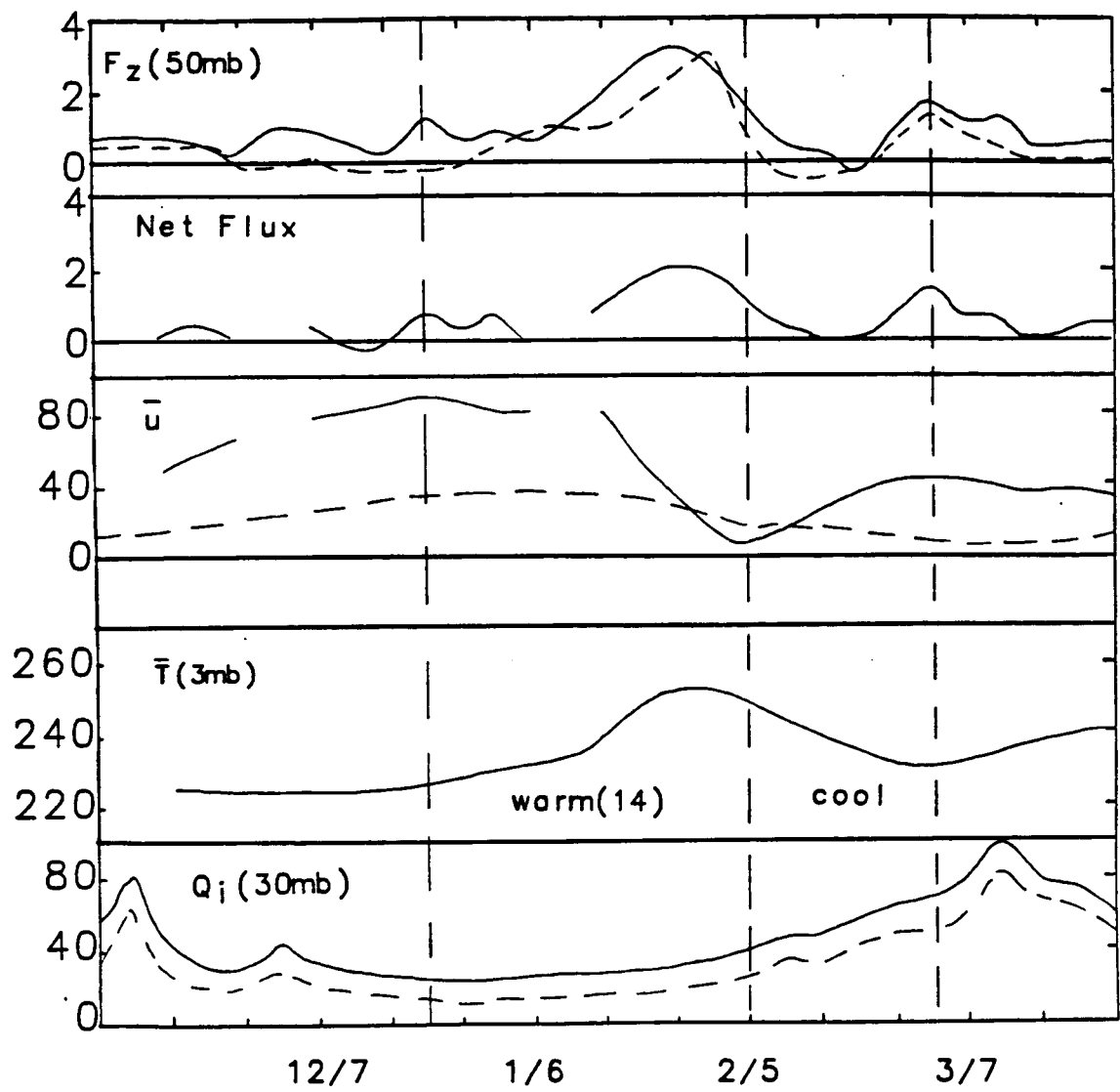
Figure 13. Same as Figure 12 for 1980-81.
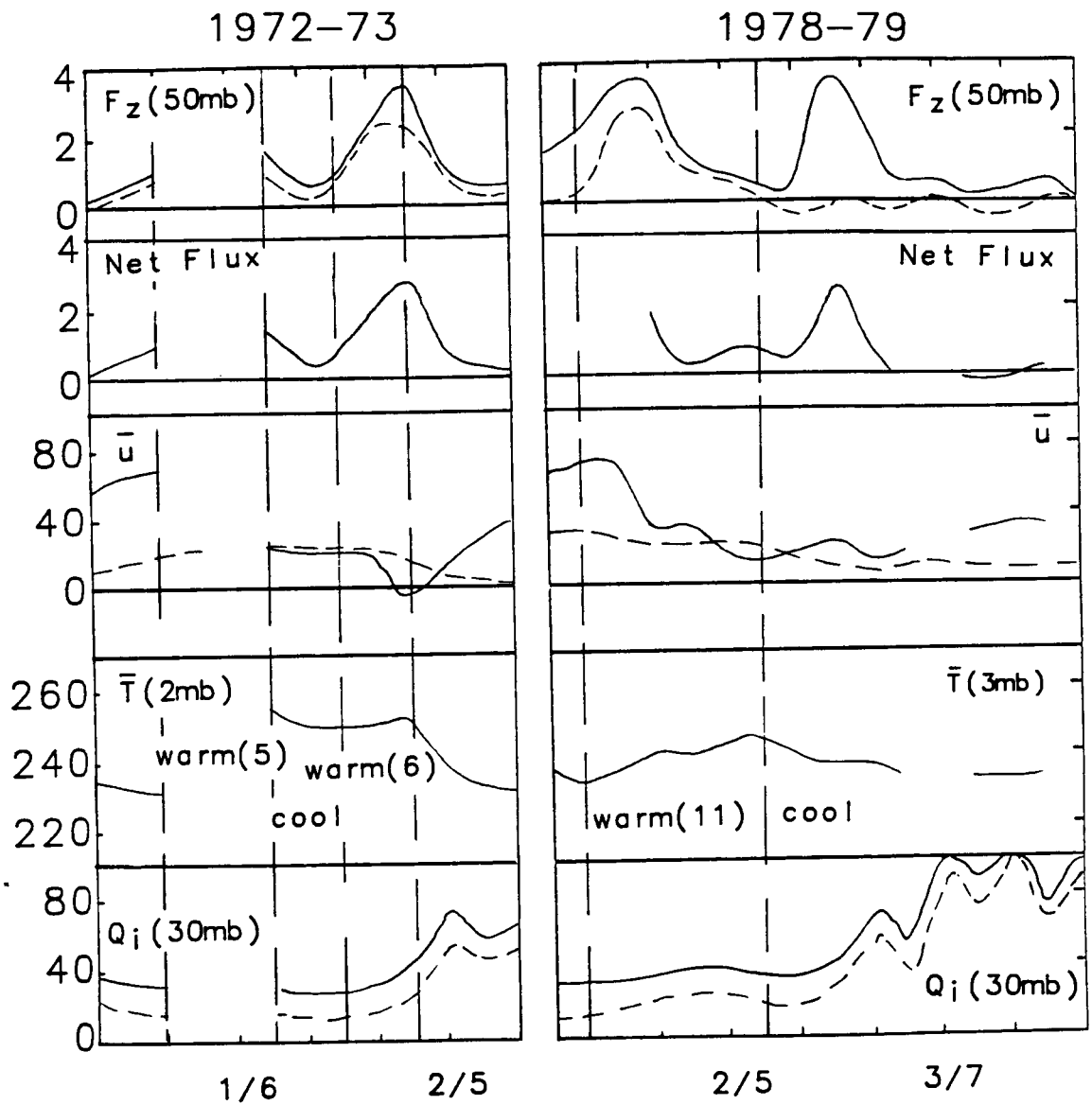
Figure 14. Same as Figure 7 for winter, 1972-73 and Figure 12 for winter, 1978-79.
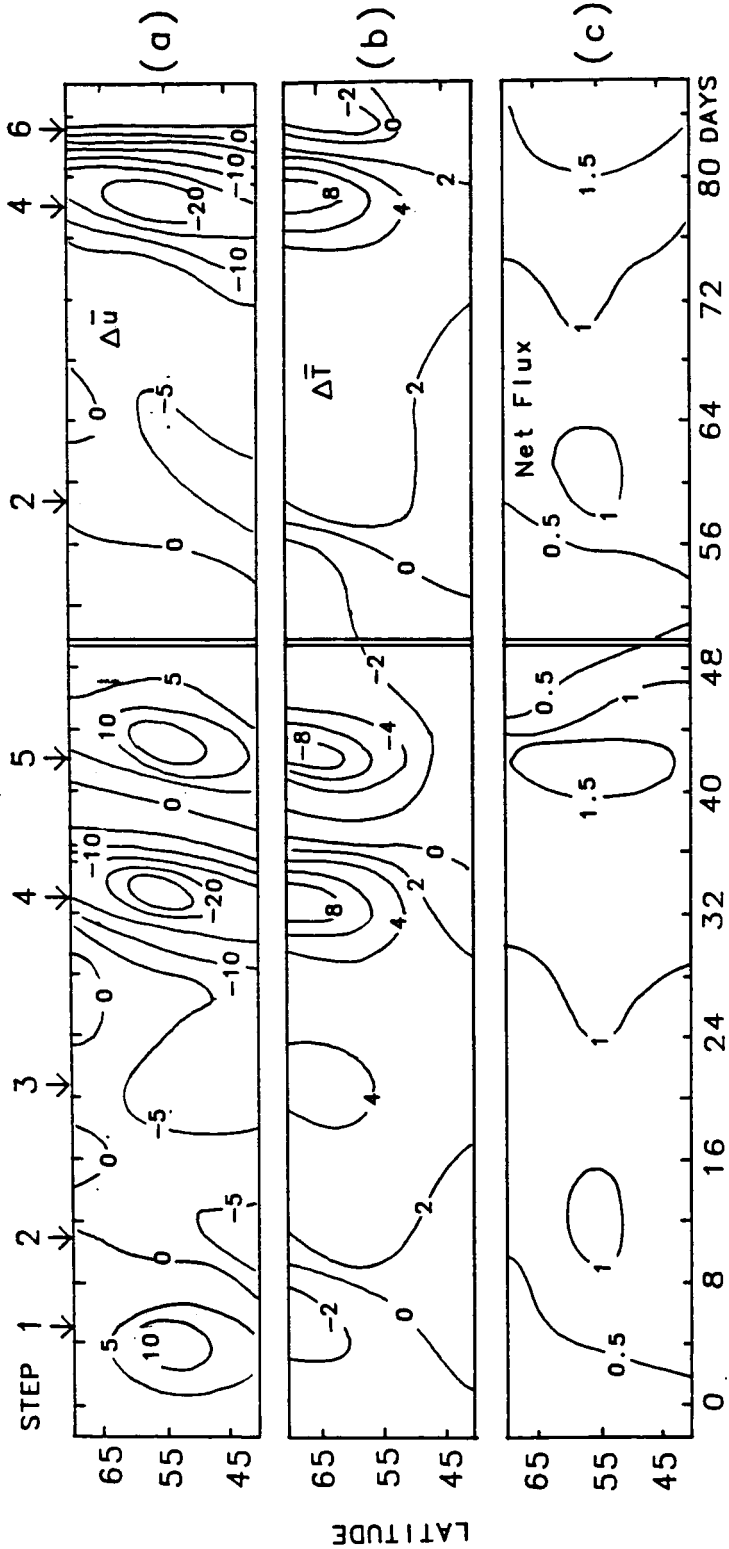
Figure 15. Time-latitude description of 5-day (a) 1 mb zonal flow tendency (m s⁻¹)
(b) upper stratosphere (2/3 mb) zonal temperature tendency (°K) and (c) net
wave flux (10¹⁵g ms⁻²) for composite mid-winter and late winter stratospheric
warmings. Characteristic steps in wave-zonal flow interaction processes are
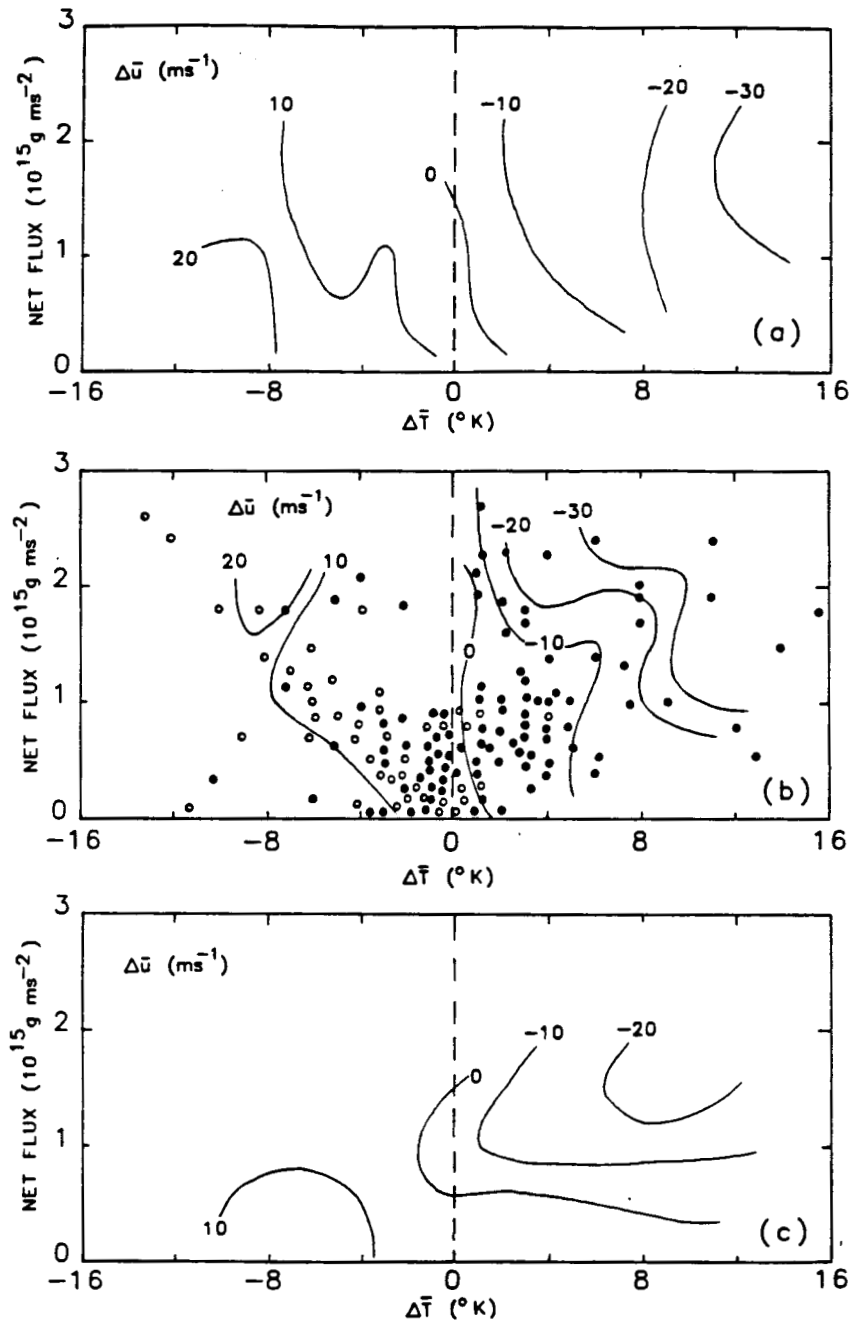indicated. See text for further explanation.

Figure 16. Diagrams showing composite 5-day 1 mb zonal flow tendency as a function of 5-day average net wave flux and 5-day upper stratospheric temperature tendency (65°N) for (a) 45°N, (b) 55°N and (c) 65°N. Dots indicate data distribution at 55°N and also the sign of $\bar{w}*$. Ascending (descending) motion is indicated by open (closed) circles.
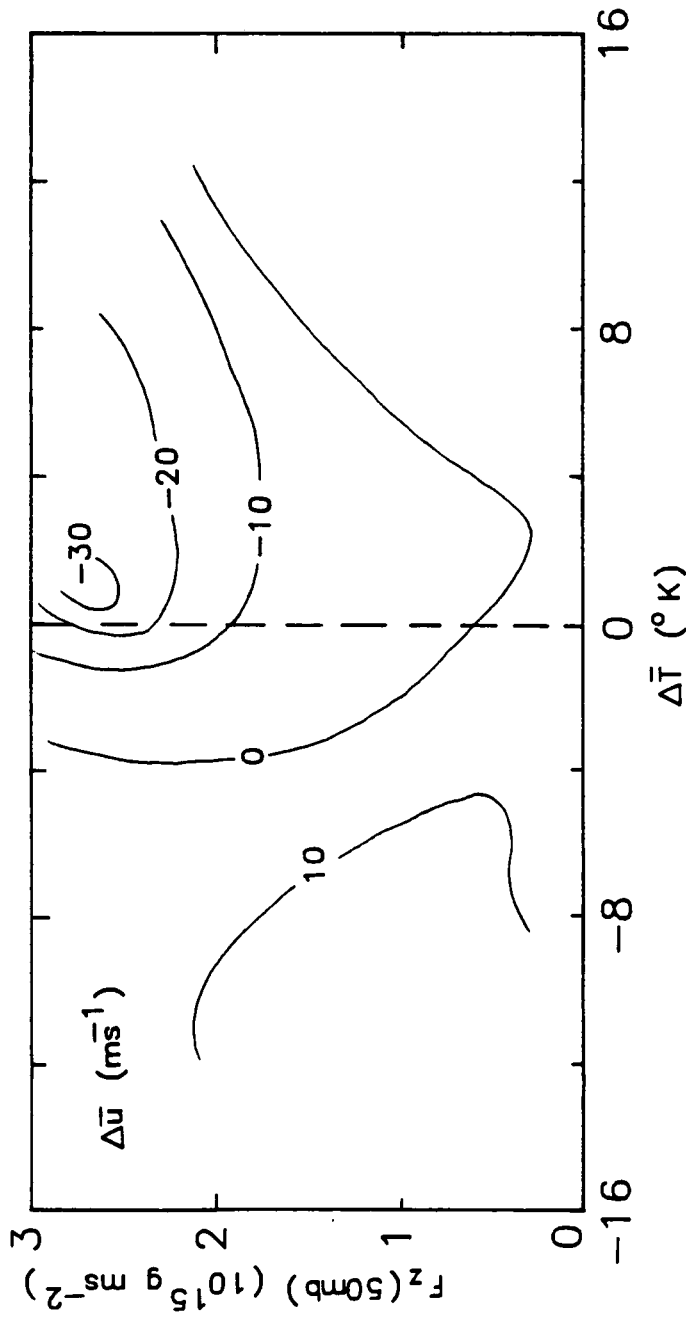
Figure 17. Composite diagram showing predictive 5-day 1 mb zonal flow tendency (55°N) as a function of current 5-day average vertical wave-flux at 50 mb and upper stratospheric temperature tendency (65°N) from the past 5 days.

PLANETARY WAVE PROPAGATION AND ZONAL FLOW INTERACTION, 0-80 KM, OBSERVED FROM NMC-SAMS DATA

Denis G. Dartt and David E. Venne

Abstract

The primary features of mid-latitude planetary wave propagation and dissipation by zonal flow interaction in the stratosphere-mesosphere are described during two northern hemispheric winters, 1979-80 and 1980-81. The analysis is based on Eliassen-Palm (EP) flux diagnostics computed from 5-day averages of daily sensible heat and momentum fluxes derived from SAMS (Stratospheric and Mesospheric Sounder) data from 30-80 km and NMC (National Meteorological Center) data downward into the lower troposphere.

Planetary waves propagating upward are observed to decelerate the mesospheric jet up to altitudes of 70 km in early winter and 60 km in late winter. Wave 1 may decelerate the zonal flow to altitudes of 70 km, while wave 2 deceleration appears to be restricted to 60 km. During large wave events, evidence of a two-cell residual circulation exists similar to the model results of Dunkerton, et al. (1981).

Above 65 km, a region of EP flux divergence leading to zonal flow acceleration of 5 $ms^{-1}day^{-1}$ frequently occurs during winter in mid-latitudes. This EP flux divergence is primarily associated with a sharp equatorward gradient of wave 2 EP flux, as propagation of this wave is restricted in the easterly shear region above the mesospheric wind maximum in high latitudes. The time variation of EP flux divergence, however, is poorly correlated with geostrophic flow variation at these altitudes suggesting that planetary wave forcing is small compared to forcing by other processes.

Much of the synoptic variability of upward propagating wave activity in the middle atmosphere appears to be related to the intermittent baroclinicity of the lower stratosphere which can be described in terms of the constructive and destructive interference of zonally propagating waves with a prominent quasi-stationary component. There is also evidence of intermittent small scale, latitude-altitude, anomalies of the planetary waves in the mesosphere which exist on a 5-day basis.

1. Introduction

In the stratosphere, the large-scale dynamics during winter can be described in terms of the interaction of upward propagating planetary waves with the zonal flow and a zonal residual diabatic circulation which is modulated during wave events (Palmer, 1981; O'Neill and Youngblut, 1982). In the mesosphere, the dynamics becomes more complex as gravity wave drag and a large Coriolis torque from the observed meridional flow affect the zonal circulation (Holton, 1982). Observationally, the presence of planetary wave type disturbances in the winter mesosphere is known from LIMS (Limb Infrared Monitor of the Stratosphere) and SAMS data (Dunkerton and Delisi, 1985; Labitzke and Barnett, 1985). Dunkerton and Delisi (1985) show that the winter mesospheric zonal flow from LIMS in 1978-79 was strongly influenced by planetary waves propagating upward from below. The analysis described here is based on SAMS data and describes the major planetary wave activity in the two following winters.

Model studies indicate complex planetary wave, gravity wave and zonal flow interactions: Holton (1983) and Dunkerton and Butchart (1984) suggest that gravity wave propagation from the troposphere to the mesosphere would be suppressed during large planetary wave events associated with sudden warmings because of

the occurrence of unfavorable winds (easterlies) lower down in the atmosphere which limit vertical transmissivity. Miyahara (1985) indicates that upward propagating gravity waves produce drag forces on the velocity perturbations of planetary waves and greatly suppress their amplitude. Holton (1984) postulates that planetary waves may be generated in the mesosphere as a consequence of the breaking of upward propagating gravity waves whose source and/or selective transmission is a function of longitude.

Local measurements of zonal flow acceleration by gravity waves near 80 km range from -20 ms^{-1} day^{-1} to approximately -50 ms^{-1}day^{-1} as described by momentum flux divergence observations of small scale motion in the mesosphere (Vincent and Reid, 1983; Fritts, 1986). This drag approximately balances the Coriolis torque of the observed meridional flow which during winter at 52°N, 80 km is from the south at about 5 ms^{-1} (Manson et al., 1985). The drag on the zonal flow in middle latitudes by the planetary waves (or deceleration as given by the EP flux convergence) is described below for altitudes up to 80 km. The time change in zonal flow results primarily from a net force based on the balance of the Coriolis torque, planetary wave drag and gravity wave drag.

The current analysis focuses on the description of planetary wave 1 and 2 propagating upward from below and their relation to winds and the index of refraction in the upper atmosphere. Further, the occurrence of anomalous wave activity in the mesosphere is noted which may be indicative of the planetary wave generation process described by Holton (1984) or perhaps barotropic instability (Dunkerton and Delisi, 1985). The two winters analyzed have quite different wave 1 behavior as indicated by episodes of baroclinic wave 1 development in the lower atmosphere. The 1979-80 winter had several distinct episodes of short duration, while the 1980-81 winter had a month-long episode which resulted in a very strong stratospheric warming. In the stratosphere each winter indicates an interaction between zonally propagating waves and a very strong quasi-stationary wave component of geopotential height.

2.   Data and Computation

As SAMS temperatures are a relatively new data source, some comparison tests were performed at 30 mb with Berlin temperature maps and at 10 mb with NMC grid points. Generally, large

planetary scale features in the Berlin and NMC temperature fields are reproducible in SAMS analyses, although single grid point differences are typically 2-5°K. In regions of sharp horizontal gradients, grid point temperature differences may be as large as 20°K. Other comparisons of SAMS derived fields and corraborative data are described in Barnett and Corney (1984), in MAP Handbook 12 (Rodgers, 1984) and in Grose and Rodgers (1986). One caveat in using SAMS limb scanner temperatures is the possible longitudinal displacement of temperature measurements in regions of large east-west temperature gradient. This may artificially cause a local baroclinic perturbation in the transition from NMC (10 mb) to SAMS (3 mb) geopotential height. However, this problem should be reduced for planetary waves which are based on zonally averaged integration.

In the hydrostatic computation of geopotential height from 10-.01 mb, SAMS temperature, which is an average based on observations near 1500 LT and 2100 LT, was directly combined with temperature and geopotential height from NMC at 1200Z. Initially, a local time analysis of the stratosphere-mesosphere was considered using 1800 LT time interpolated NMC height and temperature at 10 mb. However, this time interpolation at 10 mb did not improve SAMS-NMC temperature agreement and thus was not employed.

The computation of planetary wave parameters from NMC and
SAMS is described in Dartt (1986a). All winds are based on
geostrophy. However, the geostrophic momentum flux for each
planetary wave was corrected for zonal flow variations using the
formulation described by Robinson (1986). In the vicinity of the
mesospheric jet such corrections can significantly change the
values of EP flux divergence. Typically, SAMS data are available
on about 3 out of 4 days. Thus, 5-day averages are used to
describe variability throughout the winter. The basic SAMS
latitude range for computing winds and EP-fluxes is 35-65°N,
and for NMC grids is 35-75°N. EP flux divergence above 10 mb
was only calculated at internal grid points, at 45 and 55°N.
The squared value of the index of refraction was computed by
using a 4th degree polynominal to express the latitude
variability of $\bar{u}/(a \cos\phi)$ at each standard pressure level.
Latitude derivatives were then estimated analytically. The
details of this computation are described in Dartt (1986b).

A comparable data source to 1 mb for this period is based on
the NOAA 6 and TIROS N Stratospheric Sounding Units (SSU) and
the TIROS Operational Vertical Sounder (TOVS) system on NOAA 6
and 7. Monthly averages of planetary wave statistics from that
data are described in Geller et al. (1984). A detailed
comparison of SAMS and SSU planetary wave statistics was not
attempted. However, there are some differences in the two sets

of data. For example, the extreme values of SSU zonal wind at
1 mb (140 ms^{-1}) in December 1979 is not apparent from SAMS
derived winds (100 ms^{-1}).

3. **Planetary Wave Dynamics**

   a. **1979-80**

   The relation between planetary wave activity in the middle
and lower atmosphere can be seen from EP flux diagrams below.
The direction of propagation of wave activity over a 5-day
interval is given by the unit flux vector; the magnitude of EP
flux is indicated by logarithmic contours which follow the
dissipating wave activity with height. Figure 1 shows two
primary winter baroclinic episodes in 1979-80 when wave 1 from
the troposphere propagates upwards into the stratosphere:
Dec. 22-Jan. 6, and Feb. 15-Mar. 1. On certain days during these
episodes, unit vectors indicate that wave activity is propagating
vertically from the upper stratosphere into the mesosphere. (The
stratopause is at about 48 km.) In both episodes, the amplitude
of EP flux in the upper stratosphere and mesosphere increases
with time as the events progress.

   As a baroclinic episode develops, the unit vectors in the
upper troposphere and lower stratosphere become normal to the

almost horizontal contours indicating substantial vertical propagation. Typically, the unit vectors become gradually directed equatorward and the angle between unit vectors and contours diminishes with increasing altitude, until near 70 km the unit vectors are nearly parallel to the almost horizontal contours. At this height, further upward propagation will cease.

Wave 1 activity in the mesosphere does not always propagate equatorward. There is evidence of poleward propagation at high latitudes (55-65°N) on Dec. 22, Feb. 25 and Mar. 1. Poleward propagation at low latitudes (35-45°N) occurs on Jan. 6. There is also evidence of anomalous downward fluxes above 50 km on Jan. 6 and Mar. 1. These occurrences of non-equatorward flux do not appear associated with the transition from NMC to SAMS data which occurs at 30 km, but appear to occur as a result of the internal variation of SAMS temperature.

Two sequences of wave 2 baroclinic development are shown in Fig. 2, Jan. 1-16 and Feb. 5-20. For both episodes, wave 2 propagates vertically out of the troposphere into the stratosphere where it propagates equatorward. However, the EP flux vectors have a significant vertical component in the upper stratosphere from 35-45°N (Jan. 6, Feb.5-15) which suggests that wave 2 may propagate into the mesosphere at these latitudes. This is also indicated by the EP flux contours which

move upward with time into the mesosphere and exhibit a characteristic downward slope towards high latitudes. Wave 2 also shows examples of in situ mesospheric variability with EP flux divergence occurring above 50 km near 50°N from Jan. 1-6.

Figure 3 indicates the time evolution of zonal flow at 55°N throughout the winter along with the EP flux divergence of planetary waves (1-6). In the transformed Eulerian mean description of dynamics, the convergence of EP wave flux is a direct measure of wave forced deceleration of the zonal flow (Palmer, 1981). Up to altitudes near 70 km, the effect of the nonconservative wave action is to decelerate zonal flow, particularly the mesospheric jet. Intervals of large EP flux convergence correspond to the times of major flow deceleration. Figure 4 indicates the separate contributions to EP flux convergence by waves 1 and 2. The previously mentioned episodes of wave 1 and 2 baroclinicity produce the major wave forcing of the zonal flow. Waves 1 and 2 appear to decelerate the zonal flow up to altitudes of 70 and 60 km, respectively.

Figure 5 shows cross sections of zonal flow prior to (Dec. 22 and Feb. 10) and following (Jan. 11 and Mar. 1) the two baroclinic episodes. During the late Dec.-early Jan. episode of wave 1 and wave 2 baroclinicity, the mesospheric jet near 60 km, 35°N weakens considerably from 100 to 40 ms^{-1} and west winds

strengthen from 40-60 ms^{-1} in high latitudes. Dunkerton and

Delisi (1985) indicate similar behavior of the mesospheric winds

in the previous year during an early winter period of wave

propagation. During the Feb. baroclinic activity, the westerly

flow above 30 km in high latitudes is completely destroyed. In

late Feb., Fig. 1 shows that wave 1 EP fluxes are polar focused

into the lower stratosphere contributing to enhanced EP flux

convergence and zonal flow deceleration.

Cross sections of Matsuno's (1970) quasi-geostrophic squared

value of the index of refraction (Q_1) for wave 1 are shown in

Fig. 6 for the same days as in Fig. 5. This parameter indicates

the effects of the zonal wind field on the wave 1 propagation in

terms of refraction (O'Neill and Youngblut, 1982; Karoly and

Hoskins, 1982) and also, dissipation (Smith, 1983). In late

Dec., Q_1 shows a large equatorward gradient between 10-20 km.

Above 20 km, Q_1 decreases with altitude becoming negative in

the upper stratosphere and mesosphere of polar regions. Wave 1

in Fig. 1 propagates upward and equatorward towards the larger

values of the index of refraction in low latitudes and away from

the negative region in high latitudes. By Jan. 11, Q_1 has

increased below 40 km, and the equatorward gradient of this

parameter from 10-20 km in high latitudes has been relaxed.

These conditions appear to favor increased wave dissipation in

the stratosphere as well as restricting equatorward propagation.

During Feb., Q_1 becomes still larger throughout the lower

stratosphere. This is the region of maximum flow deceleration,

Fig. 5.

b. 1980-81

This winter had a very pronounced sustained mid-winter warming event with large zonal flow deceleration. Figure 7 shows the evolution of the zonal flow at 55°N throughout the winter along with the EP flux divergence of planetary waves 1-6. Throughout Jan. there is sustained EP flux convergence in excess of 10 $ms^{-1}day^{-1}$ from 40-65 km which is well correlated with zonal flow deceleration. Above 65 km, EP flux divergence is indicated throughout much of the early and middle winter. Figure 8 shows the EP flux divergence for waves 1 and 2, individually. The mid-winter flow deceleration occurs primarily as a result of wave 1; however, the component that contributes most to the EP flux divergence above 65 km is wave 2.

Detailed cross sections of wave 1 EP flux during the mid-winter event are shown in Fig. 9. The event began on Dec. 27 with upward and poleward wave fluxes observed from 30-60 km, poleward of 45°N. Shortly thereafter, upward wave 1 EP flux occurs from 35-65°N from near the surface to near 40 km. From Jan. 1 to Jan. 26 the EP flux magnitude increases substantially throughout the stratosphere and into the mesosphere. The contour which represents $10^{15}g$ ms^{-2} increases in altitude from 15 to near 40 km, and the $10^{14}g$ ms^{-2} contour increases in altitude from 40 to near 60 km and

the 10^{13}g ms^{-2} contour increases in altitude from 60 to above

70 km. After Jan. 26, the EP flux magnitude in the upper

atmosphere gradually begins to weaken, although the baroclinicity

of the unit flux vectors upwards from the troposphere remains

basically unchanged until Feb. 10. In the mature stage of the

event, wave 1 has a poleward component in the altitude range

10-30 km.

Selected zonal wind cross sections indicating the breakdown

of the westerly zonal flow are shown in Fig. 10. In early Jan.

the mesospheric jet near 50 km has moved from 45°N to 65°N,

its position on Jan. 16 just prior to major deceleration.

Throughout the remainder of Jan. and early Feb., zonal flow is

rapidly reduced in the meridional plane in response to the upward

propagating wave 1 activity, and the jet is destroyed. Toward

the middle of Feb., westerly zonal flow continues to decelerate

in the high latitude stratosphere, perhaps as a result of the

poleward focused wave 1 activity seen in Fig. 9. However, the

low latitude, (35°N) mesospheric jet is again re-established

near 60 km.

The squared value of the index of refraction for wave 1

during zonal flow breakdown is shown in Fig. 11. As zonal flow

diminishes, this parameter increases from 20-50 km indicating

increased planetary wave dissipation. Also, as the event

progresses, the region of negative Q_1, in the polar mesosphere
is gradually reduced and vanishes altogether on Feb. 5. Thus,
wave 1 should be increasingly able to propagate poleward as the
event progresses. This generally occurs as wave 1 polar focusing
increases with time and leads to dissipation via zonal flow
deceleration in the lower polar stratosphere.

The wave 2 EP flux divergence above 65 km noted in Fig. 8
has values exceeding 10 ms^{-1}day^{-1} on two occasions, Dec. 17
and Jan. 31, although typical values are one-half that large.
Figure 4b also shows the EP flux divergence occurred above 70 km
in late winter, 1979-80. As EP flux divergence may be indicative
of the generation of new wave activity, this aspect is considered
further. Figure 12 shows the 5-day average EP flux vectors for
wave 2 during the two occasions of conspicuous EP flux forced
acceleration above 60 km in 1980-81. On Dec. 17 and Jan. 31, the
EP flux magnitude indicates a sharp equatorward gradient above 60
km with values at 45°N typically 5-10 times larger than at
65°N. As the unit vectors are primarily directed equatorward,
the large scale equatorward gradient of EP flux characterizes the
divergence. The pattern of EP flux divergence has contours of EP
flux magnitude sloping downward with increasing latitude with
more EP flux in low than high latitudes.

-97-

C - 2

The wave 2 divergence may be a result of the large region of negative index of refraction in the high latitude mesosphere. According to WKB theory (Smith, 1983), the group velocity of wave 2 would become quite small both in low latitudes where Q_2 is very large, but also where Q_2 is very small and positive, just equatorward of the region of negative index of refraction in high latitudes. The upward propagating wave flux would then be split, refracted both towards low latitudes and also toward high latitudes in conjunction with the lower group velocity on the flanks of the wave pulse. This would naturally create a local region of EP flux divergence and zonal flow acceleration. Most of the wave activity would appear to propagate in the low latitude branch, as indicated by the slope of the contours in Fig. 12.

There are also alternative explanations of the EP flux divergence above 65 km:

(1) It may occur artificially as a consequence of base level geopotential errors that propagate hydrostatically in the vertical from 10 mb, as a result of retrieval error in the temperature profiles or as a result of the coarse vertical resolution of SAMS data. EP flux divergence is a highly derived parameter based on second order derivatives of geopotential height, and small errors in basic structure

may be compounded in the highly derived fields. The almost synoptic occurrence of the wave 2 divergence indicates that it is not a bias; also, the occurrence is not particularly correlated with EP-wave convergence below. Such symptoms could be indicative of such problems. Generally, the basic amplitude and phase structure of wave 2 in temperature above 65 km is not much different from SAMS (Rodgers, 1984) and from PMR (Barnett and Corney, 1985) in earlier years. Also, below 65 km the evolution of EP flux convergence during wave events from SAMS is similar to calculations from LIMS, Dunkerton and Delisi, (1985). Thus, at this time, there is no specific reason to suspect the EP flux divergence noted here.

2) The wave 2 EP flux divergence at high altitudes may indicate wave growth caused by an instability associated with the mesospheric jet. Dunkerton and Delisi (1985) find negative latitude gradients of zonal potential vorticity on the northward flank of the jet and in the subtropical mesosphere on some days from LIMS data. Hartmann (1983) has also found fast moving barotropic instabilities for wave 1 and 2 in the neighborhood of the stratospheric polar night jet in the southern hemisphere. Within the limited latitude domain (35-65°N) considered here, the 5-day average latitudinal gradient of zonal potential vorticity is almost

always positive. The smallest values occur in the easterly shear zone above the mesospheric wind maximum which is the preferred altitude of EP flux divergence. However, time changes in zonal potential vorticity gradient and EP flux divergence do not appear to be correlated, which they should be, if the flow is locally unstable.

3) Another possible mesospheric source of wave 2 EP flux divergence is breaking gravity waves as described by Holton (1984). It is natural to associate the observed anomalous small spatial scale variations in planetary wave EP flux in the mesosphere with possible breaking gravity waves. These small scale features do not appear to contribute significantly to the divergence of wave 2 which is based on the large scale equatorward gradient of EP flux, as discussed previously.

4. Residual Circulation

Figure 13a indicates the meridional component of the transformed Eulerian Mean residual circulation in 1980-81 at 55°N, calculated according to Dartt (1986a). An enhanced poleward component occurs when the EP flux is strongly convergent, Fig. 7b. However, above 65 km the residual circulation is equatorward when the EP flux is divergent. On these occasions, the role of the residual circulation is to decelerate the flow, the opposite of what occurs in the stratosphere.

The vertical component of the residual circulation at 65°N is shown in Figure 13b. An ascending branch of the residual circulation above the mesospheric jet is driven by the mid-winter wave event along with a strengthened descending branch lower down in the stratosphere. The ascending branch decreases in altitude with time as the baroclinic wave activity progresses. The ascending branch produces adiabatic cooling above the primary zone of planetary forced deceleration.

The residual circulation thus opposes the forcing of the zonal flow by the planetary waves both below 65 km where the waves are decelerating the flow and above where the waves are accelerating the flow. The upper (mesosphere) and lower (stratosphere) cells during Jan. in Fig. 13 are very similar to the pattern described by Dunkerton, et al. (1981). They indicate that the residual circulation arises solely as a mechanism for adjusting the thermal balance of the surrounding zonal mean state to the effects of wave forcing at a given altitude and latitude. However, their description of wave forcing did not include a region of mesospheric divergence by planetary waves as observed here.

Above 65 km, the Coriolis torque of the computed residual circulation opposes the observed EP flux divergence which itself is not particularly well correlated with observed flow change.

This may signal a breakdown of the transformed Eulerian Mean formalism. When the planetary wave forcing is no longer dominant in describing zonal flow change, the residual circulation becomes ambiguous.

5. Quasi-Stationary and Transient Wave Interactions

To investigate the intermittent baroclinicity of the lower atmosphere where much of the planetary wave activity of the middle atmosphere appears to originate, filters were used to separate the stationary and relatively slow moving, zonally propagating components. The relative phase and amplitude of these components were then analyzed throughout the winter to see how waves interacted during baroclinic episodes.

The filtering procedure described in Dartt (1986b) was applied to daily planetary wave Fourier coefficients of NMC geopotential height at 30 mb to separate the quasi-stationary (QS) and westward and eastward propagating components (with periods in the range 12 to 35 days). SAMS data at high altitudes were not filtered because of their intermittency. Figures 14 and 15 show the relationship between the various wave 1 components at 30 mb, 65°N, a latitude where the propagating components attain maximum amplitude. During both winters the amplitude of the QS component is much larger than the propagating components. Note

in Fig. 14, the similarity in phase of all three components on Jan. 1 and on Feb. 15. These dates mark the time of strong lower stratospheric baroclinic development within episodes described earlier in Fig. 1. In contrast, downward EP flux in the lower stratosphere may occur when the propagating components are 180° out of phase with the QS component. Thus, much of the variability of EP flux in the lower stratosphere appears to be the result of the constructive and destructive interference of QS and propagating components. This process has been described in other years by Madden (1983), Salby (1984) and in Dartt (1986b). The amplification of the westward propagating component in Fig. 14 between Dec. 17 and Jan. 31 occurs while phase of the QS component is moving westward in longitude. Between these dates, the eastward propagating component is being dissipated. Changes in location of continental scale forcing could create such wave behavior. If such change occurs slowly, the QS component is primarily affected; rapid change will result in the amplification of propagating components.

Figure 15 shows that the baroclinic episode during Jan. 1981 results from amplification of the QS component. Towards the end of January, the QS component weakens and both transient components grow rapidly, resulting in an amplified standing wave. Again, there is constructive wave interference at 30 mb, 65°N on Jan. 1 and Jan. 31 which are dates of strong vertical EP flux in Fig. 9.

Amplification of zonally propagating wave components may also occur if the QS component is trapped at a higher altitude and the wave activity is reflected downward. At 65°N, the occurrence of standing waves, a region of negative index of refraction near 40 km (Figs. 6 and 11) and the occasional appearance of downward EP flux (Figs. 1 and 9) are suggestive of trapping, especially for components from below that initially are directed poleward. Ray tracing analysis (O'Neill and Youngblut, 1982) would be necessary to verify this process in more detail.

6.   Conclusion

Planetary wave propagation and subsequent dissipation through zonal flow interaction in the upper stratosphere-mesosphere have been analyzed for two winters of NMC-SAMS data to near 80 km. Planetary waves propagating up from below are observed to decelerate the mesospheric jet up to altitudes of 70 km in early winter and 60 km in late winter. In mid-latitudes, wave 1 can propagate upwards to near 70 km and wave 2 to near 60 km. EP flux cross sections indicate that upward-propagating wave 2 generally avoids polar regions in the upper mesosphere. This can also be seen on a climatological basis (Barnett and Corney, 1985) where amplitudes of geopotential height in the high latitude mesosphere during winter months for wave 2 are less than 200 m while wave 1 amplitude is typically in

the range 200-500 m. Above 65 km, EP flux divergence by the
planetary waves can occur during winter resulting in wave forced
acceleration of zonal flow by about 5 $ms^{-1}day^{-1}$. However,
this wave forcing is not well correlated with zonal flow change
and may be minor compared to gravity wave drag which appears to
be several times larger. The EP flux divergence is primarily
associated with the wave 2 component. The acceleration occurs in
mid-latitudes and would seem to occur as upward and equatorward
propagating wave activity is divided into two branches, one going
towards low latitudes, and the other towards a region of negative
index of refraction in the polar mesosphere.

A two-cell residual circulation occurs in the mesosphere and
stratosphere during strong upward propagating wave events. This
cell is similar to the model pattern described by Dunkerton, et
al. (1981) with ascending motion and equatorward flow above the
primary altitude of EP flux convergence and descending motion and
poleward flow below. Planetary wave EP flux divergence above 65
km appears to generally occur independently of EP flux
convergence lower in the atmosphere.

Much of the weekly variability of upward propagating EP flux
in the middle atmosphere would appear to result from intermittent
baroclinicity in the lower stratosphere which can be described in
terms of the interference of zonally propagating and

quasi-stationary planetary wave components. While the propagating components amplify during the stratospheric warming process, their amplitude is considerably weaker than the quasi-stationary component.

Within the SAMS data, there is evidence of small spatial scale disturbances which exist on a 5-day average basis. These structures appear intermittently and may be related to gravity wave dissipation, local instabilities, or possibly even errors.

References

Barnett, J.J. and M. Corney, 1985: Middle atmosphere reference
model derived from satellite data. Middle Atmospheric
Program, Handbook for MAP, Vol. 16 (edited by K. Labitzke,
J.J. Barnett and B. Edwards), 47-143.

Barnett, J.J. and M. Corney, 1984: Temperature comparisons
between NIMBUS 7 SAMS, rocket/radiosondes and the
NOAA 6 SSU. J. Geophys. Res., 89, 5294-5302.

Dartt, D., 1986a: Winter planetary wave influences on zonal flow
near the stratopause from SCR and SAMS data. (Submitted for
publication)

Dartt, D., 1986b: The interaction of quasi-stationary and
zonally propagating planetary waves during winter, 1973-74.
(Submitted for publication)

Dunkerton, T. and D. P. Delisi, 1985: The subtropical
mesospheric jet observed by the Nimbus 7 Limb Infrared
Monitor of the Stratosphere. J. Geophys. Res., 90,
10681-10692.

Dunkerton, T. and N. Butchart, 1984: Propagation and selective
transmission of internal gravity waves in a sudden warming.
J. Atmos. Sci., 41, 1443-1460.

Dunkerton, T., C. P. F. Hsu and M. E. McIntyre, 1981: Some
Eulerian and Lagrangian diagnostics for a model
stratospheric warming. J. Atmos. Sci., 38, 819-843.

Fritts, D.C., 1986: Gravity waves in the middle atmosphere,
Middle Atmosphere Program, Handbook for MAP, Vol. 20 (edited
by S. A. Bowhill and B. Edwards), 1-12.

Geller, M.A., M. F. Wu and M.E. Gelman, 1984:
Troposphere-stratosphere (surface-55 km) monthly winter
general circulation statistics for the northern
hemisphere-interannual variations. J. Atmos. Sci., 41,
1726-1744.

Grose, W. L. and C. D. Rodgers, 1986: Coordinated study of the
behavior of the middle atmosphere in winter: monthly mean
comparisons of satellite and radiosonde data and derived
quantities. Clarendon Laboratory, Atmospheric Physics
Memorandum 816.1, U. of Oxford, 31pp.

Hartmann, D.L., 1983: Barotropic instability of the polar night jet stream. <u>J. Atmos. Sci.</u>, <u>40</u>, 817-835.

Holton, J.R., 1984: The generation of mesospheric planetary waves by zonally asymmetric gravity wave breaking. <u>J. Atmos. Sci.</u>, <u>41</u>, 3427-3430.

Holton, J.R., 1983: The influence of gravity wave breaking on the general circulation of the middle atmosphere. <u>J. Atmos. Sci.</u>, <u>40</u>, 2497-2507.

Holton, J. R., 1982: The role of gravity wave induced drag and diffusion in the momentum budget of the mesosphere. <u>J. Atmos. Sci.</u>, <u>39</u>, 791-799.

Karoly, D.J. and B.J. Hoskins, 1982: Three dimensional propagation of planetary waves. <u>J. Met. Soc. Japan</u>, <u>60</u>, 109-122.

Labitzke, K. and J.J. Barnett, 1985: Stratospheric and mesospheric large-scale height and temperature fields during the November/December 1980 Energy Budget Campaign. <u>J. Atmos. & Terr. Phys.</u>, <u>47</u>, 173-182.

Madden, R.A., 1983: The effect of the interference of traveling and stationary waves on time variations of the large-scale circulation. <u>J. Atmos. Sci.</u>, <u>40</u>, 1110-1125.

Manson, A. H., C. E. Meek, M. J. Smith and G. J. Fraser, 1985: Direct comparisons of prevailing winds and tidal wind fields (24-, 12-h) in the upper middle atmosphere (60-105 km) during 1978-80 at Saskatoon (52N, 107W) and Christchurch (44S, 173E). <u>J. Atmos. & Terr. Phys.</u> <u>47</u>, 403-476..

Matsuno, T., 1970: Vertical propagation of stationary planetary waves in the winter Northern Hemisphere. <u>J. Atmos. Sci.</u>, <u>27</u>, 871-883.

Miyahara, S., 1985: Suppression of stationary planetary waves by internal gravity waves in the mesosphere. <u>J. Atmos. Sci.</u>, <u>42</u>, 100-107.

O'Neill, A. and C.E. Youngblut, 1982: Stratospheric warmings diagnosed using the transformed Eulerian-mean equations and the effect of the mean state on wave propagation. <u>J. Atmos. Sci.</u>, <u>39</u>, 1370-1386.

Palmer, T. N., 1981: Diagnostic study of a wavenumber-2 stratospheric sudden warming in a transformed Eulerian-Mean formalism. J. Atmos. Sci., 38, 844-855.

Robinson, W.R., 1986: The application of the quasi-geostrophic Eliassen-Palm Flux to the analysis of stratospheric data. J. Atmos. Sci., 43, 1017-1023.

Rodgers, C.D., 1984: Coordinated Study of the behavior of the middle atmosphere in winter, Middle Atmosphere Program, Handbook for MAP, Vol. 12, 154 pp.

Salby, M.L., 1984: Transient disturbances in the stratosphere: Implications for theory and observing system. J. Atmos. & Terr. Phys., 46, 1009-1047.

Smith, A.K., 1983: Stationary waves in the winter stratosphere: Seasonal and interannual variability. J. Atmos. Sci., 40, 245-261.

Vincent, R.A. and I.M. Reid, 1983: HF Doppler measurements of mesospheric gravity wave momentum fluxes. J. Atmos. Sci., 40, 1321-1333.
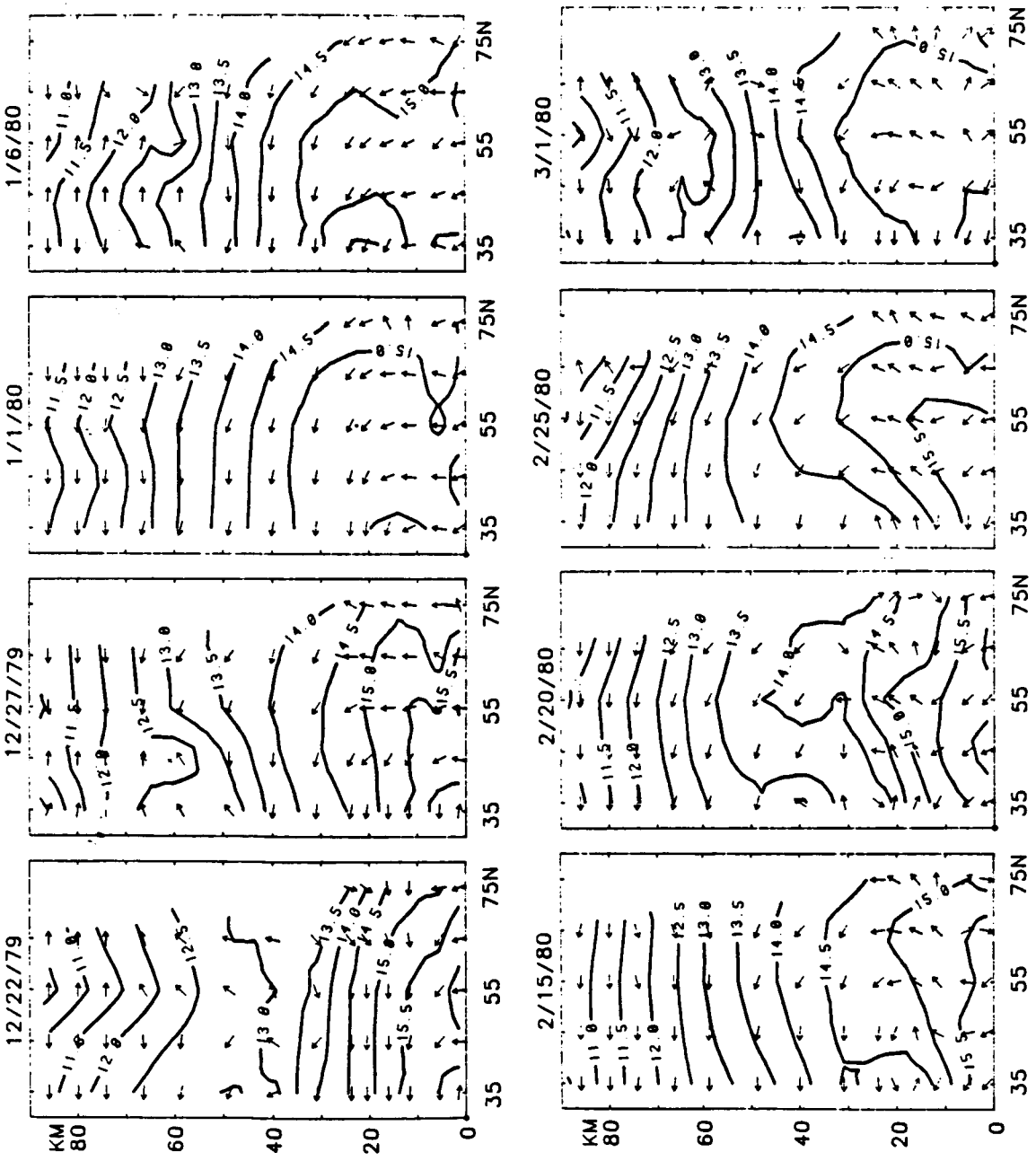
Figure 1. EP flux vector cross sections during the 1979-80 winter for planetary wave 1. Contours represent the $\log_{10}$ of the EP flux amplitude (g ms^{-2}).
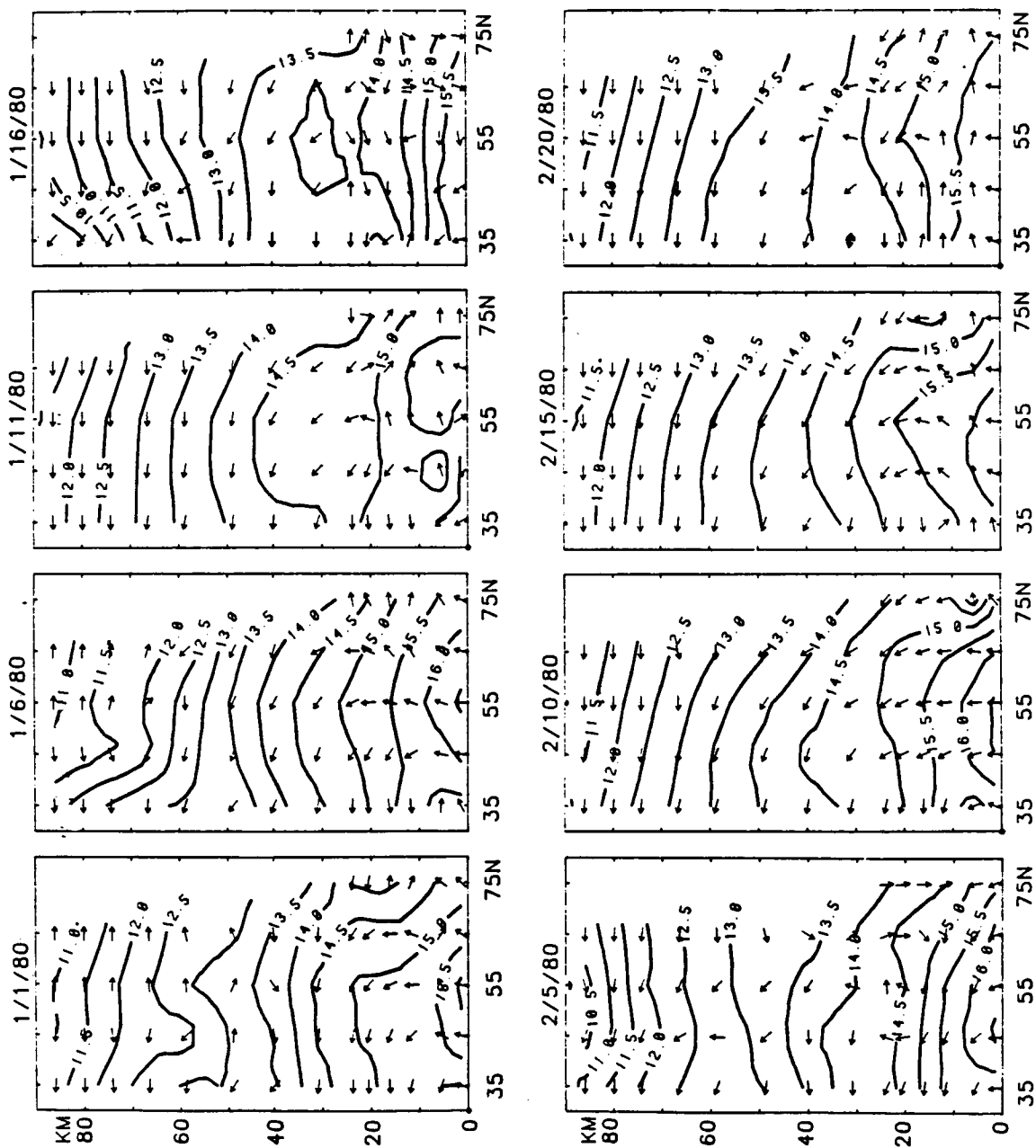
Figure 2. Same as Figure 1 for planetary wave 2.
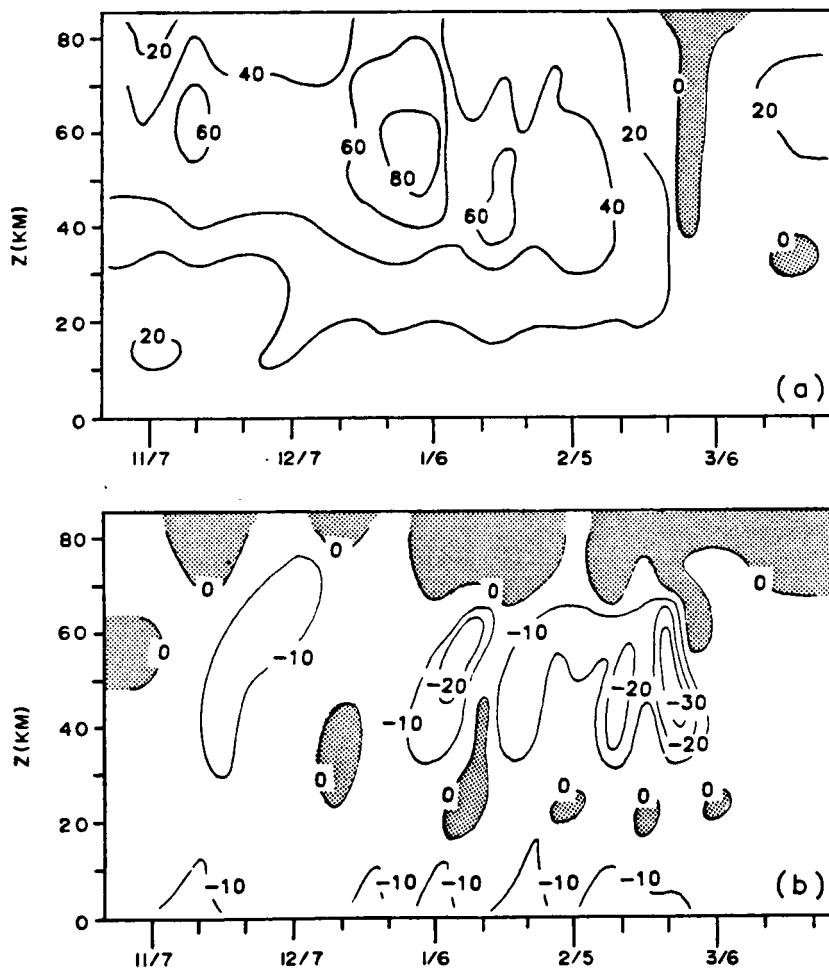
Figure 3. Time-altitude sections at 55°N of (a) zonal flow (ms^{-1}) and (b) planetary wave EP flux divergence $(ms^{-1}day^{-1})$ for winter 1979-80. In (a) easterlies are shaded; in (b) positive EP flux divergence is shaded.
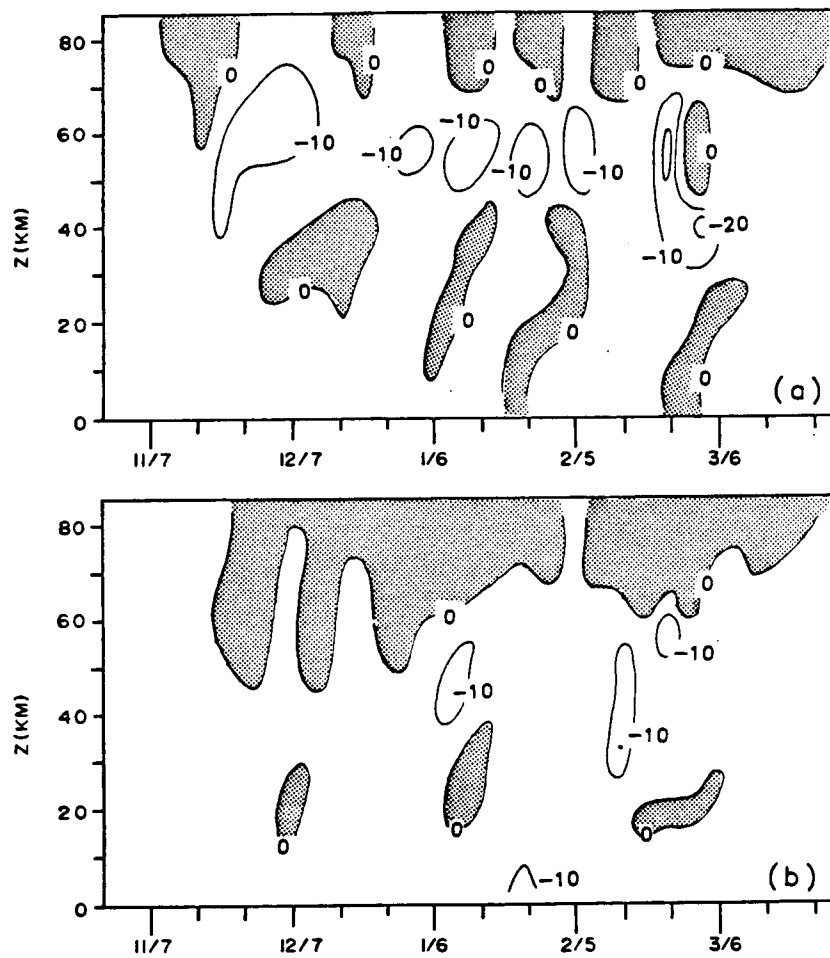
Figure 4. Time-altitude sections at 55°N of (a)
planetary wave EP flux divergence for
wave 1 and (b) wave 2 for winter 1979-80.
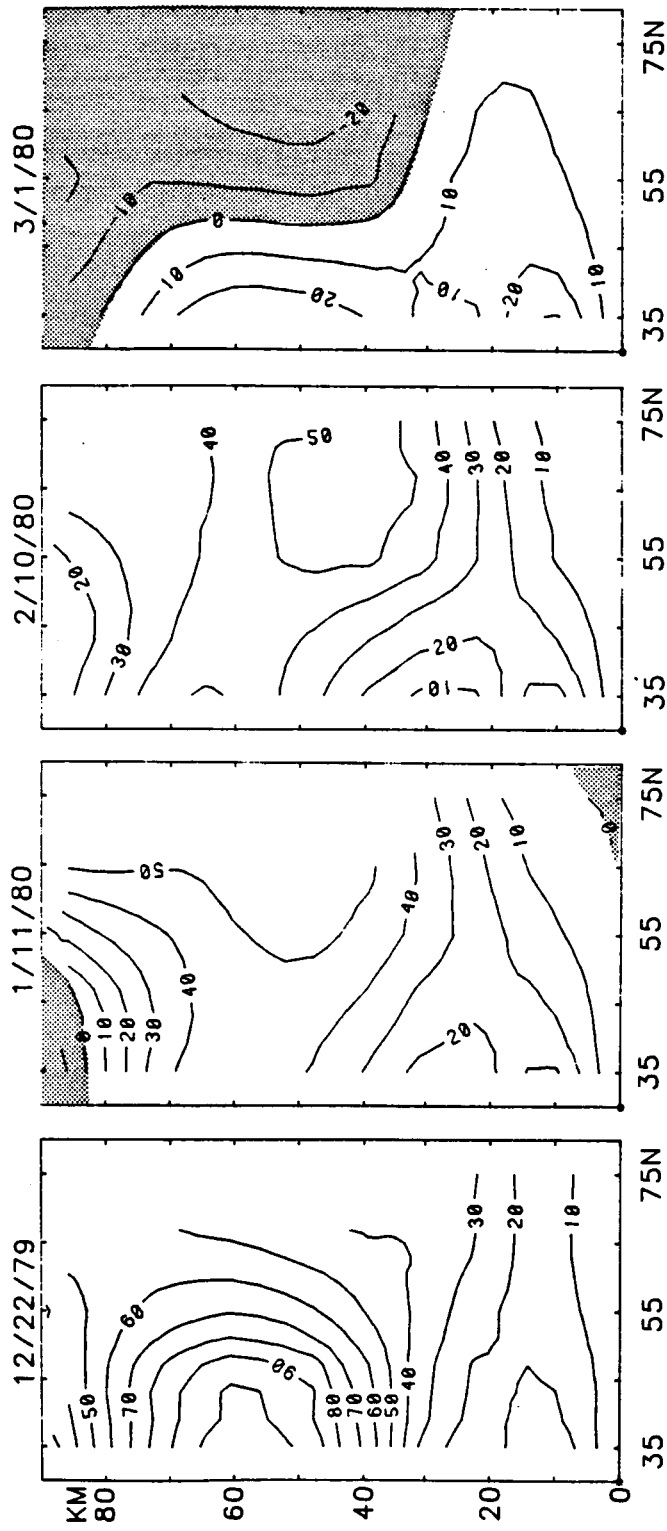
Figure 5. Zonal flow (ms^{-1}) cross sections during the 1979-80 winter. Easterlies are shaded.
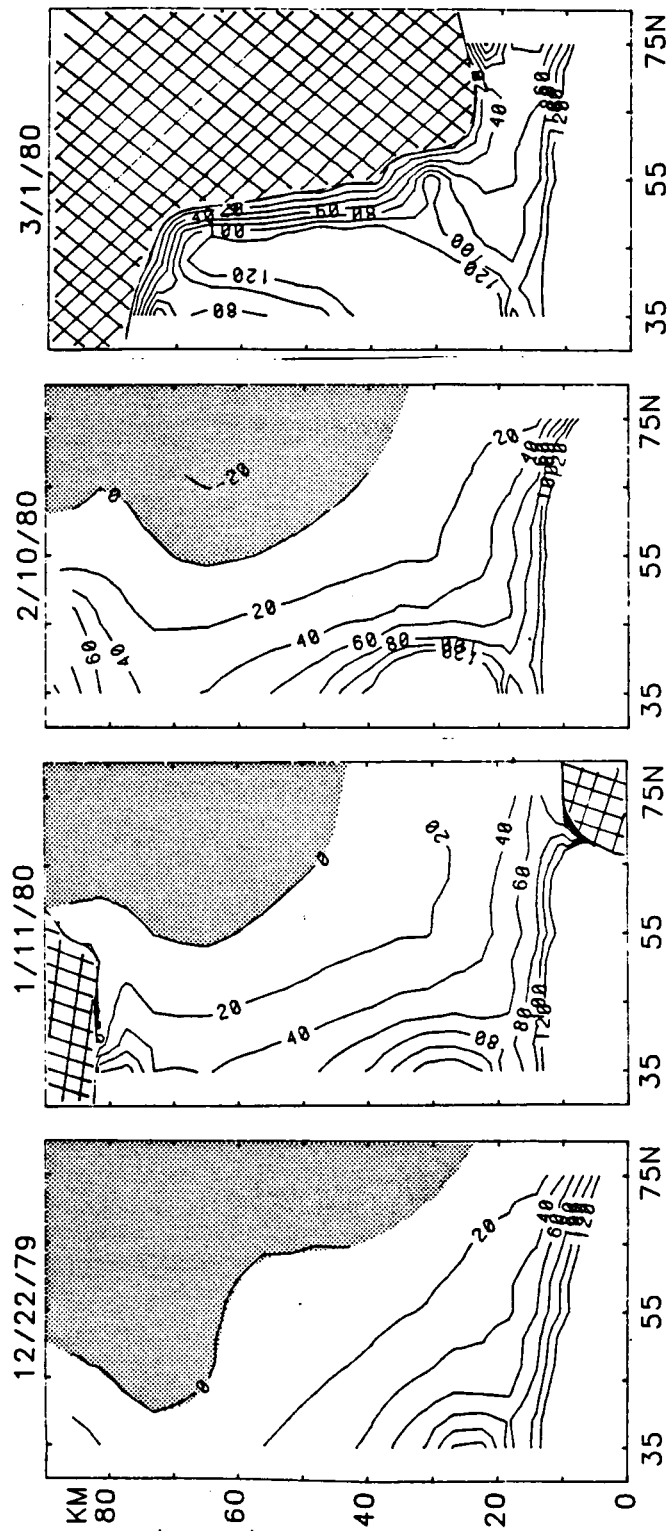
Figure 6. The index of refraction for stationary wave 1 during the 1979-80 winter. Negative values are shaded. Regions where the zonal flow is easterly are cross-hatched.
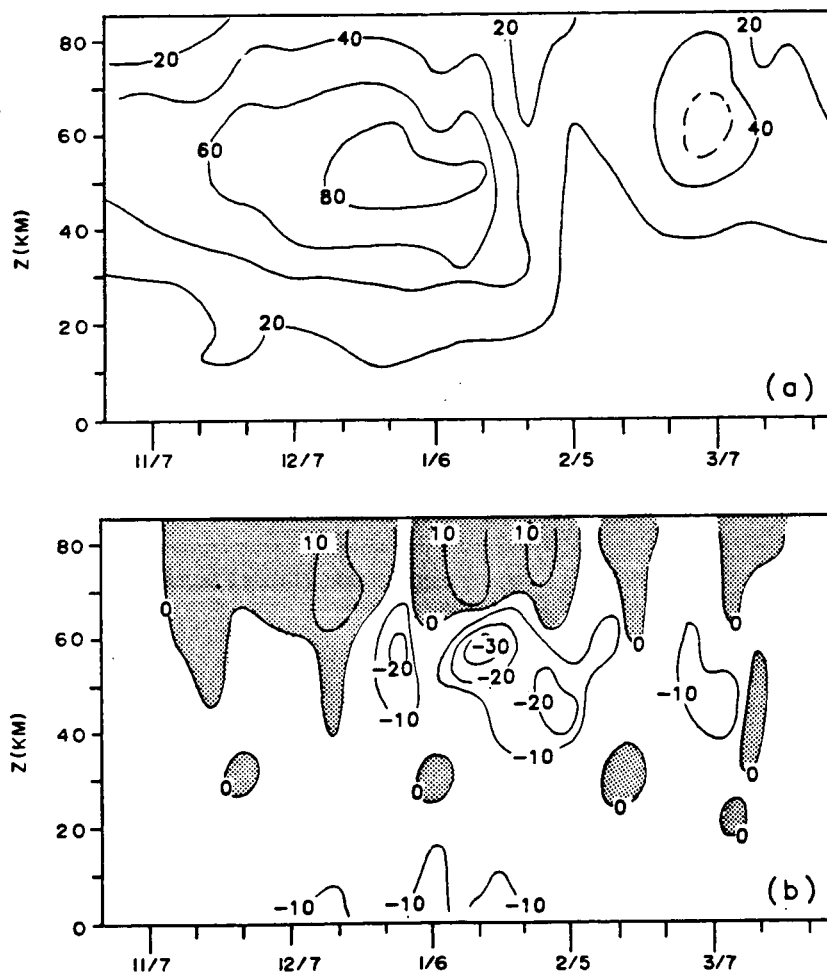
Figure 7.   Same as Figure 3 for winter, 1980-81.
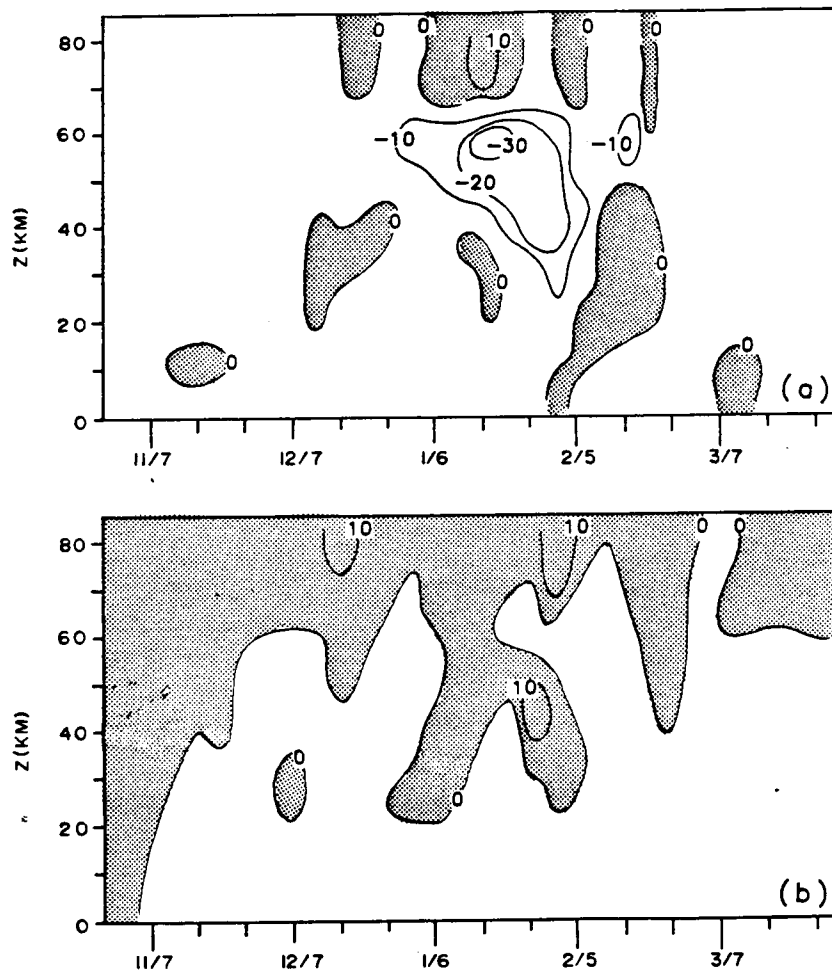
Figure 8. Same as Figure 4 for winter, 1980-81.
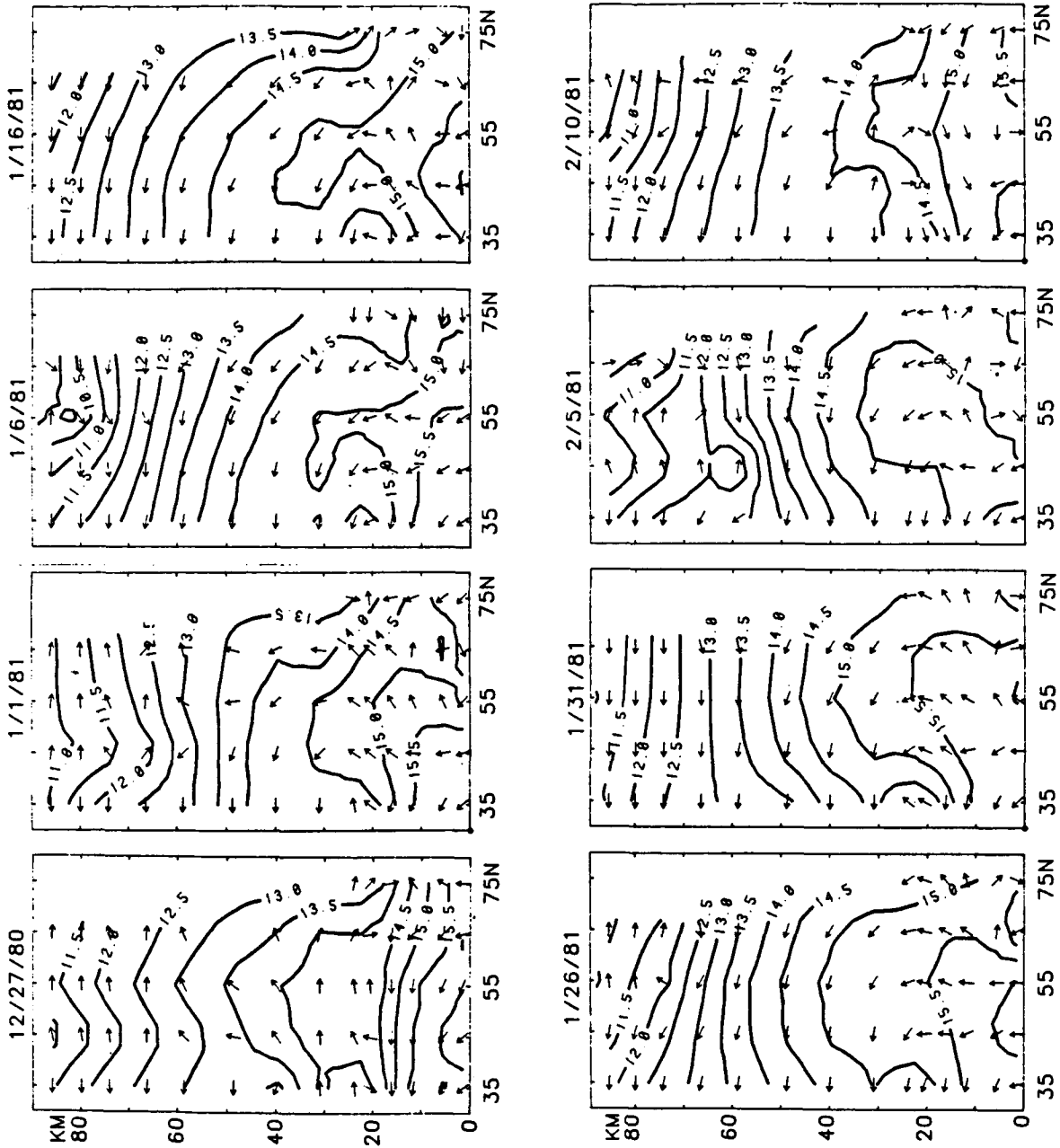
Figure 9. Same as Figure 1 for winter, 1980-81.
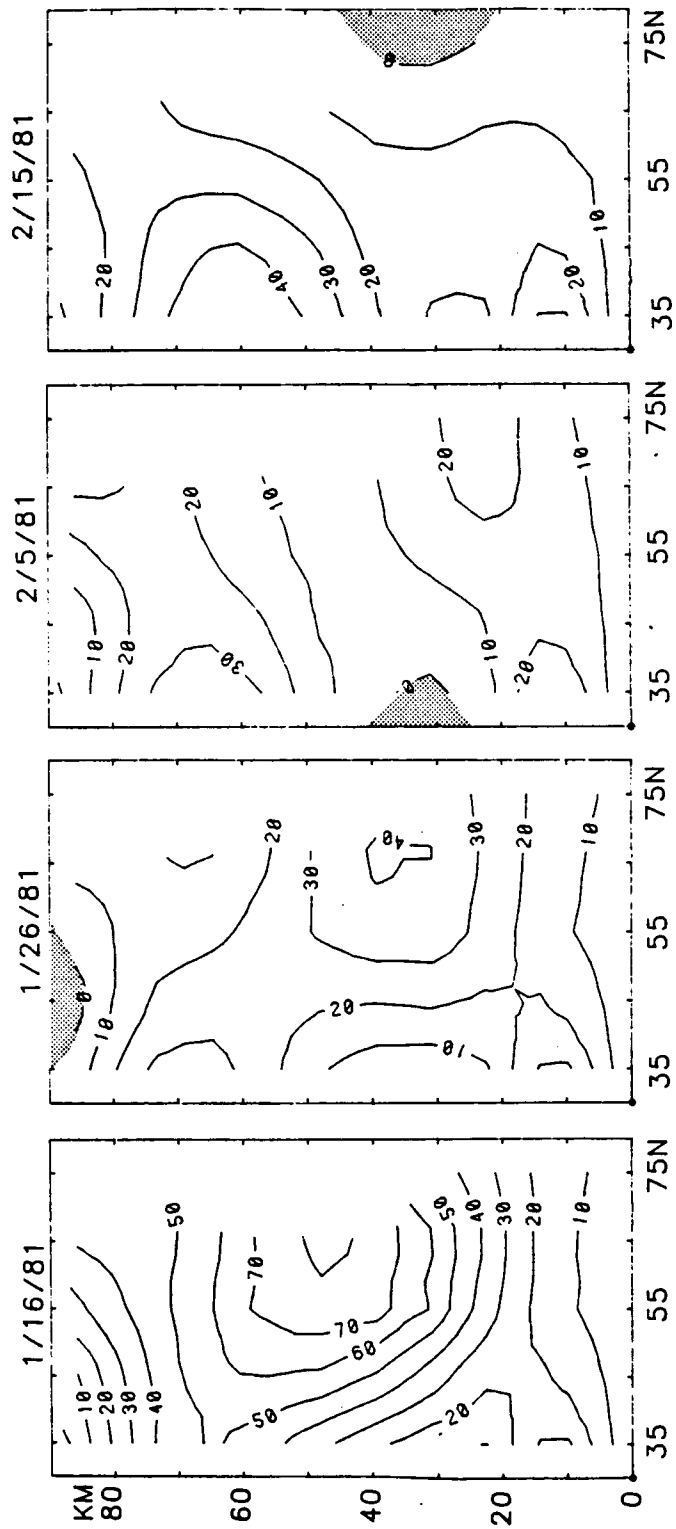
Figure 10. Same as Figure 5 for winter, 1980-81.
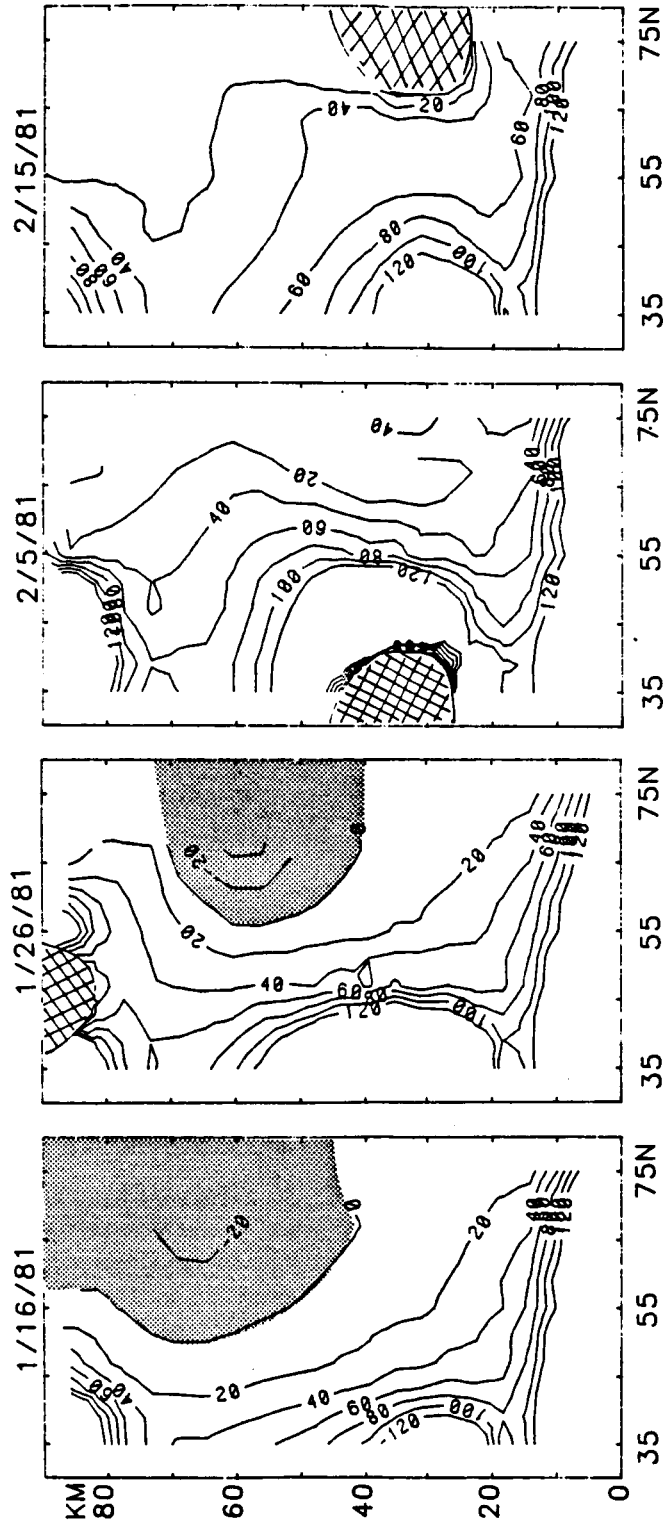
Figure 11. Same as Figure 6 for winter, 1980-81.
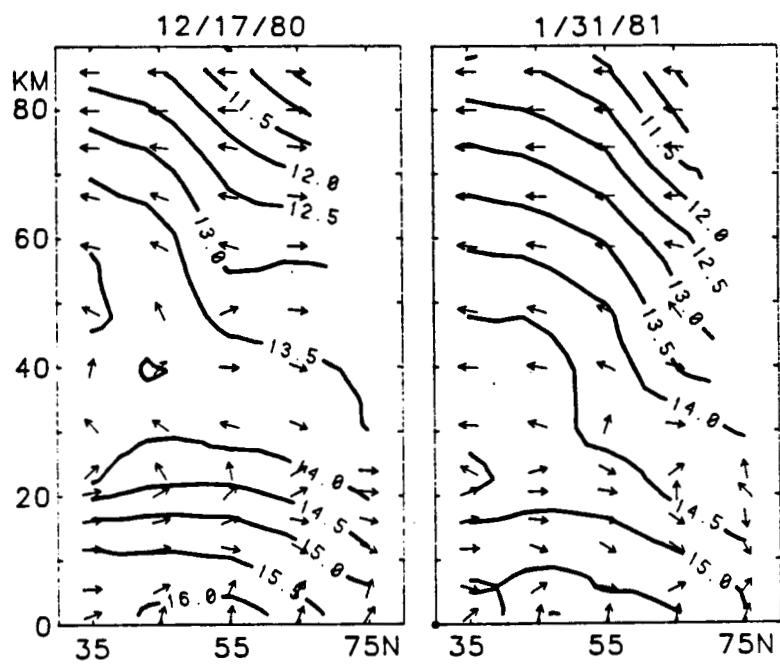
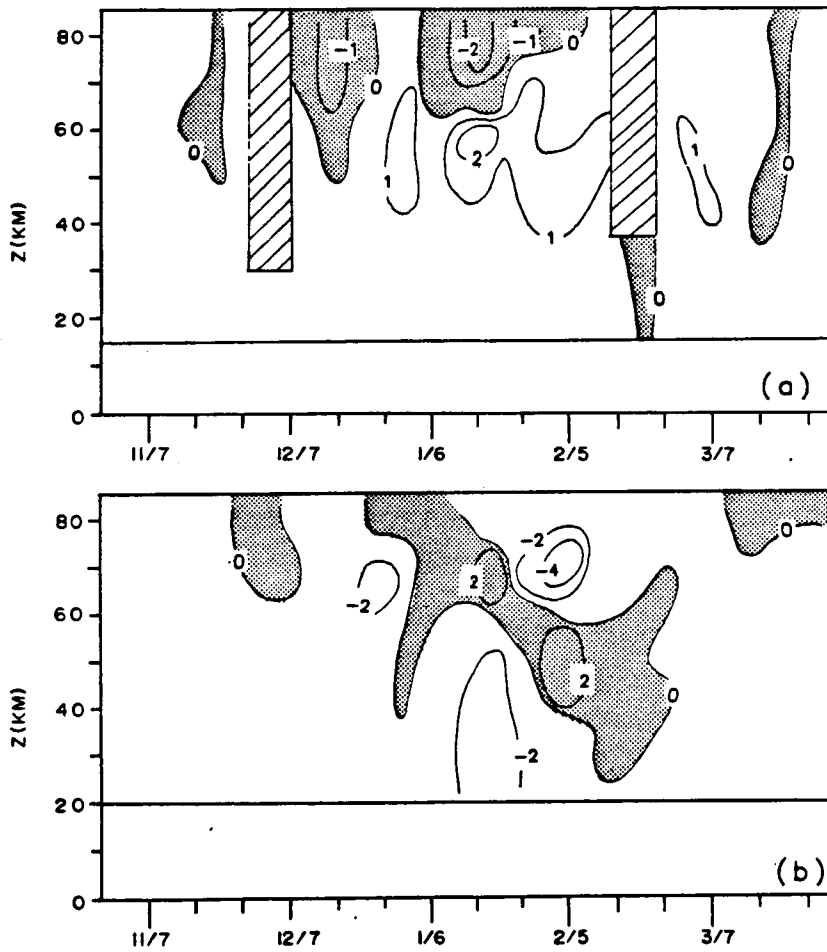Figure 12. EP flux vector cross sections for wave 2 on Dec. 17, 1980 and Jan. 31, 1981.

Figure 13. Time-altitude sections of residual
circulation during 1980-81: (a) meridional
component at 55°N (ms^{-1}) and (b) vertical
component at 65°N (10^{-3}ms^{-1}). In (a) winds
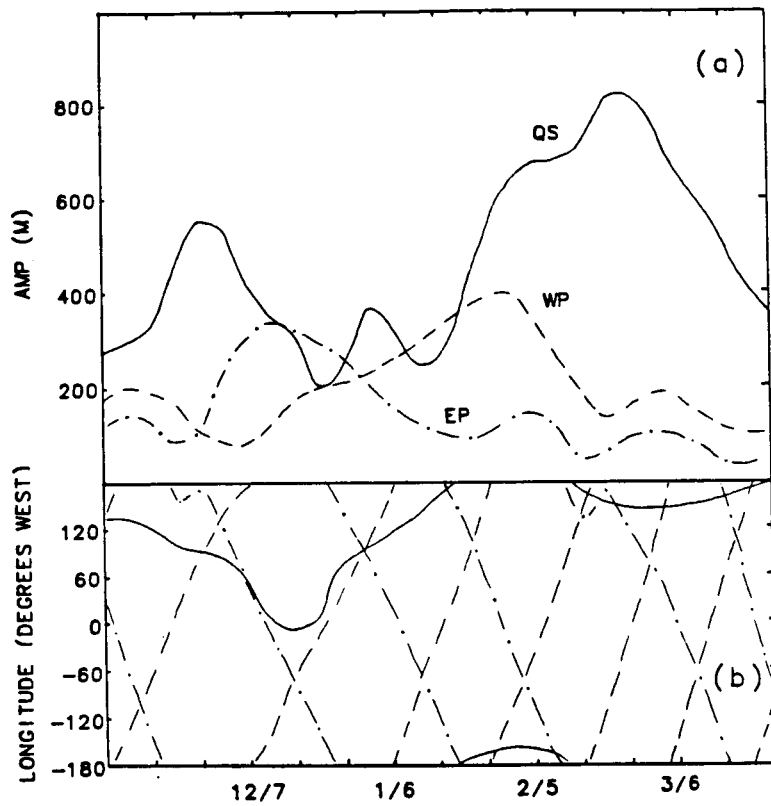from the north are shaded; in (b) upward
motion is shaded.

-123-

Figure 14. Time variations of (a) amplitude and (b) phase of quasi-stationary, westward propagating and eastward propagating wave components at 30 mb, $65°N$ during winter 1979-80.
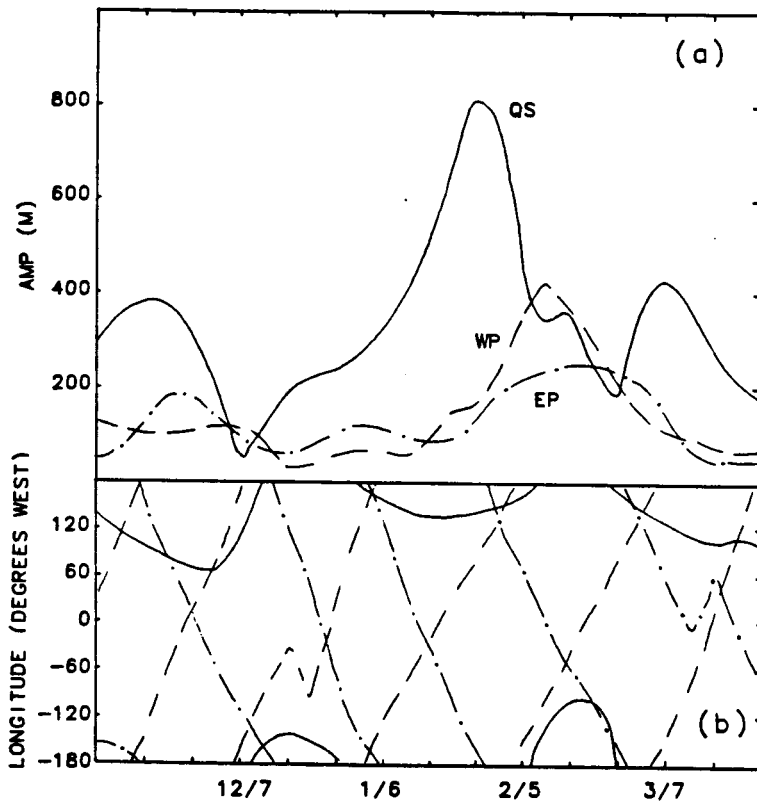
Figure 15.   Same as figure 14 for winter
1980-81.